UNIVERSITY OF HELSINKI REPORT SERIES IN PHYSICS

HU-P-D105

PHENOMENOLOGICAL ASPECTS OF FOUR-NEUTRINO MODELS

ANNA KALLIOMÄKI

Theoretical Physics Division
Department of Physical Sciences
Faculty of Science
University of Helsinki
Helsinki, Finland

ACADEMIC DISSERTATION
To be presented, with the permission of the Faculty of Science of the University of Helsinki, for public criticism in the Small Auditorium (E204) at Physicum, Gustaf Hällströmin katu 2, on June 17th, 2003, at 12 o'clock.

Helsinki 2003

ISBN 952-10-0575-0
ISSN 0356-0961
ISBN 952-10-0576-9 (pdf-version)
http://ethesis.helsinki.fi
Yliopistopaino
Helsinki 2003

Preface

This thesis is based on research carried out at the Theoretical Physics Division of the Department of Physical Sciences at the University of Helsinki during the years 1999 – 2003. I wish to thank the personnel of the Theoretical Physics Division, especially Liisa Koivisto, for an encouraging and pleasant working environment. I also thank the Academy of Finland and the Graduate School in Particle and Nuclear Physics, the Jenny and Antti Wihuri Foundation and the Ella and Georg Ehrnrooth Foundation for financial support.

I want to thank my supervisor Prof. Jukka Maalampi for excellent guidance and for initiating my interest in neutrino physics. To him, Doc. Juha Peltoniemi and Doc. Iiro Vilja I am grateful for careful reading of the manuscript and their valuable comments. Also Doc. Hannu Kurki-Suonio has read through parts of the manuscript and given comments which are greatly appreciated. I am truly thankful to Prof. Christofer Cronström for helping me in practical arrangements during the final stages of writing the thesis. It has been a great pleasure to collaborate with Prof. Jukka Maalampi, Prof. Morimitsu Tanimoto and Dr. K.R.S. Balaji who I also wish to thank.

I am indebted to many fellow students and colleagues for their friendship, encouragement and support. Among others, I would like to acknowledge especially Dr. S.M. Harun-or-Rashid, Samuli Hemming, Ville Honkkila, Dr. Elina Keihänen, Dr. Petteri Keränen, Dr. Ismo Napari, Ville Sipiläinen and Dr. Antti Sorri.

Especially I want to express my gratitude to my family, my parents Jaakko and Raija, my sister Laura and my brothers Mikko and Ossi, for continuous love and support. For Kai I am grateful for so many things that I wouldn't know where to start. I want to thank you all for being there. This thesis is dedicated to my late grandmother who taught me that being wise has nothing to do with education.

Helsinki, May 2003

Anna Kalliomäki

A. Kalliomäki: Phenomenological Aspects of Four-neutrino Models, University of Helsinki, 2003, 87 p.+appendices, University of Helsinki, Report Series in Physics, HU-P-D105, ISSN 0356-0961, ISBN 952-10-0575-0 (printed version), 952-10-0576-9 (pdf-version).

Classification (INSPEC): A1310, A1315, A1460G, A2340B, A1130E
Keywords: neutrinos, neutrino mass, double beta decay, CP invariance

Abstract

Neutrino physics has been an active and successful research field in recent years, especially experimentally. As a result of a series of great experimental discoveries neutrino oscillations are today a well established phenomenon indicating non-vanishing neutrino masses. If all the existing evidences of oscillation, coming from the atmospheric and the solar neutrino experiments and the laboratory experiment LSND, are described jointly, at least four neutrino flavors are needed. The fourth flavor must be sterile with respect to the Standard Model interactions since experiments show that only three neutrino flavors couple to the Z-boson.

In this thesis various phenomenological aspects of sterile neutrinos have been investigated. We have studied the prospects of probing the possible leptonic CP violation in the proposed neutrino factory experiments. We make a comparison of the ordinary three-neutrino case and the four-neutrino case and show that these two cases are quite different in respect to the fake CP-violation effect caused by the matter in Earth's crust. We have also examined the bounds on neutrino masses and mixing parameters one can obtain from the future neutrinoless double beta decay experiments. Also in this study we have studied particularly a four-neutrino model taking into account the LSND evidence for neutrino oscillations. The lightness of the sterile neutrino, required by the oscillation data, is a challenging problem for theoretical model building. In the third original paper of this thesis we consider this issue. There the idea of the so-called pseudo-Dirac neutrino is revisited in the light of the recent experimental information on neutrino masses and mixing.

In the introduction part of the thesis the theoretical background of the topics discussed in original publications is presented. Also some of the most important present and future neutrino experiments are described. The introduction part contains also some phenomenological considerations e.g. on different methods to study the absolute mass scale of neutrinos and to search for leptonic CP violation. Finally the present status of four-neutrino models is briefly described.

Contents

Chapter 1

Introduction

A hypothetical particle, later to be baptized neutrino, was suggested in 1931 by W. Pauli to explain a curious experimental observation concerning beta radioactivity. In 1914 experiments by J. Chadwick showed that the beta particles emitted in radioactive decay show a continuous spectrum, in contrast with what was expected, and this observation made some physicists even question the very profound principles of physics – the conservation of energy and momentum. Pauli solved the puzzle by suggesting that the missing energy might be carried off by a new light neutral particle which would have extremely strong penetrating power to escape detection. The name "neutrino", which is Italian and means "little neutral one", was given to the Pauli's hypothetical particle by E. Fermi who in 1934 introduced his theory of beta decay which included a massless neutrino [1]. In the famous experiment by F. Reines and C. Cowan [2] in the late 1950's electron antineutrinos, produced in a nuclear reactor, were detected for the first time through the inverse beta decay reaction

$$\overline{\nu}_e + p \rightarrow e^+ + n\,. \tag{1.1}$$

The muon neutrino was discovered in 1962 in experiments at Brookhaven National Laboratory and CERN [3], and the third neutrino, the tau neutrino, was discovered in 2000 [4], although its existence was indirectly verified already in 1975 when the tau lepton was discovered [5].

Already in 1968 the first solar neutrinos were detected and the long-standing solar neutrino problem was conceived. Solar neutrino problem means that some of the electron neutrinos produced in nuclear fusion reactions in the Sun seem to disappear on their way to the Earth. The similar kind of deficit in the flux is measured also for the muon neutrinos produced in the atmosphere by cosmic rays.

Originally neutrinos were introduced as massless particles mainly because the experimental upper limit on the neutrino mass was, and still is, known to be much smaller than the masses of other particles and no indication of non-zero mass was seen in experimental data. However, in theoretical considerations the idea of small but nonzero neutrino mass and neutrino oscillations is old: the possibility

of *neutrino* $\leftrightarrow$ *antineutrino* transitions was discussed by B. Pontecorvo already in 1957 [6]. A few years later, in 1962, Maki, Nakagawa and Sakata proposed a model in which the fields of the two "weak" neutrinos, ν_e and ν_μ, are linear orthogonal superpositions of the fields of the massive neutrinos ν_1 and ν_2 so that the transition $\nu_\mu \rightarrow \nu_e$ is possible [7]. The possibility that the neutrino oscillations could explain the solar neutrino problem was realized soon after the deficit in solar neutrino flux was discovered, but it took several decades and lots of experimental effort to establish the fact that the Standard Model (SM) of particle physics, which gradually evolved from the Fermi's theory, needs to be extended to include neutrino masses and that the neutrino oscillations truly do take place.

Today neutrino oscillations are observed also in experiments using man-made neutrino beams. Especially interesting results from the point of view of this thesis are those of the LSND accelerator experiment at the LAMPF facility, Los Alamos. If one wants to describe all the three positive oscillation signals, i.e. solar, atmospheric and the LSND signal, jointly, one should have three squared mass differences $\Delta m^2_{ji} = m^2_j - m^2_i$ of different orders of magnitude, and thus at least four neutrino flavors instead of the three ordinary ones which are included in the SM. The number of light neutrinos which couple to the Z-boson is experimentally restricted to three, however, and therefore the fourth neutrino flavor must be sterile with respect to the SM interactions. Because the LSND oscillation signal is not confirmed by other experiments, in contrast with the solar and atmospheric oscillation results, it is in many analyses simply ignored. However, it should be kept in mind that the LSND results have not been excluded by other experiments, either. This is true also for the recent cosmological observations, e.g. the data of the Wilkinson Microwave Anisotropy Probe (WMAP) [8], which are quite restrictive from the point of view of the LSND result [9] but not yet exclusive [10, 11]. The upcoming MiniBooNE experiment has the sensitivity to confirm or disprove the LSND result.

The case for sterile neutrinos has weakened during the last few years, however. At the time the Paper I and Paper II of this thesis were under preparation, active-sterile neutrino oscillations were a viable solution to the solar neutrino problem and the four-neutrino model that we considered was consistent with experimental results. The SNO experiment, whose first results were announced in 2001, was able to tell, for the first time, whether the solar electron neutrinos oscillate into active or sterile flavors. The SNO results indicate very clearly (at 5.3 σ C.L.) that in a simple two-flavor analysis oscillations take place between electron neutrino and some combination of active flavors ν_μ and ν_τ. This important observation made many neutrino models disfavored and out of date. It should be emphasized, however, that although active-sterile oscillations as dominant oscillation modes are now ruled out, both the solar and the atmospheric data still allow for a substantial active-sterile mixing [12–14].

This thesis consists of an introduction part and three original publications.

In the introduction part the following topics will be discussed. In Chapter 2 the basic theoretical background of neutrino mass models, neutrino oscillations, neutrinoless double beta decay and leptonic CP violation are described. Experimental neutrino physics has taken giant steps forward in the recent years; Chapter 3 is devoted to a description of some of the most important solar, atmospheric and terrestrial neutrino experiments. Also the future long-baseline projects are briefly described there. Chapter 4 contains phenomenological considerations on the search of leptonic CP violation and the absolute mass scale of neutrinos. Also some characteristics of the three-neutrino analyses on solar and atmospheric data and the present situation of the four-neutrino models is described. Concluding remarks are presented in Chapter 5.

1.1 Summary of the original papers

Paper I: Search for CP violation at a neutrino factory in a four-neutrino model

Reprinted from Physics Letters, B469, Anna Kalliomäki, Jukka Maalampi and Morimitsu Tanimoto, Search for CP violation at a neutrino factory in a four-neutrino model, 179–187, Copyright (1999), with permission from Elsevier Science.

In this paper we studied the leptonic CP violation in the framework of a four-neutrino model in which there exists a sterile neutrino along with the three ordinary neutrinos and neutrino masses are divided into two nearly degenerate pairs. The present day experiments are not sensitive to the CP violating effects, but the proposed neutrino factory experiments will provide a way to probe them. However, distinguishing the matter induced "fake" CP violation from the genuine CP violation effect, caused by the CP violating phase or phases in the neutrino mixing matrix, is a difficult task. We estimated, assuming constant matter density, the magnitude of the matter effect in long baseline experiments using approximative analytical formulas for the probability differences $\Delta P_{\alpha\beta} \equiv P(\nu_\alpha \to \nu_\beta) - P(\overline{\nu}_\alpha \to \overline{\nu}_\beta)$ between CP-conjugate channels. We found that in the four-neutrino model the matter effect is generally small compared with the genuine CP violation term. This is not the case in the three-neutrino model where with certain parameter values the matter effect can be as large as the genuine CP violation term.

Paper II: Neutrinoless double beta decay in four-neutrino models

Reprinted from Physics Letters, B484, Anna Kalliomäki and Jukka Maalampi, Neutrinoless double beta decay in four-neutrino models, 64–72, Copyright (2000), with permission from Elsevier Science.

The oscillation experiments are sensitive to the squared mass differences $\Delta m^2_{ji} = m^2_j - m^2_i$, but not to the neutrino masses themselves. Assuming that neutrinos are Majorana particles, the neutrinoless double beta decay ($0\nu\beta\beta$) process, on the

other hand, provides information on the absolute mass scale and the Majorana CP-phases of neutrinos since the quantity probed in the $0\nu\beta\beta$ experiments is the absolute value of the effective Majorana mass

$$\langle m \rangle = \sum_i m_i U_{ei}^2 \,. \tag{1.2}$$

In our work we studied the constraints the proposed GENIUS experiment sets on the neutrino masses and mixings in a four-neutrino model. We used a mass model in which neutrino masses are divided into two degenerate pairs with masses m and $m + \Delta m$. The value of the mass gap between the pairs, Δm, is constrained by cosmology, the LSND and other short baseline experiments. We concentrated in the CP-conserving case in which case the Majorana mass has the form $\langle m \rangle = \sum_i \eta_i m_i |U_{ei}|^2$ with eight different patterns of the relative CP-numbers $\eta_i = \pm 1$. We determined, in every possible CP-number configuration separately, what kind of limits the GENIUS experiment yields on m and certain mixing angles in case it does not detect $0\nu\beta\beta$. We found that the most stringent bounds are obtained when all the relative CP-numbers are equal in which case a negative result from GENIUS would set an upper limit $m \lesssim 0.001\,\mathrm{eV}$.

Paper III: Revisiting pseudo-Dirac neutrinos

In this paper we re-examined pseudo-Dirac mixing of left- and right-handed neutrinos in one-generation case, assuming that the Majorana masses M_L and M_R are small compared with the Dirac mass M_D. In our study we assumed that oscillations between the two nearly degenerate (in mass) neutrinos solves the solar neutrino problem with the squared mass difference corresponding to the so-called VAC solution, $\Delta m^2 \simeq 10^{-10}\,\mathrm{eV}^2$. In our simple model the effective Majorana mass $\langle m \rangle$, which is measured by $0\nu\beta\beta$ experiments, is actually M_L, and the negative results in search for $0\nu\beta\beta$ therefore gives an upper bound on M_L. By making general assumptions about the mechanism which generates Majorana masses for the left-handed neutrinos, also a lower bound for M_L can be derived. Because of the relation $\Delta m^2 \simeq 2M_D(M_L + M_R)$, which follows from the pseudo-Dirac mass ordering, a closed bound on M_L yields a simple closed bound also on M_D. We found that a phenomenologically consistent scenario is achieved with values $M_L = M_R \simeq 10^{-7}\,\mathrm{eV}$ and $M_D \simeq 10^{-5} - 10^{-4}$ eV. Even the most sensitive one of the planned future $0\nu\beta\beta$ experiments is sensitive only down to $\langle m \rangle \sim 10^{-3} - 10^{-2}$, and would not therefore be able to measure M_L. If, on the other hand, a positive signal for the effective Majorana mass is observed with $\langle m \rangle \gtrsim 10^{-3}\,\mathrm{eV}$, the pseudo-Dirac scenario cannot explain the solar neutrino anomaly in terms of VAC oscillations.

Chapter 2

Neutrinos in gauge field theories

2.1 Neutrinos in the Standard Model

The Standard Model (SM) of electroweak and strong interactions is the name given to the current theory of elementary particles and their interactions, excluding gravitational interaction. The Standard Model was developed in the 1960's and 70's [15–18]. It incorporated all that was at that time known about elementary particles, and it has predicted accurately the outcome of a great number of experiments performed thereafter.

The basic constituents of the SM are six quarks and six leptons and forces acting between them. The quarks are named up (u), down (d), charm (c), strange (s), top (t) and bottom (b), and the leptons consist of the electron (e), muon (μ) and tau (τ) and their corresponding neutrinos ν_e, ν_μ and ν_τ. In addition, all these particles have their antiparticles, with the possible exception of neutrinos. These spin-1/2 fermions are grouped into three families, each consisting of a quark pair and a lepton pair: (u, d, e, ν_e), (c, s, μ, ν_μ) and (t, b, τ, ν_τ). The forces described by the SM are responsible for the electromagnetic (felt by quarks and charged leptons e, μ and τ), strong (felt by quarks) and weak (felt by all left-handed fermions) interactions.

Today the SM is a well established theory, precisely tested and widely applicable in particle physics processes. Nevertheless, there are strong reasons to believe that there is physics beyond it, i.e. that the SM is only a low-energy effective theory which may have to be modified at higher energies, possibly already at the TeV scale. From the theoretical point of view, the SM has a disturbingly large number of parameters, e.g. all particle masses, whose values the theory leaves undetermined. A complete theory is expected not just to describe but to *explain* the values of particle masses, as well as to answer the other open questions, such as why the number of particle families is three. Also, as mentioned, the SM does

not describe gravity. Often in practical situations this does not matter since in particle reactions tested in laboratory the gravitational interactions have ignorable effects, but the final theory should include a quantum description of gravitational interactions, too.

At the time the SM was formulated, the experimental results gave no reason to expect neutrinos to have mass, and so the theory was built in such a way that it predicted strictly massless neutrinos. Lately this feature has been under serious reconsideration. There are both theoretical and phenomenological reasons (which will be discussed in section 2.2) to believe that neutrinos, like other fermions, indeed are massive. In contrast to the masslessness of photon, there is no symmetry principle forbidding massive neutrinos, and thus modifying the SM to include neutrino masses does not ruin the ideas behind it. This can be seen by considering the way fermions acquire masses in the theory, which will be briefly summarized in this section. Because neutrinos have no strong interactions, only the electroweak part of the SM, introduced by Glashow, Weinberg and Salam [15], is of interest in this thesis. A detailed description of the SM can be found e.g. in [19].

The standard electroweak model is a local gauge field theory based on the symmetry group $SU(2)_L \times U(1)_Y$. The condition of a local symmetry can only be fulfilled if spin-1 fields, called *gauge fields*, are introduced into the theory. The exchange of the quanta of the gauge fields, called gauge bosons, describes forces between particles whose corresponding fields transform non-trivially under the local symmetry.

The weak isospin group $SU(2)_L$ is generated by the weak isospin operator, $\vec{I}$, for which the fundamental spin-1/2 representation is given by the Pauli matrices: $\vec{I} = \vec{\sigma}/2$. The subscript L in $SU(2)_L$ is to remind that $SU(2)$ gauge bosons $\vec{A}_\mu = (A^1_\mu, A^2_\mu, A^3_\mu)$ couple only to left-handed fermions. In other words, left-handed components of fields, $\psi_L = \frac{1}{2}(1-\gamma_5)\psi$, form isospin doublets, whereas right handed components, $\psi_R = \frac{1}{2}(1+\gamma_5)\psi$, are isosinglets. The group $U(1)_Y$ is generated by the weak hypercharge operator Y which is defined so that

$$I_3 + Y/2 = Q \tag{2.1}$$

is the electric charge, I_3 being the third component of $\vec{I}$. Since ψ_L and ψ_R have different values of weak hypercharge Y, the $U(1)$ gauge boson B_μ couples with different strengths to them. For the electron and its neutrino the isospin and hypercharge quantum numbers for the fields in the $SU(2)$ doublet $E_L = (\nu_{eL},\, e_L)^T$ and the singlet field e_R are given as follows:

	I	I_3	Y
ν_{eL}	1/2	1/2	-1
e_L	1/2	-1/2	-1
e_R	0	0	-2

For quarks in the first fermion family the corresponding charge values for fields in the $SU(2)$ doublet $Q_L = (u_L,\, d_L)^T$ and the singlet fields u_R and d_R are given by

	I	I_3	Y
u_L	1/2	1/2	1/3
d_L	1/2	-1/2	1/3
u_R	0	0	4/3
d_R	0	0	-2/3

The quantum numbers of the other families (c, s, μ, ν_μ) and (t, b, τ, ν_τ) are given similarly.

It is important to note here that the electroweak model, and thus the SM, does not include right-handed neutrino fields. Since no neutrino masses were observed at the time the SM was formulated, and because it was known that only left-handed neutrino fields (and right-handed antineutrino fields) participate in the weak interactions, it was natural to assume that right-handed neutrinos do not exist in nature.

Restricting the discussion to the first fermion family, the $SU(2)_L \times U(1)_Y$ invariant Lagrangian for fermions and gauge bosons is given by

$$\begin{aligned}\mathcal{L}_{L+B} &= -\overline{E}_L\gamma^\mu D_\mu E_L - \bar{e}_R\gamma^\mu D_\mu e_R \\ &\quad -\overline{Q}_L\gamma^\mu D_\mu Q_L - \bar{u}_R\gamma^\mu D_\mu u_R - \bar{d}_R\gamma^\mu D_\mu d_R \\ &\quad -\frac{1}{4}\vec{F}^{\mu\nu}\vec{F}_{\mu\nu} - \frac{1}{4}G^{\mu\nu}G_{\mu\nu}\,, \end{aligned} \tag{2.2}$$

where $\vec{F}_{\mu\nu} = \partial_\mu\vec{A}_\nu - \partial_\nu\vec{A}_\mu + g(\vec{A}_\mu \times \vec{A}_\nu)$, $G_{\mu\nu} = \partial_\mu B_\nu - \partial_\nu B_\mu$, and D_μ is the covariant derivative

$$D_\mu = \partial_\mu - ig\vec{I}\cdot\vec{A}_\mu - ig'(\frac{Y}{2})B_\mu\,, \tag{2.3}$$

where g and g' are $SU(2)_L$ and $U(1)_Y$ gauge coupling constants, respectively. The Lagrangian in eq. (2.2) is invariant under the local gauge transformation on left- and right-handed fermion fields,

$$\psi_{L,R} \to U\psi_{L,R} = \exp\left\{ig\vec{I}\cdot\vec{\alpha}(x) + ig'(\frac{Y}{2})\beta(x)\right\}\psi_{L,R}\,, \tag{2.4}$$

where $\vec{\alpha}(x)$ and $\beta(x)$ are spacetime dependent gauge functions, as long as the gauge fields transform as

$$\vec{I}\cdot\vec{A}_\mu \to U\left[\vec{I}\cdot\vec{A}_\mu - \frac{i}{g}U^{-1}(\partial_\mu U)\right]U^{-1} \quad \text{and} \quad B_\mu \to B_\mu + \partial_\mu\beta(x)\,. \tag{2.5}$$

The Lagrangian $\mathcal{L}_{L+B}$ describes massless fermions and massless gauge bosons. Electromagnetic interactions are long-range and mediated by massless photons,

whereas weak interactions are known to be short-range, indicating massive force carrier particles. Explicit mass terms such as $\frac{1}{2}M^2 B_\mu B^\mu$ and $-m\bar{\psi}\psi$ cannot be added into the Lagrangian since they are not invariant under the gauge transformations. Instead, particle masses can be generated by the Higgs mechanism [17], which results from a spontaneous breaking of the gauge symmetry. It was shown by 't Hooft [18] in the early 1970's that if gauge boson masses are generated by the Higgs mechanism, the theory remains renormalizable.

To break the gauge symmetry spontaneously, and to generate masses for the gauge bosons and fermions, one introduces scalar fields, called Higgs fields, into the theory. The simplest possibility for such a field is a weak isospin doublet with the hypercharge value $Y = 1$:

$$\phi = \begin{pmatrix} \phi^+ \\ \phi^0 \end{pmatrix}, \tag{2.6}$$

where $\phi^+ \equiv (\phi_1 + i\phi_2)/\sqrt{2}$ and $\phi^0 \equiv (\phi_3 + i\phi_4)/\sqrt{2}$ are complex scalar fields. In order to generalize the Lagrangian of eq. (2.2) to include the Higgs doublet in such a way that the total Lagrangian $\mathcal{L} = \mathcal{L}_{L+B} + \mathcal{L}_H$ continues to be $SU(2)_L \times U(1)_Y$ invariant and renormalizable, the simplest choice that leads to a vacuum state with non-trivial charge is

$$\mathcal{L}_H = (D_\mu \phi)^\dagger (D^\mu \phi) - \mu^2 \phi^\dagger \phi - \lambda (\phi^\dagger \phi)^2 , \tag{2.7}$$

with real unknown parameters μ^2 and λ (> 0).

Because one of the gauge bosons, the photon, must remain massless, the $SU(2)_L \times U(1)_Y$ symmetry must be broken in such a way that the abelian symmetry $U(1)_{EM}$, corresponding the electromagnetic interactions, remains unbroken. To achieve this, the coefficient μ^2 is taken to be negative so that the potential $V = \mu^2 \phi^\dagger \phi + \lambda (\phi^\dagger \phi)^2$, and thus the total energy of the Higgs field, has a degenerate minimum at $|\phi|^2 = -\mu^2/2\lambda \equiv v^2/2$. The vacuum state can be chosen so that the Higgs field has the following vacuum expectation value:

$$\langle \phi \rangle_0 = \frac{1}{\sqrt{2}} \begin{pmatrix} 0 \\ v \end{pmatrix} . \tag{2.8}$$

The ground state is not invariant under the $SU(2)_L \times U(1)_Y$ gauge transformations. However, the gauge symmetry $U(1)_{EM}$, generated by $Q = I^3 + Y/2$, remains unbroken. Consequently, the electric charge is conserved and the photon remains massless.

For excitations above the vacuum, ϕ may be reduced to the form

$$\phi(x) = \frac{1}{\sqrt{2}} \begin{pmatrix} 0 \\ v + H(x) \end{pmatrix} , \tag{2.9}$$

where H is a real scalar field with $\langle H \rangle_0 = 0$. The gauge boson mass terms can then be identified in the Lagrangian $\mathcal{L}_H$ as follows:

$$(D_\mu \phi)^\dagger (D^\mu \phi) = (\frac{1}{2} v g)^2 W_\mu^+ W^{-\mu} + \frac{1}{8} v^2 (g^2 + g'^2) Z_\mu Z^\mu + \dots , \tag{2.10}$$

where $W^{\pm}_{\mu} = (A^1_{\mu} \mp iA^2_{\mu})/\sqrt{2}$, and in terms of the weak mixing angle $\theta_W = \tan^{-1}(g'/g)$,

$$\begin{aligned} Z^0_{\mu} &= -\sin\theta_W B_{\mu} + \cos\theta_W A^3_{\mu}, \\ A_{\mu} &= \cos\theta_W B_{\mu} + \sin\theta_W A^3_{\mu}\,. \end{aligned} \tag{2.11}$$

The following masses for the $W^{\pm}$ and Z^0 bosons can be extracted from eq. (2.10):

$$M_W = \frac{gv}{2} \quad \text{and} \quad M_Z = \frac{gv}{2\cos\theta_W}, \tag{2.12}$$

whereas A_{μ}, identified as the photon, is left massless. According to experimental data on gauge boson masses and the strength of electroweak interactions one has approximately $\sin^2\theta_W = 1 - M^2_W/M^2_Z \simeq 0.22$ and $v \simeq 246$ GeV.

The gauge couplings of leptons, given in eq. (2.2), obtain the following form when expressed in terms of the mass eigenstate gauge boson fields:

$$\mathcal{L}_{int} = ig(J^{\mu+}_W W^+_{\mu} + J^{\mu-}_W W^-_{\mu}) + i\frac{g}{\cos\theta_W} J^{\mu}_Z Z^0_{\mu} + ie j^{\mu}_{em} A_{\mu}\,, \tag{2.13}$$

where $g\sin\theta_W = g'\cos\theta_W$ has been identified as the electron charge e, and the charged, the neutral and the electromagnetic currents are given by

$$\begin{aligned} J^{\mu+}_W &= \frac{1}{\sqrt{2}}(\overline{\nu}_{eL}\gamma^{\mu}e_L + \overline{u}_L\gamma^{\mu}d_L)\,, \\ J^{\mu-}_W &= \frac{1}{\sqrt{2}}(\overline{e}_L\gamma^{\mu}\nu_{eL} + \overline{d}_L\gamma^{\mu}u_L)\,, \\ J^{\mu}_Z &= \overline{\nu}_{eL}\gamma^{\mu}(\frac{1}{2})\nu_{eL} + \overline{e}_L\gamma^{\mu}(-\frac{1}{2} + \sin^2\theta_W)e_L + \overline{e}_R\gamma^{\mu}(\sin^2\theta_W)e_R \\ &\quad + \overline{u}_L\gamma^{\mu}(\frac{1}{2} - \frac{2}{3}\sin^2\theta_W)u_L + \overline{u}_R\gamma^{\mu}(-\frac{2}{3}\sin^2\theta_W)u_R \\ &\quad + \overline{d}_L\gamma^{\mu}(-\frac{1}{2} + \frac{1}{3}\sin^2\theta_W)d_L + \overline{d}_R\gamma^{\mu}(\frac{1}{3}\sin^2\theta_W)d_R\,, \\ j^{\mu}_{em} &= \bar{e}\gamma^{\mu}(-1)e + \overline{u}\gamma^{\mu}(+\frac{2}{3})u + \overline{d}\gamma^{\mu}(-\frac{1}{3})d\,. \end{aligned} \tag{2.14}$$

The spontaneous breaking of the $SU(2)_L \times U(1)_Y$ symmetry also generates masses to the leptons and quarks via the so-called Yukawa couplings of the Higgs doublet ϕ. Let us now generalize the discussion to all three fermion families by denoting the family index with $l, k = 1, 2, 3$, so that for example $e^1_R = e_R$, $e^2_R = \mu_R$ and $e^3_R = \tau_R$. The Yukawa terms are given by

$$\begin{aligned} -\mathcal{L}_Y \;=\; & \sum_{l,k}\Big[h^{lk}_u(\overline{Q}^l_L\tilde{\phi}\,u^k_R + \overline{u}^k_R\tilde{\phi}^{\dagger}Q^l_L) + h^{lk}_d(\overline{d}^k_R\phi^{\dagger}Q^l_L + \overline{Q}^l_L\phi\,d^k_R) \\ & +\; h^{lk}_e(\overline{e}^k_R\phi^{\dagger}E^l_L + \overline{E}^l_L\phi\,e^k_R)\Big]\,, \end{aligned} \tag{2.15}$$

where h^{lk}'s are the Yukawa coupling constants and $\tilde{\phi} = i\sigma_2\phi^*$. After spontaneous symmetry breaking the following mass terms appear:

$$-\mathcal{L}_m = \sum_{l,k} \left[\overline{u}_L^l M_u^{lk} u_R^k + \overline{d}_L^l M_d^{lk} d_R^k + \overline{e}_L^l M_e^{lk} e_R^k + h.c. \right], \tag{2.16}$$

where $M_f^{lk} = h_f^{lk} v/\sqrt{2}$ $(f = u, d, e)$. As mentioned, neutrinos remain massless because the SM lacks right-handed neutrino fields ν_R.

The fields appearing in eq. (2.16) describe the states which are produced and destroyed in weak interaction processes. They are not necessarily the same states that describe the physical particles with a definite mass. To find the physical states, one has to diagonalize the mass matrices M_f, which can be done with a biunitary transformation:

$$V_f^\dagger M_f U_f = m_{diag}\,. \tag{2.17}$$

Two unitary matrices are needed since the mass matrix is in general not symmetric. Therefore, the mass matrices are diagonalized by redefining the left- and right-handed fields by

$$f_L^i = V_f^{ij} f_L'^j\,, \quad f_R^i = U_f^{ij} f_R'^j\,, \tag{2.18}$$

where $f'_{L,R}$'s describe physical states. The neutral and electromagnetic currents are diagonal in flavor basis, as can be seen from eqs. (2.14). The charged current is instead non-diagonal and therefore, in the quark sector, the so-called Cabibbo-Kobayashi-Maskawa (CKM) matrix $V_{CKM} = V_u^\dagger V_d$ [20, 21] appears in the interaction Lagrangian in the mass basis. According to general convention V_{CKM} is connected to the flavor eigenfields d, s, b and the mass eigenfields d', s', b' of the down-type quarks,

$$\begin{pmatrix} d \\ s \\ b \end{pmatrix} = V_{CKM} \begin{pmatrix} d' \\ s' \\ b' \end{pmatrix}, \tag{2.19}$$

leaving the up-type quarks transforming into themselves $u^i = u'^i$. The similar kind of matrix does not appear in the leptonic sector in the SM. This is because massless neutrino fields can always be redefined so that their interactions are diagonal as the interactions are the only way to identify massless neutrinos. Naturally, if the SM is modified to include right-handed neutrinos and neutrino masses, the V_{CKM}-type mixing matrix appears also in the lepton sector.

2.1.1 Number of neutrino flavors

The number of neutrino flavors has been deduced indirectly from the experimental study of Z boson, performed at the Large Electron-Positron (LEP) collider at CERN. From measurements of total cross section and forward-backward asymmetries one can determine the total width of the intermediate state, Γ_Z, as well as the partial decay widths corresponding to Z decays into hadrons (Γ_{hadrons})

and charged leptons (Γ_l). Partial decay width to neutrinos, Γ_ν, cannot be measured directly for obvious reasons, but the SM gives a very reliable prediction for the ratio $(\Gamma_\nu/\Gamma_l)_{\rm SM} = 1.991 \pm 0.001$ [22]. After subtracting the visible partial widths $\Gamma_{\rm hadrons}$ and Γ_l from the total width, one ends up with the invisible width, $\Gamma_{\rm inv}$, which is assumed to be due to N_ν light (masses less than $m_{Z^0}/2 \approx 45$ GeV) neutrino species. Each neutrino species contributes to $\Gamma_{\rm inv}$ by the value Γ_ν as given by the SM. The combined result for the number of light neutrino species from the four LEP experiments is given by [23]:

$$N_\nu = \frac{\Gamma_{\rm inv}}{\Gamma_l}\Big(\frac{\Gamma_l}{\Gamma_\nu}\Big)_{\rm SM} = 2.984 \pm 0.008\,. \tag{2.20}$$

Therefore, a fourth light neutrino with the standard interactions is excluded, indicating that there exists just three fermion families. This result is of crucial importance for neutrino physics and also for the considerations presented in this thesis. If nature contains more than three light neutrino flavors, the extra neutrinos must not couple to Z^0, at least not as strongly as the so-called active neutrino flavors ν_e, ν_μ and ν_τ. These kind of hypothetical particles, usually referred as *sterile* neutrinos, will be discussed in the later sections.

An independent upper limit for the number of neutrino types is given by the primordial nucleosynthesis argument in the Big Bang cosmology. For a given baryon to photon ratio, η, the expansion rate of the universe prior to nucleosynthesis can be deduced from the observed value of primordial ^{4}He abundance. The expansion rate, on the other hand, depends on the energy density contributed by light (mass $\ll$ MeV) particle species, usually quantified as the number of effective allowed neutrino species, N_ν^{eff}. Therefore, knowing the primordial ^{4}He abundance and determining η by separate analysis sets a bound on N_ν^{eff}. Using the value of η determined by the recent data from the Wilkinson Microwave Anisotropy Probe (WMAP) [8, 24] and the highest measured helium abundance with conservative errors the following upper limit on N_ν^{eff} (at 95 % C.L.) was obtained in ref. [9]:

$$N_\nu^{eff} < 3.4. \tag{2.21}$$

This bound is very important because it not only places an upper limit to the number of active neutrino species in thermal equilibrium, but it can also be used to constrain the possible active-sterile neutrino mixing parameters. Because sterile neutrinos do not have weak interactions with background matter, they decoupled from the thermal equilibrium early and thus contribute significantly less to N_ν^{eff} than active neutrino species. However, oscillations between active and sterile species, if they occur before the active species is decoupled, can bring sterile neutrinos, at least partly, back into thermal equilibrium, and thereby increase the expansion rate of the universe. This in turn would increase the amount of primordial ^{4}He. Also, oscillations between electron neutrino and sterile neutrino, taking place after electron neutrino has decoupled from thermal equilibrium, would

lead to depletion of the ν_e population. This affects the rates of the chemical equilibrium reactions of nucleons ($n + \nu_e \leftrightarrow p + e^-, n + e^+ \leftrightarrow p + \overline{\nu}_e$ and $n \leftrightarrow p + e^- + \overline{\nu}_e$) affecting the eventual neutron to proton ratio, which again has an effect on primordial helium abundance. Overall, the Big Bang Nucleosynthesis explanation of the light element abundances, and thus the constraint (2.21), yields rather stringent limits on active-sterile neutrino mixing, as was first discussed in refs. [25, 26]. To see how the bound (2.21) transforms into constraints on the active-sterile mixing parameters, one has to solve the appropriate quantum kinetic equations numerically (see e.g. [26, 27]).

The recent data on the cosmic microwave background (CMB) radiation from the WMAP experiment [8] and the large scale structure (LSS) from the 2 degree Field (2dF) Galaxy Redshift Survey power spectrum [28] places an upper limit for the radiation density present at the time of recombination (at the temperature $T = 0.3$ eV) which also translates into a limit on the effective number of neutrino species, N_ν^{eff}. According to ref. [11], the present constraint coming from CMB and LSS data (together with other cosmological data) is given by $N_\nu^{eff} = 4.0^{+3.0}_{-2.1}$ (at 95 % C.L.). If BBN data (light element measurements on ^{4}He and D) are taken into account, the bound is much tighter: $N_\nu^{eff} = 2.6^{+0.4}_{-0.3}$ (95 % C.L.) [11].

2.2 Description of neutrino mass

From the theoretical point of view massive neutrinos are more appealing objects than massless neutrinos. A naive argument for non-vanishing neutrino masses is the fact that all the other fermions do have masses. If one adds right-handed neutrinos into the SM, there are no symmetry principles forbidding neutrino mass terms, as already mentioned. Another theoretical reason for the existence of neutrino masses is that in grand unified theories (GUT), which unify the strong, electromagnetic and weak interactions, it is more natural to have massive than massless neutrinos [29]. For example, in the $SO(10)$ model massive neutrinos arise naturally since there quarks and leptons reside in the same irreducible representation and the mechanism which generates the quark masses automatically makes also neutrinos massive (see ref. [30]).

Theoretical arguments for neutrino masses are persuasive, but the decisive evidence for neutrino masses comes from the experimental side. The anomalous values of solar and atmospheric neutrino fluxes as well as the results from the terrestrial experiments LSND [31], KamLAND [32] and K2K [33] can be understood in terms of neutrino oscillations, which are possible only for massive neutrinos. Neutrino experiments will be discussed in Chapter 3. In the rest of the present chapter we will discuss different neutrino mass models, as well as implications of neutrino masses, i.e. neutrino mixing, lepton number violation and leptonic CP violation.

2.2.1 Dirac and Majorana mass terms

The minimal extension of the SM which includes the neutrino masses is achieved by adding the right-handed $SU(2)$ singlet fields $\nu_{eR}, \nu_{\mu R}$ and $\nu_{\tau R}$ into the theory. The Dirac mass term

$$\mathcal{L}^D = -\sum_{l,l'=e,\mu,\tau} \overline{\nu_{l'R}} M^D_{l'l} \nu_{lL} + \text{h.c.}, \tag{2.22}$$

similar to that of other fermions in eq. (2.16), is generated with a coupling to a Higgs field of the form (2.15), as a result of spontaneous symmetry breaking. The mass matrix M_D is a complex 3×3 matrix.

If the neutrino mass term is of the form (2.22), the total Lagrangian is invariant under global gauge transformations

$$\nu_{lL} \to e^{i\alpha} \nu_{lL}\,, \quad \nu_{lR} \to e^{i\alpha} \nu_{lR}\,, \quad l \to e^{i\alpha} l\,, \tag{2.23}$$

where α is a constant. This invariance means that the total lepton number $\sum_l L_l$ is conserved.

By redefining the left- and the right-handed components of the neutrino fields

$$\nu_{iL} = \sum_l U^\dagger_{il} \nu_{lL} \quad \text{and} \quad \nu_{iR} = \sum_l V^\dagger_{il} \nu_{lR}\,, \tag{2.24}$$

where U and V are the unitary matrices that diagonalize the mass matrix M_D by a biunitary transformation, the Dirac mass term can be rewritten in the diagonal form

$$\mathcal{L}^D = -\sum_{i=1}^{3} m_i \overline{\nu}_{iL} \nu_{iR} + \text{h.c.} = -\sum_{i=1}^{3} m_i \overline{\nu}_i \nu_i, \tag{2.25}$$

where ν_i's are the physical fields with definite non-negative masses m_i.

The Dirac mass term can in general include also left-handed sterile singlet fields ν_{sL} ($s = s_1, s_2, \ldots$) which do not enter in the standard CC and NC interactions but which do mix with the active neutrino flavors. In this case the neutrino mixing relation is given by

$$\nu_{\alpha L} = \sum_{i=1}^{3+n_s} U_{\alpha i} \nu_{iL}\,, \tag{2.26}$$

where $\alpha = e, \mu, \tau, s_1, \ldots$ and n_s is the number of sterile fields. Obviously, the Dirac mass terms involving left-handed sterile fields and right-handed singlet fields ν_{lR} are as such gauge invariant with no connection to the spontaneous symmetry breaking.

A mass Lagrangian of the form of eq. (2.22) is the only Lorentz invariant mass term possible for charged particles, but for neutrinos this is not the case. In addition to the Dirac mass terms there may also exist so-called Majorana mass

terms, which have the following form if there are only the three left-handed flavor fields ν_{lL} $(l = e, \mu, \tau)$ in the theory:

$$\mathcal{L}_L^M = -\frac{1}{2} \sum_{l,l'} \overline{(\nu_{l'L})^c}\, M_{l'l}^L\, \nu_{lL} + \text{h.c.} \tag{2.27}$$

Here M^L can be shown to be symmetric (see e.g. [34]) and $(\nu_{lL})^c = C\overline{\nu_{lL}}^T$ is the charge conjugate of ν_{lL}, where C is the unitary matrix of charge conjugation which fulfills the relations $C\gamma_\alpha^T C^{-1} = -\gamma_\alpha$, $C^\dagger = C^{-1}$ and $C^T = -C$. The Majorana mass term can exist also for sterile neutrinos (e.g. for right-handed $SU(2)$ singlets), but charged leptons cannot have Majorana type mass terms because these terms would violate the conservation of the electric charge. They also violate the conservation of the total lepton number, but because lepton number is not related to any gauge symmetry in the SM, it need not be conserved.

Because M^L is a symmetric complex matrix, it can be diagonalized with an unitary transformation $U^T M^L U = m_{diag}$, so that the left-handed components of the Majorana fields with definite mass, ν_i, are given by the mixing relation

$$\nu_{iL} = \sum_l U_{il}^\dagger \nu_{lL}\,, \tag{2.28}$$

and the Majorana mass term in diagonal form is given by

$$\mathcal{L}_L^M = -\frac{1}{2} \sum_{i=1}^{3} m_i \overline{(\nu_{iL})^c} \nu_{iL} + \text{h.c.} \tag{2.29}$$

Defining Majorana fields by

$$\nu_i = \nu_{iL} + (\nu_{iL})^c\,, \tag{2.30}$$

eq. (2.29) can be rewritten as

$$\mathcal{L}_L^M = -\frac{1}{2} \sum_{i=1}^{3} m_i \overline{\nu_i} \nu_i\,. \tag{2.31}$$

If the Majorana mass terms do not exist, the physical neutrinos are Dirac particles just like the other fermions, but in the presence of the Majorana mass terms they are so-called Majorana particles. The basic difference between Majorana and Dirac fields is that Dirac fields have four degrees of freedom, in other words they describe left- and right-handed particles and their antiparticles whereas Majorana fields have only two degrees of freedom corresponding to the two spin orientations of just one particle state. This is because Majorana fields are, in contrast with the Dirac fields, self-conjugated, which means that their field operators ν_i satisfy the Majorana condition[1]

$$(\nu_i)^c = \nu_i\,. \tag{2.32}$$

[1] Actually, the general definition of Majorana condition includes an arbitrary phase, $\chi^c = e^{i\phi}\chi$, but $\phi = 0$ can always be chosen by suitably defining the fermion field χ (see e.g. ref. [30]).

For Dirac neutrinos the CPT mirror image of a neutrino with negative helicity (ν_-) is an antineutrino with positive helicity ($\overline{\nu}_+$), whereas for Majorana neutrinos it is ν_+. This means that in the rest frame the CPT transformation simply reverses the spin of Majorana neutrinos. After a 180° rotation the neutrino turns back into its original state [35]. This is why one says that a Majorana neutrino is its own antiparticle.

It is important to note here that breaking the symmetry with the usual SM Higgs field does not create mass terms like (2.27). Nevertheless, these terms are not gauge invariant and therefore also they must be created by the Higgs mechanism. The scalar sector of the SM must hence be extended, for example by introducing a triplet Higgs field [36, 37]. The Majorana mass term for sterile neutrinos (e.g. for the right-handed $SU(2)$ singlets), on the other hand, can appear as bare mass terms.

2.2.2 Dirac-Majorana mass term

Let us consider a theory with the three flavor neutrino fields ν_{lL} and three singlet fields ν_{lR} with $l = e, \mu, \tau$. The most general Lorentz-invariant mass term, the so-called Dirac-Majorana mass term, has the form

$$\mathcal{L}^{D-M} = -\frac{1}{2}\overline{(n_L)^c} M^{D+M} n_L + \text{h.c.}\,, \tag{2.33}$$

where

$$M^{D+M} = \begin{pmatrix} M^L & (M^D)^T \\ M^D & M^R \end{pmatrix} \tag{2.34}$$

with the three complex 3×3 matrices M^L, M^D and M^R, and where the left-handed column vector n_L is defined as

$$n_L = \begin{pmatrix} \nu_L \\ (\nu_R)^c \end{pmatrix} \quad \text{with} \quad \nu_L = \begin{pmatrix} \nu_{eL} \\ \nu_{\mu L} \\ \nu_{\tau L} \end{pmatrix} \quad \text{and} \quad \nu_R = \begin{pmatrix} \nu_{eR} \\ \nu_{\mu R} \\ \nu_{\tau R} \end{pmatrix}. \tag{2.35}$$

The Dirac-Majorana mass matrix $\mathcal{M}$ is symmetric, and can be diagonalized, just like in the Majorana case, with an unitary transformation $\mathcal{M} = (U^\dagger)^T m_{diag} U^\dagger$. The mass term in the diagonal form can be written as

$$\mathcal{L}^{D-M} = -\frac{1}{2}\sum_{i=1}^{6} m_i \overline{\nu_i}\nu_i\,, \tag{2.36}$$

where

$$\begin{pmatrix} \nu_1 \\ \nu_2 \\ \vdots \end{pmatrix} = U^\dagger n_L + (U^\dagger n_L)^c\,. \tag{2.37}$$

The fields ν_i satisfy the Majorana condition, $(\nu_i)^c = \nu_i$ for $i = 1, 2, \ldots, 6$ and indeed, in general case of Dirac-Majorana mass term the mass eigenfields are Majorana fields.

In one-generation case the Dirac-Majorana mass matrix reduces to the form

$$M^{D+M} = \begin{pmatrix} m_L & m_D \\ m_D & m_R \end{pmatrix} . \tag{2.38}$$

If CP invariance is assumed, m_L, m_R and m_D are real-valued parameters (see e.g. ref. [34]) and in this case $\mathcal{M}$ can be diagonalized with an orthogonal matrix ($\mathcal{O}^T = \mathcal{O}^{-1}$):

$$\mathcal{O}^T M^{D+M} \mathcal{O} = m' , \tag{2.39}$$

where $m'_{ji} = m'_j \delta_{ji}$. The diagonalizing matrix can be parameterized as

$$\mathcal{O} = \begin{pmatrix} \cos\theta & \sin\theta \\ -\sin\theta & \cos\theta \end{pmatrix} , \tag{2.40}$$

and the mass eigenvalues are given by

$$\begin{aligned} m'_1 &= \frac{m_L + m_R}{2} - \frac{1}{2}\sqrt{4m_D + (m_L - m_R)^2} , \\ m'_2 &= \frac{m_L + m_R}{2} + \frac{1}{2}\sqrt{4m_D + (m_L - m_R)^2} , \end{aligned} \tag{2.41}$$

which are positive or negative depending on the values of $m_{L,R}$ and m_D. The mixing angle θ depends on the masses as follows:

$$\tan 2\theta = \frac{2m_D}{m_R - m_L} . \tag{2.42}$$

Since the physical masses are always non-negative, one introduces sign factors $\rho_i = \pm 1$, defined by $\rho_i = \mathrm{sign}(m'_i)$ so that $m'_i = \rho_i |m'| \equiv \rho_i m_i$, where m_i are the physical masses. These sign factors have a connection to the CP parities of Majorana neutrinos (see sec. 2.5.1). Defining $\tilde{m}$ matrix as $\tilde{m}_{ji} = m_j \delta_{ji}$, the diagonalizing relation (2.39) can be rewritten as [34]:

$$U^T M^{D+M} U = \tilde{m} , \tag{2.43}$$

where $U^\dagger = \sqrt{\rho}\, \mathcal{O}^T$ and ρ is a diagonal matrix $\rho_{ji} = \rho_j \delta_{ji}$. Therefore, the CP invariance implies that the neutrino mixing matrix satisfies $U^* = U\rho$.

2.2.3 See-saw mechanism

The present experimental upper bounds on neutrino masses indicate that neutrino masses are many orders of magnitude smaller than charged lepton and quark

masses. Understanding the reason for this mass hierarchy is an challenging theoretical problem for which the so-called see-saw mechanism [38] provides a compelling solution.

In the one-generation case the see-saw mass matrix is given in (2.38) with the mass hierarchy

$$m_R \gg m_D \gg m_L \,. \tag{2.44}$$

This kind of mass pattern arises if the Dirac mass m_D has the magnitude of the same order as the charged leptons, but the mass scale of the right-handed neutrino, m_R, provided by physics beyond the SM, is considerably larger than the electroweak scale ($\sim 100\,\mathrm{GeV}$). The value of the Majorana mass m_L is controlled by the fact that the vacuum expectation value of the $SU(2)_L$ triplet field $\overrightarrow{H}$, whose Yukawa coupling $\overline{(\nu_L)^c}\, i\sigma_2\, \vec{\sigma} \cdot \overrightarrow{H} \nu_L$ is the origin of this mass term, must be small compared with that of the doublet Higgs field, since otherwise the mass ratio $M_W^2/M_Z^2 \cos^2\theta_W = \rho$ would contradict with its experimental value.

If m_L is taken to be zero for simplicity, the physical masses are given by

$$m_1 \simeq \frac{m_D^2}{m_R} \quad \text{and} \quad m_2 \simeq m_R \,, \tag{2.45}$$

with the sign factors $\rho_1 = -1$ and $\rho_2 = 1$, respectively.

Because of the mass hierarchy in eq. (2.44), one of the neutrinos is much lighter and the other one much heavier than the charged leptons. Also, as can be seen from eq. (2.42), the mixing angle θ approaches zero, which implies that ν_L and $(\nu_R)^c$ are almost completely decoupled:

$$\nu_L \simeq -i\nu_{1L} \quad \text{and} \quad (\nu_R)^c \simeq \nu_{2L}, \tag{2.46}$$

and the Majorana fields ν_1 and ν_2 depend on fields ν_L and $(\nu_R)^c$ approximately by

$$\nu_1 \simeq i[\nu_L - (\nu_L)^c] \quad \text{and} \quad \nu_2 \simeq \nu_R + (\nu_R)^c \,. \tag{2.47}$$

In realistic situations one naturally has to generalize the treatment to three generations of neutrinos so that one ends up with the light SM neutrinos ν_e, ν_μ and ν_τ, at the expense of three heavy predominantly right-handed neutrinos. For a detailed description, see e.g. [37].

2.2.4 Pseudo-Dirac neutrino

The see-saw mechanism generates a large mass difference between the predominantly active ($\simeq \nu_L$) and the predominantly sterile ($\simeq \nu_R$) neutrino. In the so-called pseudo-Dirac scheme, first introduced by Wolfenstein [39], the situation is intrinsically different. The original pseudo-Dirac scheme concerned the mixing of two active neutrinos, described by the Majorana mass Lagrangian

$$\mathcal{L}_m = -\frac{1}{2}\overline{(\nu_L)^c}\mathcal{M}\nu_L + h.c. \,, \tag{2.48}$$

where

$$\nu_L = \begin{pmatrix} \nu_{eL} \\ \nu_{\mu L} \end{pmatrix} \quad \text{and} \quad \mathcal{M} = \begin{pmatrix} m_{ee} & m_{e\mu} \\ m_{e\mu} & m_{\mu\mu} \end{pmatrix} . \tag{2.49}$$

The eigenvalues of the mass matrix $\mathcal{M}$ can be read from eq. (2.41) by substituting $(m_L, m_R, m_D) = (m_{ee}, m_{\mu\mu}, m_{e\mu})$. If one assumes that $m_{ee} + m_{\mu\mu} = 0$ in (2.49) the physical masses of the two Majorana fields become degenerate,

$$m \equiv m_1 = m_2 = \sqrt{m_{e\mu}^2 + m_{\mu\mu}^2} \tag{2.50}$$

with $\rho_1 = -1$ and $\rho_2 = 1$, and the mass Lagrangian gets the form

$$\mathcal{L}_m = -\frac{1}{2} m(\overline{\nu_1}\nu_1 + \overline{\nu_2}\nu_2) , \tag{2.51}$$

where the fields ν_i are given by

$$\nu_i = \sqrt{\rho}\, \mathcal{O}^T \nu_L \, + (\sqrt{\rho})^* \, \mathcal{O}^T (\nu_L)^c \tag{2.52}$$

with a diagonal matrix $\sqrt{\rho} = \mathrm{diag}(\, i \,, 1\,)$ and the orthogonal matrix $\mathcal{O}$ which can be parameterized as in eq. (2.40). The fields ν_i clearly satisfy the Majorana condition $\nu_i^c = \nu_i$.

By defining a new field

$$\psi = \frac{1}{\sqrt{2}}(\nu_1 - i\nu_2), \tag{2.53}$$

which yields $\psi^c = (\nu_1 + i\nu_2)/\sqrt{2}$, one realizes that the mass Lagrangian can be written in the Dirac form

$$\mathcal{L}_m = -m\overline{\psi}\psi \, . \tag{2.54}$$

The field ψ is called the pseudo-Dirac neutrino field for the following reason. Considering only the lowest order mass matrix, field ψ appears to be a Dirac field. However, when one takes into account higher-order weak interaction corrections to the masses, the mass degeneracy between the fields ν_1 and ν_2 is removed and they do not any more combine into a single Dirac field ψ but appear as two separate Majorana fields [39].

One can also construct an one-generation version of the pseudo-Dirac neutrino by using the Dirac-Majorana mass matrix defined in eq. (2.38) and the fields

$$\nu = \begin{pmatrix} \nu_L \\ (\nu_R)^c \end{pmatrix} . \tag{2.55}$$

In this case ν_L is an active particle which takes part in the SM interactions, whereas ν_R (or $(\nu_R)^c$) is sterile.

Nowadays the term "pseudo-Dirac" usually refers to the situation where

$$m_{e\mu} \gg |m_{ee}|, |m_{\mu\mu}| \quad \text{or} \quad m_D \gg |m_L|, |m_R| \, . \tag{2.56}$$

This kind of mass pattern generates two nearly degenerate (in mass) Majorana neutrinos with masses

$$m_{1,2} \simeq m_{e\mu(D)} \mp \frac{m_{ee(L)} + m_{\mu\mu(R)}}{2} \,. \tag{2.57}$$

This case differs from the original pseudo-Dirac scheme in such a way that the constraint (2.56) fixes the mixing angle to $\theta \simeq \pi/4$, whereas in the original scheme the mixing angle can have any values.

In Paper III [40] we investigated the pseudo-Dirac mixing of left- and right-handed neutrinos assuming that the Majorana masses M_L and M_R are small compared with the Dirac mass M_D. As mentioned above, this scenario leads to close-to-maximal mixing between the Majorana pair of neutrinos with almost degenerate masses, and we considered the possibility that this mixing could explain the solar neutrino deficit (see Sec. 3.1) in terms of the so-called vacuum (VAC) solution (with $\Delta m^2 = m_2^2 - m_1^2 \simeq 10^{-10}\,\mathrm{eV}^2$) in such a way that the masses of other flavor neutrinos can be neglected. In such a case the effective Majorana mass $\langle m \rangle$, measured by the neutrinoless double beta decay ($0\nu\beta\beta$) experiments (see Sec. 2.4.1 and Sec. 3.4) is actually M_L, and therefore a negative result in search for $0\nu\beta\beta$ gives an upper bound for M_L. Also a lower bound for M_L is easily derived by making very general assumptions about the Majorana mass generation mechanism. A closed bound on M_L yields a closed bound of different order of magnitude on M_D because of the relation $\Delta m^2 = 2M_D(M_L + M_R)$, which follows from the pseudo-Dirac mass ordering. A consistent scenario for the pure $\nu_e \leftrightarrow \nu_s$ vacuum oscillation is achieved with $M_L, M_R \simeq 10^{-7}$ eV and $M_D \simeq 10^{-5} - 10^{-4}$ eV. Unfortunately the sensitivities of the planned future $0\nu\beta\beta$ experiments are many orders of magnitude above $\langle m \rangle \simeq 10^{-7}$ eV. On the other hand, if the future experiments do observe a positive signal for $0\nu\beta\beta$, the pseudo-Dirac scenario cannot explain the solar neutrino anomaly in terms of VAC oscillations.

2.2.5 Neutrino masses in models with extra dimensions

In the see-saw mechanism a large right-handed Majorana mass m_R, which is usually assumed to have values from $\sim 10^{10}\,\mathrm{GeV}$ to $10^{15}\,\mathrm{GeV}$, suppresses the mass eigenvalues leading to $m_\nu \sim m_{fermion}^2/m_R$. This super-heavy mass scale does not fit into models with large extra dimensions in which the fundamental scale of quantum gravity, M_f, can be as small as $\mathcal{O}(\mathrm{TeV})$ and there does not naturally exist any larger mass scale. However, small neutrino masses, both in Dirac and Majorana cases, do have explanations also in high-dimensional models, and in these models small mass terms arise naturally also for sterile neutrinos [41, 42].

In models with large extra dimensions the weakness of the gravitational force is explained by its spread into n (≥ 2) new space dimensions. All the SM particles are spatially localized on a 3-dimensional wall, the so-called 3-brane, embedded in the bulk of n large extra dimensions, while gravitons and other particles which are

singlets under the SM symmetry group can freely propagate in the bulk. Dirac neutrino masses are naturally small if they arise from a coupling between a left-handed neutrino on the 3-brane and a right-handed bulk neutrino (or any SM singlet bulk fermion). This is because generally the couplings between the the Higgs field on the 3-brane, h, the bulk neutrino (denoted here as ν_R) and the brane neutrino (ν_L) are suppressed by the volume of the extra dimensions, V_n, and have the form [42]:

$$\frac{1}{\sqrt{M_f^N V_n}}\, h\, \overline{\nu}_L \nu_R\,, \tag{2.58}$$

where $V_n = R_1 R_2 \ldots R_N$, and R_i is the size of the i - compact extra dimension. To understand where the coefficient comes from, let us consider the model with one extra dimension y. The interaction term between neutrinos and the Higgs fields is given by

$$S = \int d^4x dy\, \kappa\, (\phi^0(x))^* \overline{\nu}_L \nu_R(x,y)\delta(y)\,, \tag{2.59}$$

where ϕ^0 the neutral component of $SU(2)$ doublet Higgs field and κ is a dimensional Yukawa coupling. As the right-handed bulk neutrinos are Fourier expanded (the Kaluza-Klein expansion)

$$\nu_R(x,y) = \sum_n \frac{1}{\sqrt{2\pi R}} \nu_{Rn}(x) e^{iny/R}\,, \tag{2.60}$$

and by setting $\langle \phi^0 \rangle = v/\sqrt{2}$, we see that the interaction term generates a Dirac mass term between ν_L and the zero mode ν_{R0}, which is suppressed by the size of the extra dimension,

$$m_D = \kappa \frac{v}{\sqrt{2R}}\,. \tag{2.61}$$

The form of $\kappa = \kappa'/\sqrt{M_f}$, where κ' is a dimensionless constant, is determined by dimensional analysis and by the fact that M_f is the only natural mass scale in the theory.

By Gauss' law the volume V_n is related to the fundamental Planck scale in $4+n$ dimensions, M_f, and to the observed (reduced) Planck scale, $M_P = (4\pi G_N)^{-1/2} = 3.4 \cdot 10^{18}\,\mathrm{GeV}$, where G_N is the Newton constant, by [43]

$$M_P = M_f \sqrt{M_f^N V_N}\,. \tag{2.62}$$

Therefore the Dirac mass equals to

$$m_D = \frac{\kappa' v\, M_f}{\sqrt{2} M_P} = 3 \cdot 10^{-16}\, \frac{\kappa' v\, M_f}{\sqrt{2}\mathrm{TeV}}\,. \tag{2.63}$$

Inserting $v/\sqrt{2} = 174\,\mathrm{GeV}$ and assuming, for instance, that $M_f \simeq 1\,\mathrm{TeV}$ and $\kappa' = 1$, neutrino mass gets the value $m_D \simeq 5 \cdot 10^{-5}$ eV.

One can write kinetic terms also for the bulk neutrinos, and after Fourier expanding the bulk neutrino fields and integrating over the fifth coordinate y the following Dirac mass terms appear [41, 42]:

$$\sum_{k=-\infty}^{+\infty} m_k \overline{\nu}_{kR} \nu_{kL} + \text{h.c.}\,, \quad m_k \equiv \frac{k}{R}\,. \tag{2.64}$$

In n dimensions the masses of the Kaluza-Klein states in given by [42]

$$m_{k_1,k_2,\ldots,k_n} = \sqrt{\sum_i \frac{k_i^2}{R_i^2}}\,. \tag{2.65}$$

Also small Majorana masses can be generated with different methods in models with extra dimensions (see e.g. ref. [41]).

2.3 Neutrino mixing and oscillations

According to the neutrino mixing hypotheses the flavor neutrino fields ν_l, identified through their charged current interactions, are unitary superpositions of the mass eigenfields ν_i,

$$\nu_{lL} = \sum_{i=1}^{3+n_s} U_{li} \nu_{iL}\,, \tag{2.66}$$

where $l = e, \mu, \tau$ and $i = 1, 2, \ldots, 3 + n_s$ with n_s indicating the number of the possible sterile neutrino species. In the mass eigenfield basis the charged current terms for neutrinos can be written as

$$\mathcal{L}_{int}^{cc} = \frac{ig}{\sqrt{2}} \sum_{l,i} \overline{l}_L \gamma^\mu U_{li} \nu_{iL} W_\mu^- + \text{h.c.} \tag{2.67}$$

The unitary mixing matrix U can be parameterized with rotation angles and phase factors. The phase factors generate, just like in the quark sector, CP violation in neutrino interactions (see Sec. 2.5). Some of the phases in the most general unitary mixing matrix are unphysical since they can be absorbed into the field redefinitions. The Majorana condition $\chi^c = \eta\chi$, however, does not allow phases to be absorbed into Majorana neutrino fields[2]. In general, the number of the CP violating phases depends both on the nature of neutrinos and on the number of neutrino flavors. In the case of N flavors, the mixing matrix of Majorana neutrinos contains $N(N-1)/2$ physical phases, but that of Dirac only $(N-1)(N-2)/2$ phases. Obviously, the number of rotation angles, $N(N-1)/2$, is the same in both cases.

[2]To be precise, phases can be absorbed to the Majorana fields, but in that case they are hidden in the Majorana condition for the modified Majorana fields and nonetheless have physical implications [44].

The most general unitary 3×3 matrix can be parameterized with 3 angles and 6 phases, for example in the following way:

$$U_{3\times 3} = P_2 R_{23} R_{13} P_1 R_{12} P_3 \,, \tag{2.68}$$

where R_{ij} are real rotation matrices with Euler angles θ_{ij} describing the rotations on the ij-plane,

$$R_{23} = \begin{pmatrix} 1 & 0 & 0 \\ 0 & c_{23} & s_{23} \\ 0 & -s_{23} & c_{23} \end{pmatrix}, R_{13} = \begin{pmatrix} c_{13} & 0 & s_{13} \\ 0 & 1 & 0 \\ -s_{13} & 0 & c_{13} \end{pmatrix}, R_{12} = \begin{pmatrix} c_{12} & s_{12} & 0 \\ -s_{12} & c_{12} & 0 \\ 0 & 0 & 1 \end{pmatrix}, \tag{2.69}$$

where $c_{ij} = \cos\theta_{ij}$ and $s_{ij} = \sin\theta_{ij}$, and P_i are diagonal phase matrices

$$P_1 = \begin{pmatrix} 1 & 0 & 0 \\ 0 & e^{i\alpha} & 0 \\ 0 & 0 & 1 \end{pmatrix}, P_2 = \begin{pmatrix} 1 & 0 & 0 \\ 0 & e^{i\beta_2} & 0 \\ 0 & 0 & e^{i\beta_3} \end{pmatrix}, P_3 = \begin{pmatrix} e^{i\gamma_1} & 0 & 0 \\ 0 & e^{i\gamma_2} & 0 \\ 0 & 0 & e^{i\gamma_3} \end{pmatrix}. \tag{2.70}$$

The parameterization (2.68) is equivalent to [45]

$$U_{3\times 3} = P U_{23} U_{13} U_{12} \,, \tag{2.71}$$

where $P = P_1 P_2 P_3$ and

$$U_{23} = \begin{pmatrix} 1 & 0 & 0 \\ 0 & c_{23} & \tilde{s}_{23}^* \\ 0 & -\tilde{s}_{23} & c_{23} \end{pmatrix}, U_{13} = \begin{pmatrix} c_{13} & 0 & \tilde{s}_{13}^* \\ 0 & 1 & 0 \\ -\tilde{s}_{13} & 0 & c_{13} \end{pmatrix}, U_{12} = \begin{pmatrix} c_{12} & \tilde{s}_{12}^* & 0 \\ -\tilde{s}_{12} & c_{12} & 0 \\ 0 & 0 & 1 \end{pmatrix} \tag{2.72}$$

with the definitions $\tilde{s}_{ij} = \sin\theta_{ij} e^{i\delta_{ij}}$ and

$$\begin{aligned} \delta_{12} &= \gamma_1 - \gamma_2, \\ \delta_{13} &= \gamma_1 - \gamma_3, \\ \delta_{23} &= \alpha + \gamma_2 - \gamma_3. \end{aligned} \tag{2.73}$$

The phase factor P may always be removed by a charged lepton phase rotation, and therefore the 3×3 neutrino mixing matrix, i.e. the so-called Maki-Nakagawa-Sakata matrix [7], can be parameterized in the following way:

$$U_{MNS} = U_{23} U_{13} U_{12} \tag{2.74}$$

$$= \begin{pmatrix} c_{13}c_{12} & c_{13}s_{12}e^{-i\delta_{12}} & s_{13}e^{-i\delta_{13}} \\ -c_{23}s_{12}e^{i\delta_{12}} & c_{23}c_{12} & c_{13}s_{23}e^{-i\delta_{23}} \\ -s_{13}s_{23}c_{12}e^{i(\delta_{13}-\delta_{23})} & -s_{13}s_{23}s_{12}e^{i(\delta_{13}-\delta_{12}-\delta_{23})} & \\ s_{23}s_{12}e^{i(\delta_{23}+\delta_{12})} & -s_{23}c_{12}e^{i\delta_{23}} & c_{13}c_{23} \\ -s_{13}c_{23}c_{12}e^{i\delta_{13}} & -s_{13}c_{23}s_{12}e^{i(\delta_{13}-\delta_{12})} & \end{pmatrix}.$$

In the Majorana case all the three irremovable phases δ_{ij} are physical. The Dirac phase, which appears for example in oscillation probabilities, is in this parameterization given by

$$\delta = \delta_{13} - \delta_{23} - \delta_{12}\,. \tag{2.75}$$

The parameterization (2.74) can be easily generalized for four neutrino mixing [46]:

$$U_{4\times4} = U_{23}U_{13}U_{03}U_{12}U_{02}U_{01}\,, \tag{2.76}$$

where

$$U_{01} = \begin{pmatrix} c_{01} & \tilde{s}^*_{01} & 0 & 0 \\ -\tilde{s}_{01} & c_{01} & 0 & 0 \\ 0 & 0 & 1 & 0 \\ 0 & 0 & 0 & 1 \end{pmatrix}. \tag{2.77}$$

This parameterization of the $U_{4\times4}$ mixing matrix has been used in Paper I [47] and Paper II [48] of this thesis, where we have studied the effects of the CP-phases for long-baseline neutrino oscillations and neutrinoless double beta decay in the presence of a fourth neutrino.

2.3.1 Neutrino oscillations in vacuum

Neutrino oscillation, analogous to the for long known $K^0 - \overline{K}^0$ oscillation, is a quantum mechanical phenomenon that is a consequence of neutrino mixing. The idea of neutrino oscillations dates back to late 1950's when it was first discussed by Pontecorvo [6].

As the one-neutrino state $|\nu_\alpha\rangle$ is created by the field operator $\nu^\dagger_\alpha$, it follows from eq. (2.66) that the state vector of the flavor neutrino ν_α produced in the weak interaction is the following superposition of the state vectors of the physical particles ν_k with definite masses m_k:

$$|\nu_\alpha\rangle = \sum_k U^*_{\alpha k}\,|\nu_k\rangle\,. \tag{2.78}$$

For antineutrinos the unitary matrix U^* is replaced with its complex conjugate U. A neutrino created in a weak interaction process is one of the flavour states but it propagates as a superposition of mass states.

One can assume that the 3-momenta $\vec{p}$ of different beam components are the same, but the difference in masses leads to difference in their energies according to the relativistic energy-momentum relation

$$E_k = \sqrt{p^2 + m_k^2} \simeq p + \frac{m_k^2}{2p}\,, \tag{2.79}$$

where $p = |\vec{p}|$ and the approximation is valid if $m_k \ll p$, i.e. if neutrinos are extremely relativistic. The flavor neutrino states evolve in time as

$$|\nu_\alpha\rangle_t = e^{-iH_0 t}\,|\nu_\alpha\rangle\,, \tag{2.80}$$

where $|\nu_\alpha\rangle$ is the state vector at the initial moment of time $t = 0$ and H_0 is the free Hamiltonian:

$$H_0 \, |\nu_k\rangle = E_k \, |\nu_k\rangle \, . \tag{2.81}$$

From the above equations it follows that

$$|\nu_\alpha\rangle_t = \sum_k e^{-iE_k t} U^*_{\alpha k} \, |\nu_k\rangle \, , \tag{2.82}$$

and by using the unitarity of the matrix U, the time dependent state vectors $|\nu_\alpha\rangle_t$ can be expressed as superpositions of states $|\nu_\alpha\rangle$:

$$|\nu_\alpha\rangle_t = \sum_{\alpha'=e,\mu,\tau,\ldots} |\nu_{\alpha'}\rangle \sum_k U_{\alpha' k} \, e^{-iE_k t} \, U^*_{\alpha k} \, , \tag{2.83}$$

from which the probability amplitude for the transition $\nu_\alpha \to \nu_{\alpha'}$ can be inferred:

$$a(\nu_\alpha \to \nu_{\alpha'})(t) = \langle \nu_{\alpha'} | \nu_\alpha \rangle_t = \sum_k U_{\alpha' k} \, e^{-iE_k t} \, U^*_{\alpha k} \, . \tag{2.84}$$

After the relativistic approximation of eq. (2.79) is made, the corresponding transition probability reads

$$P(\nu_\alpha \to \nu_{\alpha'}) = |\langle \nu_{\alpha'} | \nu_\alpha \rangle_t|^2 = | \sum_k U_{\alpha' k} e^{-i\Delta m^2_{k1} \frac{L}{2E}} U^*_{\alpha k} \, |^2 \, , \tag{2.85}$$

where $\Delta m^2_{k1} \equiv m^2_k - m^2_1$. The time of flight ($t$) has been replaced with the distance between the source and the detector (L), and the momentum is approximated with the neutrino energy, $p \approx E$, which both are valid only for highly relativistic neutrinos.

In practical situations there is often effectively only two neutrino flavors oscillating. In that case the transition probability is given by

$$\begin{aligned} P(\nu_\alpha \to \nu_{\alpha'}) &= 2 \, |U_{\alpha' 2}|^2 |U_{\alpha 2}|^2 \Big[1 - \cos\Big(\Delta m^2 \frac{L}{2E} \Big) \Big] \\ &= \sin^2(2\theta) \sin^2 \Big(1.27 \frac{\Delta m^2(\mathrm{eV}^2) L(\mathrm{km})}{E(\mathrm{GeV})} \Big) \, , \end{aligned} \tag{2.86}$$

and the survival probability reads as

$$P(\nu_\alpha \to \nu_\alpha) = 1 - \sin^2(2\theta) \sin^2 \Big(1.27 \frac{\Delta m^2(\mathrm{eV}^2) L(\mathrm{km})}{E(\mathrm{GeV})} \Big) \, , \tag{2.87}$$

where θ is the mixing angle and $\Delta m^2 = m^2_2 - m^2_1$ is the mass-squared difference of the two mass eigenstates. Using the oscillation length defined as $L_{\mathrm{osc}} = 4\pi E / \Delta m^2$, the oscillating part of the probabilities can be written as

$$\sin^2 \Big(\frac{\Delta m^2 L}{4E} \Big) = \sin^2 \Big(\frac{L}{L_{\mathrm{osc}}} \pi \Big) \, . \tag{2.88}$$

It is important to note that an oscillation experiment is sensitive to a given value of Δm^2 only if the distance between the neutrino production and detection points L, the baseline, is of the order of the oscillation length $L_{\rm osc}$, which corresponds to $E/L \sim \Delta m^2$. If the baseline is much shorter than the oscillation length, oscillations do not have time to develop and the transition probability vanishes. If, on the other hand, the baseline is much longer than the oscillation length, $L >> L_{\rm osc}$, oscillating behavior disappears due to averaging over neutrino spectrum and the uncertainty of the baseline length, and one ends up with averaged transition and survival probabilities, $\widehat{P}(\nu_\alpha \to \nu_{\alpha'}) = \frac{1}{2}\sin^2(2\theta)$ and $\widehat{P}(\nu_\alpha \to \nu_\alpha) = 1 - \frac{1}{2}\sin^2(2\theta)$, respectively.

It is also worth noting that the usual derivation of the standard oscillation formula (2.85), described in this section, raises some questions (see e.g. [49]). For example, is it correct to assume that all the mass eigenstates $|\nu_i\rangle$ have the same momenta? Or, how can one replace time t with distance L/c, even though in the simple plane wave approach the wave has infinite space extent? It turns out that the proper treatment with the wave packet formalism [50] or alternatively in the framework of quantum field theory [49, 51] leads, in practical terms, to the same results as those presented in this section.

2.3.2 Matter enhanced oscillations

What was described in the previous section applies only to neutrinos propagating in vacuum. In practical situations, however, neutrinos often travel in a medium. For example solar neutrinos travel a long distance in solar matter, and before detection also through the Earth.

In a medium neutrinos interact with matter particles, which affects their propagation. Coherent interactions generate an additional effective potential energy, $V_e = V_{CC} + V_{NC}$, which is determined by the forward elastic scatterings due to weak charged current (V_{CC}) and neutral current (V_{NC}) interactions [52]. Because the ordinary medium is composed of electrons, protons and neutrons, but not of muons and taus, ν_e's are affected differently by the medium than ν_μ's and ν_τ's: electron neutrino "feels" both V_{CC} and V_{NC}, but ν_μ and ν_τ feel only the latter, as depicted in Fig. (2.1). Sterile neutrinos lack all interactions with the SM particles and hence their propagation is not affected by the medium.

It must be emphasized that in the coherent interactions the medium remains unchanged so that the original unscattered neutrino wave function and the scattered one interfere with each other. In that respect the word "scattering" is misleading. An analogue to the situation is a photon which obtains an effective mass in matter. The incoherent effects, which damp the oscillation, can in most cases be neglected since they are proportional to the total cross section of the neutrino in the medium, and thus G_F^2, whereas coherent effects are proportional to G_F (see ref. [37]).

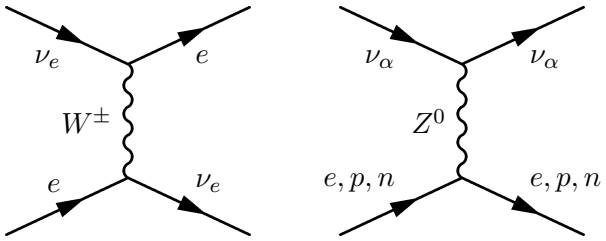

Figure 2.1: Feynman diagrams describing neutrino interactions with matter particles. W-exchange induced scattering from an electron is possible only for ν_e, whereas Z-exchange induced scattering from an electron, proton or neutron is possible for $\nu_\alpha = \nu_e$, ν_μ and ν_τ.

The potentials V_{CC} and V_{NC} are given by [37]

$$V_{CC} = \sqrt{2}\, G_F n_e \quad \text{and} \quad V_{NC} = -\frac{G_F}{\sqrt{2}} n_n \,, \tag{2.89}$$

where n_e and n_n are the electron and neutron number densities in the medium. The effect of protons and electrons cancel each other in V_{NC} if the medium is electrically neutral.

Restricting the discussion to two-neutrino oscillations, the evolution equation in vacuum for the two mass eigenstates ν_1 and ν_2 can be written as

$$i\frac{d}{dt}\begin{pmatrix}\nu_1(t)\\ \nu_2(t)\end{pmatrix} = H\begin{pmatrix}\nu_1(t)\\ \nu_2(t)\end{pmatrix}, \tag{2.90}$$

where the diagonal Hamiltonian H is

$$H = \begin{pmatrix}E_1 & 0\\ 0 & E_2\end{pmatrix} \simeq p + \begin{pmatrix}m_1^2/2p & 0\\ 0 & m_2^2/2p\end{pmatrix}. \tag{2.91}$$

In flavor basis eq. (2.90) is given by

$$i\frac{d}{dt}\begin{pmatrix}\nu_e(t)\\ \nu_\mu(t)\end{pmatrix} = H_f\begin{pmatrix}\nu_e(t)\\ \nu_\mu(t)\end{pmatrix}, \tag{2.92}$$

where, by using the 2×2 mixing matrix of eq. (2.40), the Hamiltonian H_f reads

$$H_f = UHU^\dagger = p + \frac{m_1^2+m_2^2}{4p} + \frac{\Delta m_{21}^2}{4p}\begin{pmatrix}-\cos 2\theta_V & \sin 2\theta_V\\ \sin 2\theta_V & \cos 2\theta_V\end{pmatrix}. \tag{2.93}$$

Subtracting diagonal matrix $(\Delta E)I$ changes the eigenvalues of H_f by $E_i \to E_i - \Delta E$, and the probability amplitude of eq. (2.84) gets multiplied by a phase factor $\exp[i(\Delta E)t]$. This has no physical effect since one measures the oscillation

probability, $P_{\nu_\alpha \to \nu_\beta}(L/E) = |a_{\nu_l \to \nu_{l'}}(t)|^2$, not the amplitude itself. Thus one has the effective Hamiltonian

$$H'_f = \frac{\Delta m^2_{21}}{4E} \begin{pmatrix} -\cos 2\theta_V & \sin 2\theta_V \\ \sin 2\theta_V & \cos 2\theta_V \end{pmatrix} , \tag{2.94}$$

where the approximation $p \simeq E$ is made.

Neutral current interactions are flavor diagonal and flavor independent, and thus they contribute to the effective Hamiltonian only by a multiple of an identity matrix. So they do not affect the oscillation probability. It is convenient to add the contribution due to the charged current interactions in a symmetric form [29], so that the Hamiltonian for propagation in the medium can be written as

$$\begin{aligned} H_M &= H'_f + \frac{G_F}{\sqrt{2}} n_e \begin{pmatrix} 1 & 0 \\ 0 & -1 \end{pmatrix} \\ &= \frac{\Delta M^2_{21}}{4E} \begin{pmatrix} -\cos 2\theta_M & \sin 2\theta_M \\ \sin 2\theta_M & \cos 2\theta_M \end{pmatrix} , \end{aligned} \tag{2.95}$$

where the effective mass squared difference ΔM^2_{21} and the effective mixing angle θ_M in the medium are given by

$$\begin{aligned} \Delta M^2_{21} &= \Delta m^2_{21} \sqrt{\sin^2 2\theta_V + (\cos 2\theta_V - A)^2} , \\ \sin^2 2\theta_M &= \frac{\sin^2 2\theta_V}{\sin^2 2\theta_V + (\cos 2\theta_V - A)^2} \end{aligned} \tag{2.96}$$

with the definition

$$A \equiv \frac{2\sqrt{2} G_F n_e E}{\Delta m^2_{21}} . \tag{2.97}$$

Thus the effective mixing angle in matter can be maximal, $\theta_M = \pi/4$ (which corresponds to $\cos 2\theta_V = A$), even if the vacuum mixing angle θ_V is small. In the case neutrino is propagating in a medium with varying density this may lead to an enhanced transition between neutrino flavors. This so-called Mikheyev-Smirnov-Wolfenstein effect [52, 53] seems to play an important role in the oscillations of solar neutrinos.

2.4 Lepton number violating processes

Individual lepton numbers are defined so that for single-particle states the electron number $L_e = +1$ (-1) is assigned for e^- and ν_e (e^+ and $\overline{\nu}_e$) and $L_e = 0$ for all other particles. For any state the electron number is defined by

$$L_e = N(e^-) - N(e^+) + N(\nu_e) - N(\overline{\nu}_e) , \tag{2.98}$$

where $N(e^-)$ is the number of electrons present and so on. The muon number L_μ and the tau number L_τ are defined analogously. The total lepton number is given by

$$L = L_e + L_\mu + L_\tau \,. \tag{2.99}$$

In the SM the three lepton numbers, L_e, L_μ and L_τ, are conserved separately. The observed neutrino oscillations clearly break the conservation of individual lepton numbers, and if neutrinos turn out to be Majorana particles, even the total lepton number is not conserved.

Except for neutrino oscillations, all the experimental data so far is consistent with the conservation of the three separate lepton numbers. Experiments trying to find indications of lepton number violation have studied for example[3] conversion of one charged-lepton type to another. The best limits for purely leptonic processes are on $\mu \to e\gamma$ and $\mu \to 3e$ (at 90 % C.L.) [22]:

$$\Gamma(\mu^- \to e^-\gamma) \,/\, \Gamma(\mu^- \to \text{all}\,) \,<\, 1.2 \times 10^{-11}, \tag{2.100}$$

$$\Gamma(\mu^- \to e^- e^+ e^-) \,/\, \Gamma(\mu \to \text{all}\,) \,<\, 1.0 \times 10^{-12}. \tag{2.101}$$

Also kaon decays yield very stringent limits on the following processes (at 90% C.L.):

$$\Gamma(K_L^0 \to e^\pm \mu^\mp) \,/\, \Gamma(K_L^0 \to \text{all}\,) \,<\, 4.7 \times 10^{-12} \tag{2.102}$$

$$\Gamma(K^+ \to \pi^+ e^- \mu^+) \,/\, \Gamma(K^+ \to \text{all}\,) \,<\, 2.8 \times 10^{-11}. \tag{2.103}$$

The most promising process for testing the total lepton number conservation is the neutrinoless double beta decay of the nuclei, which is the topic of the next section.

2.4.1 Neutrinoless double beta decay

Two-neutrino double beta decay ($2\nu\beta\beta$) is a process in which a nucleus emits two electrons and two neutrinos, so that the charge number Z of the nucleus changes by two units:

$$(Z, A) \to (Z + 2, A) + 2\, e^- + 2\, \overline{\nu}_e \,. \tag{2.104}$$

The decay occurs very rarely because it is a second order weak interaction process the decay width being proportional to G_F^2. Nevertheless, lepton numbers are conserved in the $2\nu\beta\beta$ process and it has been observed in several experiments [22].

More interesting processes from the neutrino physics point of view are those in which the two electrons are emitted without being accompanied by neutrinos:

$$(Z, A) \to (Z + 2, A) + 2\, e^- \,. \tag{2.105}$$

[3] For a complete list of experimental results, see ref. [22].

Such processes would violate the total lepton number conservation and therefore, if neutrinos are considered to be massive, they can take place only if neutrinos are Majorana particles. Indeed, if neutrinoless double beta decay process was observed, the long-standing question whether neutrinos are Dirac or Majorana particles could most likely finally be settled.

In what follows we will discuss the standard neutrinoless double beta decay process ($0\nu\beta\beta$), depicted by the Feynman diagram in picture 2.2, and other possibilities, for example Majoron emitting neutrinoless double beta decay process, will not be considered.

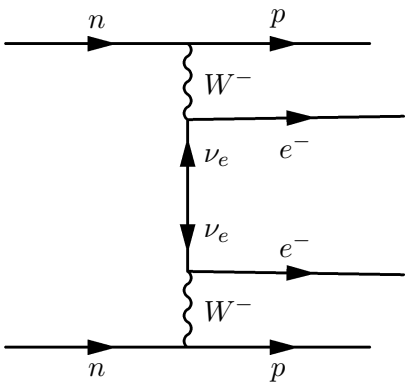

Figure 2.2: Feynman diagram for the standard $0\nu\beta\beta$ process.

As explained in Sec. 2.2.1, diagonalization of the Majorana mass Lagrangian yields mass eigenstate neutrinos of the form

$$\nu_k = \sum_l (U^\dagger_{kl}\nu_{lL} + U^T_{kl}(\nu_{lL})^c)\,, \tag{2.106}$$

and hence the electron neutrino exchanged in the $0\nu\beta\beta$ process is generally a superposition of the mass eigenstates,

$$\nu_{eL} = \sum_k U_{ek}\nu_{kL}\,. \tag{2.107}$$

The Hamiltonian density of the charged current interaction is therefore given by

$$H_{cc} = \frac{g}{2\sqrt{2}}\,W^-_\mu \sum_k i\,\overline{e}\gamma_\mu(1-\gamma_5)U_{ek}\nu_k + \frac{g}{2\sqrt{2}}\,W^+_\mu \sum_k i\,\overline{\nu}_k\gamma_\mu(1-\gamma_5)U^*_{ek}\,e\,, \tag{2.108}$$

and the lepton part of the $0\nu\beta\beta$ amplitude arises from the second-order term

$$\sum_k U^2_{ek}[\overline{e}(x)\gamma^\mu(1-\gamma_5)\nu_k(x)][\overline{e}(y)\gamma_\mu(1-\gamma_5)\nu_k(y)]\,. \tag{2.109}$$

After a slight manipulation the latter current can be written as

$$\overline{e}\gamma_\mu(1-\gamma_5)\nu_k \;\; = \;\; \overline{(e^c)^c}\,\gamma_\mu(1-\gamma_5)(\nu^c_k)^c$$

$$
\begin{aligned}
&= -(e^c)^T C^{-1}\gamma_\mu(1-\gamma_5)\, C(\overline{\nu_k^c})^T \\
&= -(e^c)^T[-\gamma_\mu(1+\gamma_5)]^T(\overline{\nu_k^c})^T \\
&= -\overline{\nu_k^c}\,\gamma_\mu(1+\gamma_5)e^c \\
&= -\overline{\nu}_k\,\gamma_\mu(1+\gamma_5)e^c\,, \qquad (2.110)
\end{aligned}
$$

where the Majorana condition $\nu_k^c = \nu_k$ and the following properties of the charge conjugation and the charge conjugation matrix C were used:

$$
\begin{aligned}
\psi^c &= C\overline{\psi}^T\,, \qquad & \overline{\psi^c} &= -\psi^T C^{-1}\,, \\
C^{-1}\gamma_\mu C &= -\gamma_\mu^T\,, \qquad & C^{-1}\gamma_\mu\gamma_5 C &= (\gamma_\mu\gamma_5)^T\,. \qquad (2.111)
\end{aligned}
$$

The fermionic part of the second order Lagrangian is hence given by

$$
\sum_k U_{ek}^2\,\overline{e}(x)\gamma^\mu(1-\gamma_5)\nu_k(x)\overline{\nu}_k(y)\,\gamma_\mu(1+\gamma_5)e^c(y)\,. \qquad (2.112)
$$

The contraction of the neutrino field operators yields the ordinary Feynman propagator:

$$
\langle 0|T(\nu_k(x)\overline{\nu}_k(y))|0\rangle = S_F(x-y) = \int \frac{d^4q}{(2\pi)^4} e^{-iq(x-y)}\,\frac{i\,(\not{q}+m_k)}{q^2-m_k^2}\,. \qquad (2.113)
$$

Only the mass part of the propagator gives a contribution to the amplitude since $(1-\gamma_5)\not{q}\gamma^\mu(1+\gamma_5) = 0$. For light neutrinos ($m_j < 10\,\mathrm{MeV}$), the mass in the denominator of the propagator can be neglected, and the resulting amplitude of the $0\nu\beta\beta$ process has the form

$$
A[0\nu\beta\beta] = \Big[\sum_k m_k U_{ek}^2\Big] \times [k - \text{Independent term}]\,, \qquad (2.114)
$$

where the second factor includes the nuclear physics of the process. The quantity

$$
\langle m\rangle \equiv \sum_k m_k U_{ek}^2 \qquad (2.115)
$$

is called the effective Majorana mass of ν_e.

Nuclear physics of the $0\nu\beta\beta$ process is complicated, and thus there are large theoretical uncertainties in the nuclear matrix elements. However, from the existing upper limits on the $0\nu\beta\beta$ rate one can infer upper limits on $\langle m\rangle$. Neutrinoless double beta decay experiments will be discussed in section 3.4.

2.5 Leptonic CP violation

There is no experimental indication that parity, time reversal or charge conjugation (denoted by P, T or C) were violated in the gravitational, electromagnetic and

strong interactions. As is well known, the weak interactions violate C and P symmetries maximally, but in most weak processes CP and T symmetries are preserved. The combination of the three discrete symmetries, CPT, is believed to be a perfect symmetry of nature, although this assumption has been under reconsideration lately [54]. One should keep in mind that the strong CP problem of QCD [55] still awaits a definite solution.

Certain rare weak process do show CP and T violation. In 1964 CP violation was first observed in a process involving neutral K mesons [56], and quite recently CP was observed to be violated also in B meson decays [57]. As was shown by Kobayashi and Maskawa [21], CP violation in weak interactions can be explained in the framework of the SM with three (or more) fermion families but the origin of the phenomenon is not yet understood. The parameter that is responsible for CP violation in the quark sector is a complex phase in the quark mixing matrix. As explained in section 2.3, the $N \times N$ mixing matrix can be parameterized with $N(N-1)/2$ mixing angles and, because quarks are Dirac particles, $(N-1)(N-2)/2$ phases since some of the phases in a general unitary matrix can be absorbed to the field redefinitions. In case of just two families, $N = 2$, the mixing matrix has one angle and no phases, and thus the theory predicts no CP violation. There must therefore exist at least three fermion families in order the SM to explain the observed CP violation, as was pointed out by Kobayashi and Maskawa in [21].

There is no experimental evidence of leptonic CP violation, but since neutrinos do mix, it is natural to expect that, parallel to the quark case, also the neutrino mixing matrix contains CP-violating phase or phases.

2.5.1 CP invariance conditions

In general the CP transformation on fields $\psi_{L,R}$ includes a phase parameter η,

$$U_{CP}\psi_{L,R}(x)U_{CP}^{-1} = \eta\,\gamma_0 C\,\overline{\psi_{L,R}}^{T}(x')\,, \tag{2.116}$$

where $x' = (x_0, -\vec{x})$ and U_{CP} is the CP-conjugation operator. If fields $\psi_{L,R}$ describe Dirac particles, the phases η can always to be chosen to be one because they are not observable parameters [58]. Requiring that the Dirac mass term

$$\mathcal{L}^D(x) = -\sum_{l,l'} \overline{\nu_{l'R}}(x) M^D_{l'l} \nu_{lL}(x) + \text{h.c.} \tag{2.117}$$

is invariant under the CP transformation, it is easy to see that the mass matrix M^D has to be real, $M^D = M^{D*}$. A real matrix can be diagonalized via the biorthogonal transformation, $M^D = \mathcal{O}'\, m\, \mathcal{O}^T$, where $\mathcal{O}'$ and $\mathcal{O}$ are orthogonal matrices and $m_{kj} = m_k \delta_{jk}$, and the neutrino mixing relation is thus given by $\nu_{lL} = \sum_k \mathcal{O}_{lk}\nu_{kL}$. Therefore, if CP invariance holds, the Dirac neutrino mixing matrix is a real, orthogonal matrix,

$$U^*_{lk} = U_{lk} = \mathcal{O}_{lk}, \quad \mathcal{O}^T\mathcal{O} = \mathbf{1}\,. \tag{2.118}$$

An alternative method to come to this same conclusion is to study the CP transformation properties of the charged current Lagrangian

$$\mathcal{L}^{cc}_{int} = \frac{ig}{\sqrt{2}} \sum_{l,i} \overline{l}_L \gamma^\mu U_{li} \nu_{iL} W^-_\mu + \text{h.c.}\,. \tag{2.119}$$

It can be shown that the Lagrangian $\mathcal{L}^{cc}_{int}$ is invariant under the CP transformation if the mixing matrix U is real (see e.g. [58]).

For Majorana particles the consequences relating to CP symmetry, whether it is conserved or not, are different from the Dirac case. If CP is conserved, each Majorana neutrino with a definite mass carries a quantum number, its intrinsic CP-parity η_{CP}, which has implications in various processes. Let us assume that the fields $\nu_L = (\nu_{eL}, \nu_{\mu L}, \ldots)^T$ transform under CP as the left-handed components of the Dirac fields, eq. (2.116). The Majorana mass Lagrangian

$$\mathcal{L}^M(x) = \frac{1}{2} \nu^T_L(x) C^{-1} M \nu_L(x) - \frac{1}{2} \overline{\nu_L}^T(x) M^\dagger C \overline{\nu_L}^T(x) \tag{2.120}$$

is invariant under CP transformation if

$$\eta M \eta = -M^\dagger. \tag{2.121}$$

If the arbitrary phase η is chosen to be equal to i, the condition (2.121), taken into account that the Majorana mass matrix is symmetric, is the same as in the Dirac case: in case of CP invariance the mass matrix is real, $M^* = M$. As was mentioned in section 2.2.2, a real symmetric matrix can be diagonalized with an orthogonal transformation. Nevertheless, one also has to require, on physical grounds, that mass eigenvalues are non-negative, and therefore the diagonalizing matrix has to be of the form

$$U^\dagger = \sqrt{\rho} \mathcal{O}^T \tag{2.122}$$

with $\rho_{ij} = \rho_j \delta_{ji}$, where $\rho_j = \pm 1$ are the signs of the eigenvalues of the matrix M.

Let us see how a massive Majorana field transforms under CP transformation. From the mixing relation $\nu_{lL} = \sum_i U_{li} \nu_{iL}$ follows that

$$\nu_{iL} = \sum_{l=e,\mu,\ldots} (U^\dagger)_{il}\, \nu_{lL}. \tag{2.123}$$

Using eq. (2.116) with $\eta = i$ and transforming back to the mass basis we find

$$U_{CP} \nu_{iL}(x) U^{-1}_{CP} = i \sum_l (U^\dagger)_{il} \gamma_0\, C \overline{\nu_{lL}}^T(x') \tag{2.124}$$

$$= i \sum_{l,k} (U^\dagger)_{il} U^*_{lk} \gamma_0\, C \overline{\nu_{kL}}^T(x')\,. \tag{2.125}$$

From $U^*_{lk} = \rho_k U_{lk}$, which follows from (2.122), we get [34]

$$U_{CP} \nu_{kL}(x) U^{-1}_{CP} = i \rho_k \gamma_0\, C \overline{\nu_{kL}}^T(x') \equiv \eta_{CP}(\nu_k) \gamma_0\, C \overline{\nu_{kL}}^T(x'), \tag{2.126}$$

where the CP parity of the Majorana field ν_k, $\eta_{CP}(\nu_k) = i\rho_k$, is determined by the sign of the corresponding eigenvalue m_k of the neutrino mass matrix [59] [4].

It is important to note that some of the formulas described above in the Majorana case depend on phase conventions [59]. For example, often the Majorana condition is used in the form $\chi_k^c(x) = \rho_k \chi(x)$, in which case the Majorana field operator is given by

$$\chi_k = (\mathcal{O}^T \nu_L)_k + \rho_k (\mathcal{O}^T C \overline{\nu_L}^T)_k \,. \tag{2.127}$$

With these phase conventions the mixing matrix obviously is a real orthogonal matrix. The CP parity of a Majorana field χ_k has values $i\rho_k$ also in this case.

[4] It should be stressed that the CP parity of a Majorana field indeed has to have values $\pm i$ (see e.g. [59]).

Chapter 3

Neutrino physics experiments

3.1 Solar neutrinos

Solar energy is generated in fusion reactions as protons are converted into helium-4, positrons and neutrinos:

$$4p \rightarrow {}^4\mathrm{He} + 2e^+ + 2\nu_e + \gamma. \tag{3.1}$$

The energy released in this process, $Q = 4m_p - m_{^4\mathrm{He}} - 2m_e \simeq 26$ MeV, is mostly radiated as photons, but a small fraction of it is carried by the neutrinos, $\langle E_{2\nu_e} \rangle = 0.59$ MeV. Several models have been developed [60, 61] to describe the dynamics of the Sun, and these models also predict the solar neutrino flux at the Earth. In this thesis the latest version of the model by Bahcall, Pinsonneault and Basu [61] (BP00) is used as the Standard Solar Model (SSM).

Two main reaction chains, the *pp* chain and the CNO cycle, are responsible of the energy production in the Sun. Electron neutrinos are created in several sub-processes belonging to these chains. The flux of the so-called *pp*-neutrinos, produced in the reaction $p + p \rightarrow {}^2\mathrm{H} + e^+ + \nu_e$, is the largest, but detection of these neutrinos is difficult since they are born with very low energy, $E_\nu < 0.42$ MeV. From the detection point of view very important solar neutrinos are the so-called beryllium neutrinos, produced in the reaction ${}^7\mathrm{Be} + e^- \rightarrow {}^7\mathrm{Li} + \nu_e$ with the energy $E_\nu = 0.86$ MeV or $E_\nu = 0.39$ MeV and the boron neutrinos, produced in ${}^8\mathrm{B} \rightarrow {}^8\mathrm{Be} + e^+ + \nu_e$ with $E_\nu < 15$ MeV. The figure 3.1 shows the solar neutrino flux on Earth originating from the reactions in the *pp* chain, according to the BP00 model [61].

The detection of solar neutrinos at present is based mainly on three detection methods, all having different energy thresholds. The sensitivity areas of these gallium, chlorine and (heavy-)water Cherenkov based detectors are shown in Fig. 3.1. Clearly, the numerous *pp*-neutrinos can be detected only in gallium-based experiments. The high-energy ${}^8\mathrm{B}$ neutrinos, on the other hand, can be observed with all

the three detection methods, but the flux is very small compared with the total solar neutrino flux, and the uncertainty in the flux is large.

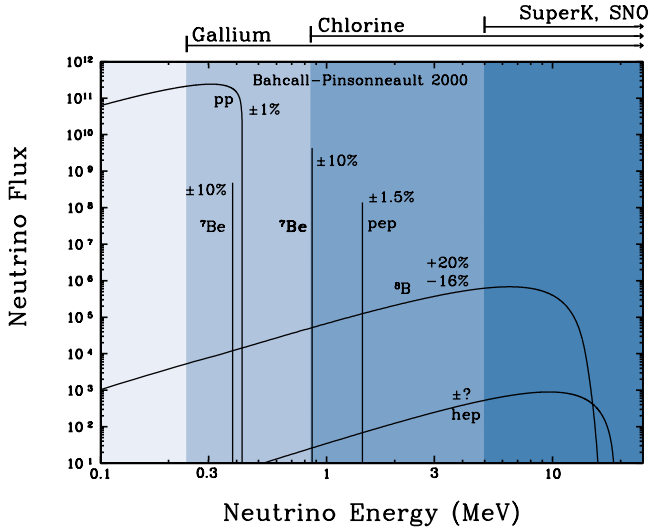

Figure 3.1: Energy spectrum of neutrino flux from the *pp* chain at the Earth, as predicted by the BP00 Standard Solar Model [61]. The continuous spectra are given in number per cm^2 per second per MeV and the monoenergetic lines are given in number per cm^2 per second. On the top of the plot the sensitivity areas of the different experiment types are shown.

3.1.1 Solar neutrino experiments

Homestake

The first detector that observed astrophysical neutrinos was built in Homestake Gold Mine in South Dakota, USA, by a collaboration led by R. Davis[1]. The Homestake experiment announced its first results on the detection of solar neutrinos in 1968 [62], and since the late 60's the experiment took data until 1994.

Neutrino detection in the Homestake experiment was based on 615 tons of perchloroethylene (C_2Cl_4) and the process

$$\nu_e + {}^{37}\mathrm{Cl} \rightarrow {}^{37}\mathrm{Ar} + e^- \tag{3.2}$$

with a threshold energy of 0.814 MeV. The resulting argon was extracted radiochemically and the number of ^{37}Ar nuclei counted by their radioactive decays. The

[1]Year 2002 R. Davis was awarded a Nobel Prize in physics for his pioneering contribution to astrophysics.

Homestake experiment did not provide information about the neutrino spectrum, arrival time or direction but measured only the total flux during its measuring periods.

The average event rate measured during the more than 20 years of operation is [63]

$$R_{\rm Cl} = 2.56 \pm 0.16 \pm 0.16 \text{ SNU}, \tag{3.3}$$

where one solar neutrino unit (SNU) equals one interaction per 10^{36} target atoms per second. The observed event rate is about one-third of the rate predicted by the SSM [61],

$$(R_{\rm Cl})_{\rm SSM} = 7.6\,^{+1.3}_{-1.1} \text{ SNU}. \tag{3.4}$$

SAGE and GALLEX/GNO

Two radiochemical experiments, SAGE (Russian-American Gallium Experiment) and GALLEX (Gallium Experiment), both using ^{71}Ga as target, started taking data in early 1990. The SAGE detector is located in Baksan Neutrino Observatory in Russia and its equipment consists of 57 tons of liquid metallic gallium. The GALLEX experiment, located in the Gran Sasso tunnel in Italy, uses 30.3 tons of ^{71}Ga in 101 tons of aqueous gallium-chloride solution ($GaCl_3$ - HCl) as a target.

In both experiments the neutrino detection is based on inverse beta decay reaction

$$\nu_e + {}^{71}\text{Ga} \rightarrow {}^{71}\text{Ge} + e^- , \tag{3.5}$$

which has a threshold energy of 0.233 MeV so that gallium experiments, unlike any other solar neutrino experiments so far, are able to detect also low energy neutrinos from the *pp* fusion. The produced ^{71}Ge is extracted radiochemically, and the number of ^{71}Ge decays is measured in a proportional counter.

Whereas the SAGE experiment is still ongoing, the GALLEX experiment was completed in 1997 and its successor Gallium Neutrino Observatory (GNO) started taking data in spring 1998.

The event rates observed in the SAGE [64], GALLEX [65] and in the combined GALLEX+GNO [66, 67] experiments are

$$R_{\rm SAGE} = 70.8\,^{+5.3\ +3.7}_{-5.2\ -3.2} \text{ SNU}, \tag{3.6}$$

$$R_{\rm GALLEX} = 77.5 \pm 6.2\,^{+4.3}_{-4.7} \text{ SNU}, \tag{3.7}$$

$$R_{\rm GALLEX+GNO} = 70.8 \pm 4.5 \pm 3.8 \text{ SNU}, \tag{3.8}$$

which all are only about 55–60% of the SSM value [61]

$$(R_{\rm Ga})_{\rm SSM} = 128\,^{+9}_{-7} \text{ SNU} \tag{3.9}$$

where the main contribution (69.7 SNU) comes from the *pp* neutrinos.

Kamiokande and Super-Kamiokande

The Kamiokande and Super-Kamiokande, located in the Kamioka underground observatory, Japan, are imaging water Cherenkov detectors — tanks containing tons of pure water and a large number of photomultiplier tubes attached to the inner surface of the tanks.

The Kamioka Nucleon Decay Experiment (Kamiokande) detector, which was originally designed to investigate the stability of matter by looking for proton decays, was running from 1987 to 1995. It contained altogether 3000 tons of pure water, 2140 tons of which was in the inner photosensitive volume viewed by 948 photomultiplier tubes.

The Super-Kamiokande (Super-K) detector, which started taking data in 1996, is considerably larger than its predecessor. It consists of 50 kilotons of water, of which 22.5 kilotons are used in solar neutrino measurements, and about 13000 photomultiplier tubes. Unfortunately in November 2001 several thousand photomultiplier tubes were destroyed accidentally. The rebuilding of the Super-K detector is still ongoing [2].

In both experiments the solar neutrinos are detected through the observation of the elastic scattering process

$$\nu_\alpha + e \to \nu_\alpha + e\,, \tag{3.10}$$

where $\alpha = e, \mu, \tau$. Thus the detection process is sensitive to all the active neutrino flavors unlike radiochemical experiments which are sensitive only to electron neutrinos. However, ν_e's give the largest contribution also in Kamiokande and Super-K detectors since their scattering cross section is about 6 times larger than that of ν_μ's and ν_τ's. The recoil electron energy threshold is rather large: ~ 7.5 MeV in the Kamiokande experiment and ~ 5 MeV in the Super-K experiment, so that only the ^{8}B neutrinos and a very small hep neutrino flux can be measured in these experiments.

The recoiled electrons are detected by their Cherenkov radiation. By reconstructing the direction of the electrons the direction of the incoming neutrinos can be determined, which makes it possible to ascertain that 'solar' neutrinos really are coming from the Sun. Furthermore, the amount of Cherenkov light produced by the recoiled electron enables a measurement of its energy.

The combined final result of Kamiokande II and III [68] and the latest measured ^{8}B solar neutrino flux in the Super-K [69] experiments are given by

$$\Phi_{\rm Kam} = (2.80 \pm 0.19 \pm 0.33) \times 10^6 \ {\rm cm}^{-2}{\rm s}^{-1}, \tag{3.11}$$

$$\Phi_{\rm Super-K} = (2.35 \pm 0.02 \pm 0.08) \times 10^6 \ {\rm cm}^{-2}{\rm s}^{-1}\,, \tag{3.12}$$

which correspond to about 40–50% of the SSM prediction [61]

$$(\Phi_{^8{\rm B}})_{\rm SSM} = 5.05\,^{+0.20}_{-0.16} \times 10^6 \ {\rm cm}^{-2}{\rm s}^{-1}\,. \tag{3.13}$$

[2] M. Koshiba has been playing leading roles both in Kamiokande and Super-K experiments and was a co-recipient of the year 2002 Nobel Prize in Physics, along with R. Davis and R. Giacconi.

Super-K has also studied the time and energy dependence of their events. Analysis of the shape of the "zenith angle spectrum", in which spectrum and daily variation analyses are combined, shows no sign of spectral distortion [69,70]. Also no significant daily variation is found: the observed day - night asymmetry in event rates is given by [70]

$$A_{\mathrm{N-D}} = 2\,\frac{\Phi_{night} - \Phi_{day}}{\Phi_{night} + \Phi_{day}} = 0.021 \pm 0.020\,^{+0.013}_{-0.012}\,. \tag{3.14}$$

SNO

Also the Sudbury Neutrino Observatory (SNO) is a water imaging Cherenkov detector. It is located in the Creighton mine near Sudbury, Canada, and it has been taking data since November 1999. The neutrino detection medium is 1 kiloton of 99.92% isotopically pure heavy water (D_2O) contained in a 12-m diameter transparent acrylic vessel. Photomultiplier tubes (9456 inward looking and 91 outward looking) are situated in a 17.8 m diameter geodesic sphere and the remaining volume in the large barrel shaped cavity is filled with 7 kilotons of ultra-pure light water (H_2O) to provide shielding from radioactivity.

SNO is sensitive to all active neutrino flavors through the charged current, the neutral current and the elastic scattering reactions:

$$\nu_e + d \to p + p + e^- \qquad \text{(CC)}, \tag{3.15}$$
$$\nu_x + d \to p + n + \nu_x \qquad \text{(NC)}, \tag{3.16}$$
$$\nu_x + e^- \to \nu_x + e^- \qquad \text{(ES)}, \tag{3.17}$$

where $x = e, \mu, \tau$. The CC reaction on the deuteron, with an energy threshold of $E_{th} = 6.8$ MeV, is sensitive only to ν_e while the NC reaction ($E_{th} = 2.2$ MeV) has equal sensitivity to all active neutrino flavors. All non-sterile neutrino flavors can also interact via elastic scattering, with reduced sensitivity for ν_μ and ν_τ ($E_{th} = 5.2$ MeV).

The SNO experiment consists of three phases, each lasting about one year. In the first phase the detector concentrated on the measurement of the CC reaction rate determined by the Cherenkov light produced by recoiled electrons. In the second phase the sensitivity for the NC reaction (3.16) is enhanced by adding NaCl to the heavy water. The free neutron is readily captured by ^{35}Cl, and a cascade of γ rays with a total energy of ~ 8.6 MeV follow as the excited state of ^{36}Cl decays to its ground state. The gamma rays scatter electrons which produce detectable light via the Cherenkov process. In the third phase of the SNO experiment the salt will be eliminated and Neutral Current Detectors (proportional counters filled with ^{3}He) will be installed inside the D_2O volume. This phase provides a consistency check with the NC results obtained with the salt because the NC measurements are subject to different systematical effects during these two phases.

The fluxes in the different reactions can be presented as follows:

$$\begin{aligned}\Phi_{CC}^{SNO} &= \Phi_e\,,\\ \Phi_{NC}^{SNO} &= \Phi_e + \Phi_{\mu\tau}\,,\\ \Phi_{ES}^{SNO} &= \Phi_e + r\,\Phi_{\mu\tau}\,,\end{aligned} \tag{3.18}$$

where $r = \sigma_\mu/\sigma_e \simeq 0.15$ is the ratio of the $\nu_e e$ and $\nu_\mu e$ ES cross sections above 5 MeV. The flux of muon and tau neutrinos, $\Phi_{\mu\tau}$, is expected to be zero in the SSM, and therefore all the three observed rates should be equal. However, the observed rates above the kinetic energy threshold of 5 MeV are [71]

$$\begin{aligned}\Phi_{CC}^{SNO} &= (1.76\,^{+0.06}_{-0.05} \pm 0.09) \times 10^6\,\mathrm{cm}^{-2}\mathrm{s}^{-1}\,,\\ \Phi_{NS}^{SNO} &= (5.09\,^{+0.44}_{-0.43}\,^{+0.46}_{-0.43}) \times 10^6\,\mathrm{cm}^{-2}\mathrm{s}^{-1}\,,\\ \Phi_{ES}^{SNO} &= (2.39\,^{+0.24}_{-0.23} \pm 0.12) \times 10^6\,\mathrm{cm}^{-2}\mathrm{s}^{-1}\,,\end{aligned} \tag{3.19}$$

assuming that the solar neutrino energy spectrum is undistorted. Using this data the ν_e component in the ^{8}B solar flux was found to be [71] $\Phi_e = 1.76 \pm 0.05 \pm 0.09 \times 10^6\,\mathrm{cm}^{-2}\mathrm{s}^{-1}$ and the non-ν_e component $\Phi_{\mu\tau} = 3.41 \pm 0.45\,^{+0.48}_{-0.45} \times 10^6\,\mathrm{cm}^{-2}\mathrm{s}^{-1}$, which is 5.3 σ above zero. The total flux of the active ^{8}B neutrinos, measured with the NC reaction, is consistent with the SSM prediction, eq. (3.13). These results are considered to be solar-model-independent evidence for neutrino flavor transition $\nu_e \to \nu_{\mu,\tau}$ at the 5.3 σ level [71].

SNO has measured also day-night asymmetries of the CC, NC and ES reaction rates and the small asymmetry in the ν_e flux, defined in eq. (3.14), was found, $A_{\mathrm{N-D}}^{CC} = 0.07 \pm 0.049\,^{+0.013}_{-0.012}$ [72], presuming that the total flux of active neutrinos has no asymmetry.

Near future: Borexino

The 300 ton real-time liquid scintillator detector of the Borexino experiment [73], is under construction in the underground Gran Sasso laboratory. The main goal of the experiment is to observe the low-energy mono-energetic (862 keV) ^{7}Be neutrinos, produced in the ^{7}Be electron capture reaction in the Sun. Neutrino detection will occur through elastic scattering processes $\nu + e^- \to \nu + e^-$ signalled by the light produced by the scattered electrons. Due to very low energy experimental threshold, 250 keV, extreme radiopurity of the detector is required. Besides detecting ^{7}Be neutrinos, Borexino is also able to detect ^{8}B neutrinos in the energy range $1.5 - 5$ MeV, which is not accessible to the higher threshold experiments, for example Super-Kamiokande or SNO. This would allow the identification of spectral distortions typical for the MSW solutions. Furthermore, Borexino will be able to search for solar antineutrinos, as well as geophysical $\overline{\nu}_e$'s from the Earth and $\overline{\nu}_e$'s from supernovae.

3.1.2 Solar neutrino problem and oscillation solution

To summarize, except for the SNO NC measurements, all solar neutrino experiments have detected only 30–60 % of the flux predicted by the SSM. The deficit varies for different experiments in a way that suggests that the effect may depend on neutrino energy. In addition to these two observations, which constitute the so-called solar neutrino problem, the recent SNO NC measurements have confirmed that the the non-ν_e component in ^{8}B solar flux is 5.3 σ above zero so that the evidence of the neutrino flavor transition from ν_e to ν_μ and/or ν_τ is solar model independent.

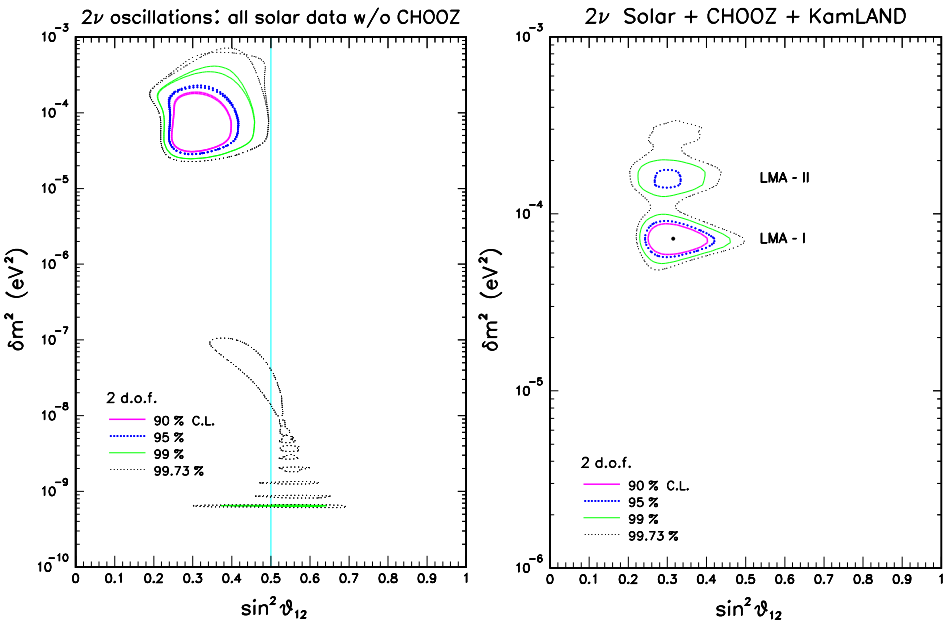

Figure 3.2: Left: Global two-neutrino analysis of the solar neutrino oscillations with and without the additional constraints given by the CHOOZ reactor experiment (by Fogli et al. in ref. [74]). The inclusion of CHOOZ results leads to slightly tighter upper bound on Δm^2. Right: Global two-neutrino analysis of the solar, CHOOZ and KamLAND neutrino data by Fogli et al. in ref. [75]. The LMA region is split into two sub-regions, LMA-I and LMA-II. The best fit point ($\sin^2\theta_{sol} = 0.315$, $\Delta m^2_{sol} = 7.3 \cdot 10^{-5}\mathrm{eV}^2$) is in the LMA-I region.

The most popular explanation for these experimental results is the neutrino oscillation hypothesis according to which ν_e oscillates into an active (ν_μ, ν_τ) and/or sterile (ν_s) neutrino. A number of alternative solutions to the solar neutrino problem has been proposed in the literature, for example non-standard neutrino interactions with matter [76] and resonance spin-flavor precession [77], but the combined analysis of the solar data by several solar neutrino experiments and the data from reactor neutrino experiment KamLAND [32] strongly favors the

oscillation hypothesis. More precisely, KamLAND results exclude non-oscillation solutions as the dominant mechanism of solar neutrino conversion, but they still can have sub-dominant effects [78]. Two-neutrino oscillation analyses clearly favor oscillations into active species due to the difference between the observed CC and NC event rates at SNO [71]. The combined fit to the CC interaction rates indicates several allowed regions in the $(\Delta m^2_{sol}, \sin^2\theta_{sol})$ parameter space. However, the absence of spectral distortion and daily variations in the Super-Kamiokande data [70] restricts the number of favoured parameter regions to two, and the measured day and night energy spectra in the SNO experiment [72] strongly favores one of those two parameter regions, the so-called large mixing angle (LMA) solution in a two-neutrino MSW oscillation analysis. Also KamLAND's first results [32] are in good agreement with the LMA MSW oscillation solution.

Figure 3.2 shows the allowed regions in the $(\Delta m^2_{sol}, \sin^2\theta_{sol})$ parameter space at present according to the global two-neutrino analysis of a) solar data [74] and b) solar data combined with the data from two reactor experiments, CHOOZ and KamLAND [75].

3.2 Atmospheric neutrinos

Atmospheric neutrinos are produced in the atmosphere as the primary cosmic rays, typically protons, collide with the air nuclei. The collision creates a shower of hadrons, mostly pions. The pion decays to a muon neutrino and a muon

$$\pi^- (\pi^+) \rightarrow \overline{\nu}_\mu (\nu_\mu) + \mu^- (\mu^+), \tag{3.20}$$

which subsequently decays to an electron, a muon neutrino and an electron neutrino

$$\mu^- (\mu^+) \rightarrow e^- (e^+) + \nu_\mu (\overline{\nu}_\mu) + \overline{\nu}_e (\nu_e). \tag{3.21}$$

Based on this kinematic chain, one predicts that the flux of muon neutrinos is approximately twice as large as the electron neutrino flux (making no difference between neutrinos and antineutrinos). This holds true actually only at relatively small energies ($\leq 1\,\mathrm{GeV}$) since the high-energy muons do not have time to decay in the atmosphere but are stopped in the earth. Also, in a more detailed calculation one has to take into account that there are also other particles, for example kaons, produced in the hadronic showers.

3.2.1 Atmospheric neutrino experiments

Atmospheric neutrinos are, just like solar neutrinos, observed in underground experiments. The predicted absolute fluxes of atmospheric muon and electron neutrinos, ϕ_{ν_e} and ϕ_{ν_μ}, are quite uncertain, but their ratio $r = \phi_{\nu_\mu}/\phi_{\nu_e}$ can be calculated in detail and it is expected to be uncertain by less than 5%. The experimental results are usually reported as the double ratio $R \equiv (\mu/e)_{\mathrm{data}}/(\mu/e)_{\mathrm{theory}}$,

Experiment		$R \equiv r_{\text{data}}/r_{\text{theory}}$	
IMB		$0.51 \pm 0.01 \pm 0.05$	[79]
Kamiokande	(sub-GeV)	$0.60\,^{+0.07}_{-0.06} \pm 0.05$	[80]
	(multi-GeV)	$0.57\,^{+0.08}_{-0.07} \pm 0.07$	[81]
Super-K	(sub-GeV)	$0.638 \pm 0.016 \pm 0.050$	[82]
	(multi-GeV)	$0.658^{+0.030}_{-0.028} \pm 0.078$	[82]
Soudan 2		$0.68 \pm 0.11 \pm 0.06$	[83]

Table 3.1: Double ratio $R \equiv r_{\text{data}}/r_{\text{theory}}$, where $r = \phi_{\nu_\mu}/\phi_{\nu_e}$, measured in some of the most recent atmospheric neutrino experiments. Contained data samples can be divided into sub-GeV events if the visible energy is below 1.33 GeV, or multi-GeV events if it is above 1.33 GeV.

where μ and e are the number of muon-like and electron-like events. The determination of the theoretical ratio $(\mu/e)_{\text{theory}}$ is based on Monte Carlo simulations [84] and $R = 1$ is expected if the simulation models the data accurately.

Table 3.1 shows the values of the double ratio R obtained in some of the recent atmospheric neutrino experiments. The double ratio is measured to be much less than one which means that experiments detect less muon neutrinos compared with the number of electron neutrinos than what is expected. The first atmospheric neutrinos were detected already in the 1960's [85], but statistically significant measurements were not done until in the 1980's.

The Kamiokande detector took data between years 1983 - 1995. The last phase, the Kamiokande-II-III, was a 4.5 kiloton water Cherenkov detector. The observed ratio of ν_μ and ν_e fluxes was smaller than the theoretical ratio both for sub-GeV [80] and multi-GeV [81] neutrinos (see Table 3.1). In addition, Kamiokande made the observation that the flux ratio R showed zenith-angle dependence in the multi-GeV data [81].

The Irvine Michigan Brookhaven Experiment (IMB), which took data between years 1982 - 1991, was also a ring-imaging 8 kiloton water Cherenkov detector. It was built in the Morton salt mine near Cleveland, Ohio, USA. Also the IMB detector observed a ratio of ν_μ-induced events to ν_e-induced events smaller than the expected ratio by a factor of about 0.5 [79].

However, the two oldest iron calorimeter experiments, Fréjus [86] and NUSEX [87], performed in France in the 1980's, found no deviation from the value $R = 1$ and therefore it was first suspected that the atmospheric neutrino deficit originates from some systematic problem with the water Cherenkov detectors.

These kind of speculations were proven wrong by the large statistics data of the Super-K experiment and especially by the conformation of the muon neutrino deficit in the iron calorimeter detector Soudan 2 (Soudan mine, Minnesota, USA, 1989-) and the liquid scintillator experiment MACRO (Gran Sasso, Italy, 1991-) [88, 89]. Also a liquid scintillator experiment Baksan Underground Scintillation Telescope (BUST) in Russia, which started taking data in 1978, has found similar results than the other atmospheric neutrino detectors [90].

Super-Kamiokande

The most compelling evidence for atmospheric neutrino deficit comes from the measurements performed at the Super-Kamiokande (Super-K) experiment since 1996. In fact, Super-K was the first atmospheric neutrino experiment which announced a strong *evidence* for ν_μ oscillation [91] based on the angular distribution of their contained[3] data event sample.

Atmospheric neutrinos are detected at Super-K as they interact with the nuclei of hydrogen and oxygen via charged current interactions

$$\nu_l(\overline{\nu}_l) + N \to l^{\mp} + X \tag{3.22}$$

in the 22.5 kiloton mass of ultra-pure water. For low energies ($E_\nu \lesssim 1$ GeV) the main interactions are the quasi-elastic scatterings, X denoting a nucleon N', whereas for higher energies ($E_\nu \gtrsim$ a few GeV) deep inelastic scattering takes place and X stands for a hadronic state for which there are a large number of possibilities. The flavor of the final-state lepton l, electron or muon, can be identified by the characteristic shape of the Cherenkov ring they produce, and from the lepton flavor the flavor of the incoming neutrino can be inferred. Also, the direction and the energy of the neutrino can be deduced by exploring the properties of the Cherenkov ring.

High-energy cosmic rays are not deflected by the Earth's magnetic field, and therefore arrive at the Earth almost isotropically. Therefore the atmospheric neutrino flux is expected to be up-down symmetric at high energies ($E_\nu \gtrsim 2$ GeV) which means that the flux should be equal for equal angles with the zenith and nadir. Besides that Super-K has observed a deviation from $R = 1$ (see Table 3.1), it has also confirmed the Kamiokande observation that the muon neutrino deficit is zenith-angle dependent. The zenith angle θ is the angle between the direction of the reconstructed path of the charged lepton and the vertical of the detector so that the vertically down-going particles correspond to $\cos\theta = 1$ and up-going to $\cos\theta = -1$. The zenith angle asymmetry can be quantified as

$$A = \frac{U - D}{U + D}\,, \tag{3.23}$$

[3]The observed event is classified as *contained event* if the charged current interaction between the incoming neutrino and the detector medium is observed directly inside the detector.

where the U (D) are the contained μ or e-like events with zenith angle in the range $-1 < \cos\theta < -0.2$ ($0.2 < \cos\theta < 1$). The value of the asymmetry for multi-GeV μ-like events obtained in the Super-K experiment is given by [92]

$$A_\mu = -0.31 \pm 0.04\,, \tag{3.24}$$

which is more than 7σ away from the expected value of zero. For high-energy electrons the up-down asymmetry A_e was indeed found to be zero. Neutrinos coming from the top of the detector (down-going neutrinos) have traveled only about $\lesssim 20$ km while neutrinos coming from the opposite direction have traversed the whole diameter of the earth, about 13 000 km. According to the result (3.24) the suppression of the contained μ-like events grows for larger $\cos\theta$ and thus for larger distances between the neutrino source and the detector.

The Super-K experiment has observed also that the deficit in flux of the through-going muons is smaller than that for the stopping muons[4], which implies that the suppression effect is weaker for neutrinos with larger energy [93].

3.2.2 Atmospheric neutrino problem and oscillation solution

To summarize, several experiments detect a deficit of about 50–60% in the observed ν_μ/ν_e ratio with respect to the predicted value. In addition, the muon neutrino flux shows a zenith-angle dependence in contrast with the electron neutrino data which is consistent with the predictions.

Again, neutrino oscillations is the most probable solution to the anomaly. There are also other proposals, for example ν_μ decay [94], decoherence effects induced by new physics (e.g. by quantum gravity) [95], and flavor changing neutrino-matter interactions which induce $\nu_\mu \to \nu_\tau$ transitions also for massless neutrinos [96], but as the dominant mechanism of atmospheric ν_μ conversion, these alternative solutions give predominantly worse fits to the data than the best oscillation solution [97].

Oscillations into electron neutrinos, $\nu_\mu \to \nu_e$, are ruled out because if they did take place, also ν_e flux should show angular dependence, in contrast with the data. Also, the CHOOZ reactor experiment, which searches for disappearance of $\overline{\nu}_e$'s, has excluded most of the parameter space capable of explaining the atmospheric neutrino problem in terms of $\nu_\mu \to \nu_e$ oscillations.

According to the Super-K and MACRO results, the two-flavor $\nu_\mu \to \nu_s$ oscillations are disfavored with 99 % C.L. with respect to $\nu_\mu \to \nu_\tau$ oscillations [89, 98]. These two cases can be distinguished because matter effects suppress the conversion probability of $\nu_\mu \to \nu_s$ for high energy neutrinos ($E_\nu > 15$ GeV), which should show especially in the through-going muon event sample. On the other hand, the

[4]The so-called *upgoing muons* are produced underneath the detector as the high energy ν_μ's and $\overline{\nu}_\mu$'s interact with the surrounding rock. An upgoing muon is called a *a stopping muon* if it does not exit the detector, and it is classified as a *through going muon* if it crosses the full detector.

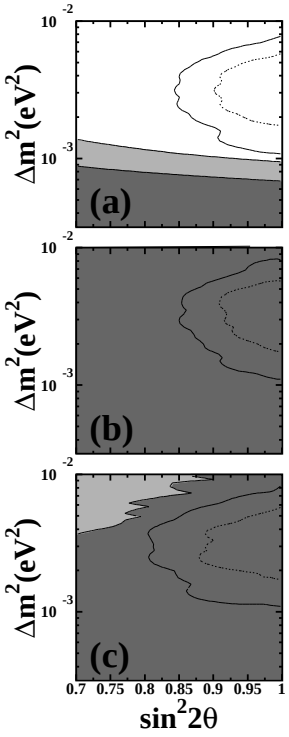

Figure 3.3: a) Excluded parameter region for the $\nu_\mu \leftrightarrow \nu_\tau$ oscillation solution. b-c) Excluded regions for the $\nu_\mu \leftrightarrow \nu_s$ oscillation solution with b) $\Delta m^2 > 0$ and c) $\Delta m^2 < 0$. The light gray region is excluded at 90 % and the dark gray at 99 % C.L. The dotted line shows the 90 % and the solid line 99 % C.L. allowed regions from the analysis of fully contained single-ring events [98].

transition probability $P(\nu_\mu \to \nu_\tau)$ takes the vacuum form because matter has the same effect on muon and tau neutrinos. The Super-K experiment has also studied the zenith angle distribution of the neutral current enhanced multi-ring event sample, which should be up-down asymmetric if conversions into sterile neutrinos took place. Oscillations into sterile neutrinos fit the low-energy charged current data, but not the neutral current and high-energy data [98].

Figure 3.3 shows the excluded regions in the $(\sin^2\theta_{atm}, \Delta m^2_{atm})$ parameter space for both the oscillation channels according to Super-K results [98]. For the $\nu_\mu \leftrightarrow \nu_\tau$ channel they find the allowed parameter values $\Delta m^2 = (1.6 - 3.9) \times 10^{-3}\mathrm{eV}^2$ and $\sin^2 2\theta > 0.92$ at 90 % C.L. Best fit points are given by $\Delta m^2 = 2.5 \times 10^{-3}\mathrm{eV}^2$ and $\sin^2 2\theta = 1$ [82].

It should be noted that the Super-K analysis described above does not exclude more complicated scenarios in which ν_μ oscillates into a mixture of other neutrino flavors. Three- and four-neutrino analyses will be discussed in Chapter 4.

3.3 Accelerator and reactor neutrinos

In addition to the experiments measuring solar and atmospheric neutrinos, there are several terrestrial laboratory experiments for neutrino oscillation study in which neutrinos are produced either in accelerators or in nuclear reactors. These experiments have the advantage of better control of the neutrino flux compared with the solar and atmospheric neutrinos and therefore they will play essential role in precision determination of neutrino oscillation parameters.

Oscillation experiments can be divided into two groups based on how they look for the oscillation signal. In a *disappearance* experiment one looks for attenuation of the neutrino beam composed of a certain neutrino flavor and in an *appearance* experiment one looks for appearance of neutrinos of different flavor not present in the beam initially.

In the following a short description of some of the most important accelerator and reactor experiments is given.

3.3.1 Short-baseline accelerator experiments

The only appearance laboratory experiment that has seen a positive oscillation signal is the Liquid Scintillating Neutrino Detector (LSND) experiment performed at Los Alamos Meson Physics Facility. It presented its first evidence for muon antineutrino to electron antineutrino oscillation in 1995.

Neutrinos in the LSND experiment are produced with an intense 800 MeV proton beam. The beam hits the target and creates, among other things, positive pions which decay mainly at rest and through the sequence

$$\begin{aligned} \pi^+ \quad &\rightarrow \quad \mu^+ \nu_\mu \\ &\quad\;\; \hookrightarrow e^+ \, \nu_e \, \overline{\nu}_\mu \, . \end{aligned} \tag{3.25}$$

The experiment investigates whether the resulting $\overline{\nu}_\mu$'s, which have the maximum energy of 52.8 MeV, oscillate into $\overline{\nu}_e$'s which are detected about 30 m away from the neutrino source by inverse beta decay reaction

$$\begin{aligned} \overline{\nu}_e \, p \quad &\rightarrow e^+ \, n \\ &\quad\;\; n \, p \rightarrow d \, \gamma \;\; (2.2 \text{ MeV}). \end{aligned} \tag{3.26}$$

Also π^-'s and μ^-'s are produced in the target but they are readily absorbed by the shielding and beam stop materials so that in the energy range $36 < E_\nu < 52.8$ MeV the $\overline{\nu}_e$ flux is calculated to be only $\sim 8 \times 10^{-4}$ as large as the $\overline{\nu}_\mu$ flux.

The structure of the LSND target allows also $\pi^+ \rightarrow \mu^+\nu_\mu$ decay in flight producing ν_μ's up to 300 MeV, and hence also charge-conjugate oscillation channel, $\nu_\mu \rightarrow \nu_e$, can be searched for by detecting higher energy decay-in-flight electron neutrinos.

As the final result the LSND collaboration has reported that they observe the total excess of $87.9 \pm 22.4 \pm 6.0$ $\overline{\nu}_e p \rightarrow e^+ n$ events in the $\overline{\nu}_\mu \rightarrow \overline{\nu}_e$ oscillation search, corresponding to an oscillation probability of $(2.64 \pm 0.67 \pm 0.45) \times 10^{-3}$ [31]. In the final analysis the event selection was optimized for the decay-at-rest energy region, below 60 MeV, and no significant signal in the decay-in-flight energy region was found[5]. In the two-flavor formalism the LSND results can be presented with the oscillation parameters shown in Fig. 3.4.

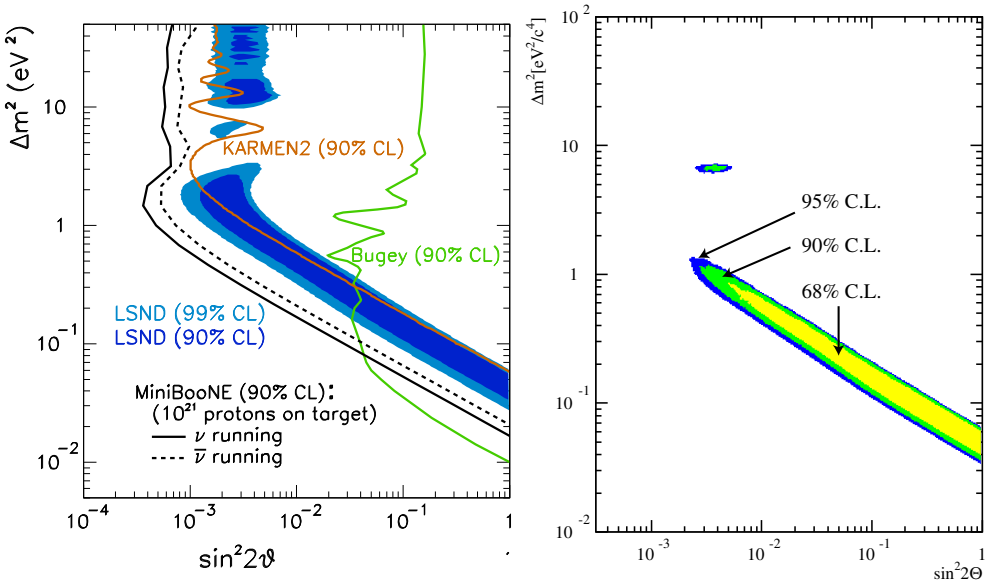

Figure 3.4: Left: A $(\sin^2 2\theta, \Delta m^2)$ oscillation parameter fit (at 90 and 99% CL) for $\overline{\nu}_\mu \rightarrow \overline{\nu}_e$ oscillations from the LSND experiment and exclusion curves (at 90% CL) from KARMEN2 and the Bugey reactor experiment. Also the expected sensitivity region (at 90% CL) from the MiniBooNE experiment is shown. Picture is from [105]. Right: Allowed region from the combined analysis of the KARMEN2 and the LSND data [104].

The parameter region corresponding to the LSND oscillation signal has been partly tested by other experiments. The large $\sin^2 2\theta$ region is explored and excluded by reactor experiments Bugey [100] and CHOOZ [101], and a part of the large Δm^2 region is tested by another accelerator experiment, the Karlsruhe-

[5]In an older analysis of 1993–1995 decay-in-flight data [99] an excess of $18.1 \pm 6.6 \pm 4.0$ events was found, corresponding to the oscillation probability of $P(\nu_\mu \rightarrow \nu_e) = (2.6 \pm 1.0 \pm 0.5) \times 10^{-3}$.

Rutherford Medium Energy Neutrino (KARMEN) experiment, performed at Rutherford Appleton Laboratory, England. The KARMEN experiment also searched for $\overline{\nu}_\mu \to \overline{\nu}_e$ oscillations using $\overline{\nu}_\mu$ from μ^+ decay at rest, but there were some important differences between the beams and detectors of these two experiments [102]. For example, the KARMEN detector was centered only about 18 meters from the target, rather than the 30 meters of LSND, and the experiments were sensitive to somewhat different Δm^2. The KARMEN experiment saw no sign of $\overline{\nu}_\mu \to \overline{\nu}_e$ oscillations [103], and it was able to exclude a part of the LSND allowed parameter space (see Fig. 3.4), but not all of it. A combined statistical analysis of the KARMEN and LSND data still leaves an allowed parameter region compatible with both experiments [104], as illustrated in Fig. 3.4.

The conclusive test of the LSND oscillation signal will be given by the MiniBooNE experiment [105], situated at Fermilab, which is currenly taking data. MiniBooNE is the first phase of the BooNE (Booster Neutrino Experiment) experiment and it searches for $\nu_\mu \to \nu_e$ oscillations with a $0.5 - 1.5$ GeV ν_μ beam, initiated by an 8 GeV primary proton beam from the Fermilab Booster. Neutrino energies are over an order of magnitude higher than those of LSND, but the baseline to neutrino energy ratio is similar, $L/E \sim 1\,\mathrm{m}/1\,\mathrm{MeV}$, since the MiniBooNE baseline is correspondingly longer, $L \sim 500$ m. MiniBooNE will be able to look for oscillation signal using both ν_μ and $\overline{\nu}_\mu$ beams, and its expected (90 % C.L.) sensitivity regions are shown in Fig. 3.4. If the LSND oscillation signal is confirmed by the MiniBooNE, the BooNE experiment proceeds to its second phase in which a second detector is built at an appropriate distance from the neutrino source so that e.g. oscillation parameters can be studied in detail.

3.3.2 Reactor disappearance experiments

The CHOOZ experiment (1997-1998) looked for disappearance of $\overline{\nu}_e$'s, i.e. $\overline{\nu}_e \to \overline{\nu}_x$ oscillations. Electron antineutrinos with a mean energy of a few MeV are produced in two nuclear reactors at the Chooz power station, and they were detected ~ 1 km away from the neutrino source in a liquid scintillator detector via the inverse beta decay reaction. Due to its relatively long baseline, the experiment was sensitive to Δm^2 values down to atmospheric neutrino range.

The CHOOZ experiments found (at 90 % C.L.) no evidence of neutrino oscillations for the parameter region $\Delta m^2 \gtrsim 7 \cdot 10^{-4}\,\mathrm{eV}^2$ at maximal mixing and $\sin^2 2\theta > 0.1$ at large Δm^2 [101]. The excluded parameter region is shown in figure 3.5. As already mentioned, the CHOOZ results rule out the $\nu_\mu \leftrightarrow \nu_e$ oscillation solution for the atmospheric neutrino problem.

The Palo Verde reactor experiment (Arizona, USA), which took data between years 1998 and 2000, has found similar results than the CHOOZ experiment. Electron antineutrinos are produced in three reactors at the Palo Verde nuclear generating station, and the detector was situated 750 m from one of them and 890 m from the other two. Also Palo Verde observed no sign of $\overline{\nu}_e$ disappearance, thus

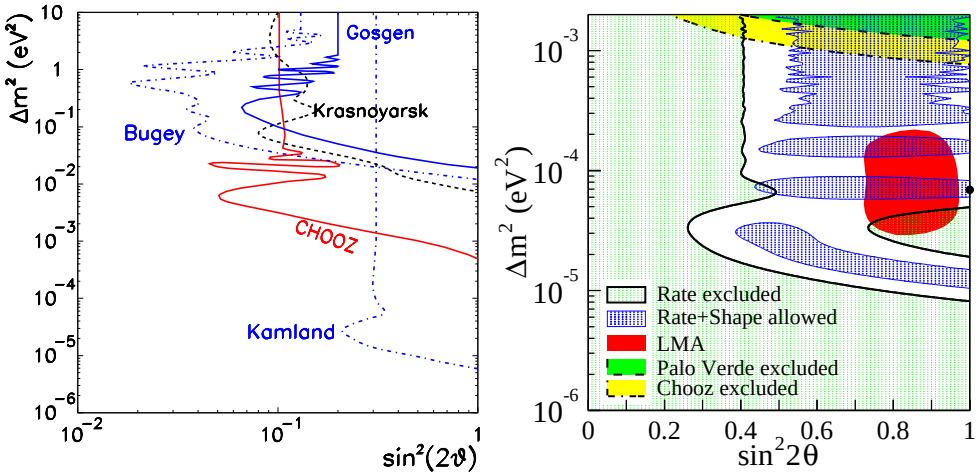

Figure 3.5: Left: Exclusion curves at 90 % C.L. for $\nu_e \leftrightarrow \nu_x$ oscillations from reactor experiments CHOOZ, Bugey, Krasnoyarsk and Gosgen. Shown is also the expected sensitivity region from the KamLAND experiment. The plot is from [106]. Right: Excluded regions for oscillation parameters based on the rate analysis and allowed regions based on the combined rate and shape analysis at 95 % C.L. from the KamLAND experiment [32].

confirming the CHOOZ results. It was able to exclude a slightly smaller parameter region than the CHOOZ experiment [107].

The figure 3.5 (Left) shows the exclusion curves also from the reactor disappearance experiments Gosgen [108], Krasnoyarsk [109] and Bugey [100] which all have shorter baselines than the CHOOZ and the Palo Verde experiments. As already mentioned, the Bugey results rule out part of the parameter region corresponding the LSND oscillation signal (see also Fig. 3.4).

The Kamioka Liquid-scintillator Anti-Neutrino Detector (KamLAND) is the latest reactor disappearance experiment, and also the one with the longest baseline. The KamLAND neutrino detector, a 1000 ton liquid scintillation detector, is located at the old Kamiokande site. It is exposed to a large flux of low energy electron antineutrinos, produced in several nuclear reactors at a variety of distances (typically 180 km). Again $\overline{\nu}_e$'s (with energies above 1.8 MeV) are detected via the inverse β-decay reaction, $\overline{\nu}_e + p \rightarrow e^+ + n$. Due to the long baseline KamLAND is sensitive to small Δm^2 values, and it is able to provide a solar model independent test for the LMA solution of the solar neutrino problem. According to the first KamLAND results [32], announced in December 2002, the ratio of the number of observed inverse β-decay events to the expected number of events in the absence of neutrino oscillations is $0.611 \pm 0.085 \pm 0.041$ for $\overline{\nu}_e$ energies $>$ 3.4 MeV. This rules out the no-oscillation hypothesis at 99.95 % C.L. Also, the observed energy spectrum shows a distortion which is consistent at 93 % C.L with

the expected spectrum in case of neutrino oscillations. In figure 3.5 (Right) are shown the allowed and excluded parameter regions for two-neutrino mixing. The KamLAND results exclude all oscillation solutions but the LMA MSW solution to the solar neutrino problem (assuming CPT invariance), and are therefore in good agreement with the recent solar neutrino results which also favor the LMA solution. Indeed, the allowed LMA region indicated by the solar neutrino data is reduced by KamLAND results as already mentioned (see Fig. 3.2). After three years of data taking KamLAND is expected to determine the solar mixing angle $\sin^2 2\theta$ to within ± 0.1 and Δm^2_{sol} to an accuracy of ± 10 % for $\sin^2 2\theta > 0.7$ (at 2σ C.L.) [110].

3.3.3 Long-baseline accelerator experiments

The KEK to Kamioka (K2K) is the first working accelerator-based long-baseline (LBL) experiment. It took data from June 1999 to July 2001, and will resume data taking as soon as the Super-K detector is rebuilt. Neutrino beam is produced by a 12 GeV proton beam from the synchrotron accelerator at the High Energy Accelerator Research Organization (KEK), Japan, and detected at the Super-K detector, 250 km away from the KEK. The beam flux and energy spectrum are precisely known because of the measurements made with a set of nearby detectors at the KEK site. The neutrino beam consists of 98% pure muon neutrinos with the mean energy of 1.3 GeV. Therefore, the K2K experiment is sensitive to the same Δm^2 region as the atmospheric neutrino experiments. Indeed, one of the main goals of the experiment is to test the oscillation solution for the atmospheric neutrino problem and to determine more precisely the oscillation parameters.

According to their latest analysis on the data, K2K has observed 56 beam-induced neutrino events in Super-K whereas the expected number in the absence of neutrino oscillations is $80.1^{+6.2}_{-5.4}$ [33]. The probability that the observed data could be explained with statistical fluctuation, without oscillations, is less than 1 %. Also, the observed neutrino spectrum shows a distortion expected from neutrino oscillation effects. Both the number of observed neutrino events and the observed energy spectrum are consistent with neutrino oscillation hypothesis with parameter values corresponding to the atmospheric neutrino oscillations.

The MINOS [111] experiment is expected to start data taking in early 2005. Neutrinos will be delivered by a 120 GeV proton beam at Fermilab and detected at the Soudan Mine, Minnesota, 735 km away. The mean energy of the ν_μ beam ("the NuMI beam") can be tuned from about 3 to 18 GeV. The low-energy beam with the average energy of 3.5 GeV yields the same L/E as the K2K experiment but due to its higher flux, MINOS will provide better precision on the oscillation parameters. It expects to confirm oscillatory behavior of ν_μ's and measure Δm^2_{atm} with 10 % error in the $\nu_\mu \to \nu_\tau$ channel. The MINOS experiment will also search for ν_e appearance due to $\nu_\mu \to \nu_e$ oscillations which in the three-neutrino framework are governed by the currently unknown mixing matrix element U_{e3}.

It expects to improve the CHOOZ upper bound on $|U_{e3}|^2$ by a factor of 2 [111]. However, the sensitivity of this oscillation channel is limited by large background.

OPERA[6] [112] in the Gran Sasso laboratory, is an approved but not yet functional long-baseline accelerator-based experiment. It will search for appearance of ν_τ's in the ν_μ beam ("the CNGS beam") generated by 400 GeV protons from SPS accelerator at CERN. The τ's produced in ν_τ charged current interactions are detected by their decays in the massive lead/emulsion – based detector. The baseline is the same as in the MINOS experiment, 735 km, and also OPERA will be sensitive to the parameter region indicated by the atmospheric neutrino anomaly.

ICARUS [113], which also will be situated in Gran Sasso laboratory, is the second detector which is proposed to measure the CNGS neutrino beam. It still awaits definite approval, although the first part of the experimental program, the ICARUS T600 detector, has already been approved, built and tested. Besides beam neutrinos, ICARUS will study also atmospheric, solar and supernovae neutrinos, and it will search for proton decay.

3.4 Present and future $0\nu\beta\beta$-decay experiments

In order to detect two-neutrino double beta decays ($\nu\nu\beta\beta$) and neutrinoless double beta decays ($0\nu\beta\beta$) one must go underground, just like when detecting atmospheric or solar neutrinos. The reason is simply that when rare events are sought, the number of background events must be reduced to a minimum.

Having not been able to detect neutrinoless double beta decay, various experiments have obtained lower limits on the half-life $T^{0\nu}_{1/2}$ of the process. From those one can infer upper limits on the effective Majorana mass $\langle m \rangle$, defined in eq. (2.115), with the relation $(T^{0\nu}_{1/2})^{-1} = (\langle m \rangle / m_e)^2 \times |M_{0\nu}|^2 \times F_{0\nu}$, where $M_{0\nu}$ is the nuclear matrix element of the relevant isotope whose calculations have large theoretical uncertainties and $F_{0\nu}$ is the analytically calculable space phase factor. Table 3.2 shows the best reported limits on $\langle m \rangle$ from some of the already existing experiments and expected sensitivities of some of the future proposals (see e.g. ref. [114] for a more complete list). The sensitivities of the future experiments should be considered as suggestive since they are based on background estimates for experiments that do not exist, yet.

As can be seen from the Table 3.2, the germanium-based experiments, especially the Heidelberg-Moscow double beta decay experiment [115, 116], which is located in the Gran Sasso laboratory, gives currently the most stringent lower limit for the half-life of the $0\nu\beta\beta$-decay. This, according to ref. [115], results from the good energy resolution and large size of germanium detectors and the fact that source is equal to the detector which allows large source strengths. The Heidelberg-Moscow experiment started data taking in 1990 and is now operated

[6] OPERA stands for Oscillation Project with Emulsion-tRacking Apparatus.

Past/present experiments	Isotope	$T^{0\nu}_{1/2}$ (y)	$\langle m \rangle$ (eV)
Heidelberg - Moscow [116]	^{76}Ge	$> 1.9 \times 10^{25}$	< 0.35
IGEX [117]	^{76}Ge	$> 1.6 \times 10^{25}$	$< 0.33 - 1.35$
MIBETA [118]	^{130}Te	$> 1.4 \times 10^{23}$	$< 1.1 - 2.6$
Gotthard [119]	^{136}Xe	$> 4.4 \times 10^{23}$	$< 1.8 - 5.2$
ELEGANT V [120]	^{100}Mo	$> 5.5 \times 10^{22}$	< 2.1
Future experiments/proposals	Isotope	Sensitivity to $T^{0\nu}_{1/2}$ (y)	Sensitivity to $\langle m \rangle$ (eV)
NEMO 3 [121] (7 kg, 5 y)	^{100}Mo	4×10^{24}	$0.25 - 0.7$
CUORE [122] (750 kg, 1 y)	^{130}Te	1.1×10^{26}	0.05
EXO [123] (1 ton, 5 y)	^{136}Xe	8×10^{26}	$0.05 - 0.14$
Majorana [124] (0.5 ton, 10 y)	^{76}Ge	4.3×10^{27}	$0.02 - 0.07$
GENIUS [125] (1 ton, 1 y)	^{76}Ge	5.8×10^{27}	$0.02 - 0.05$
GENIUS [125] (10 ton, 10 y)	^{76}Ge	6×10^{28}	$0.006 - 0.016$

Table 3.2: The $T^{0\nu}_{1/2}$ and $\langle m \rangle$ sensitivities (at 90 % C.L.) of some of the past and present experiments as given by the authors in the cited papers. Shown is also expected sensitivities (acquired after run time shown in the parenthesis) from some of the proposed experiment as well as NEMO 3 experiment which is currently under construction or taking data.

with five detectors (crystals made of Ge) with total active mass of 10.96 kg enriched to 86 % in $\beta\beta-$emitter ^{76}Ge (while the isotopic abundance of ^{76}Ge in natural Ge is only 7.8 %). Location in the underground laboratory reduces the external muon flux significantly, and a further shielding is provided by the lead box and nitrogen flushing of the detectors. Detectors are calorimeters which measure the two-electron sum energy with excellent energy resolution. A pulse shape discrimination analysis is used to identify and reject multi-site events, for instance multi Compton scattering events, which also reduces the background. The main sources of background have been located in the copper parts of the cryostats. This has inspired the GENIUS (GErmanium NItrogen Underground Setup) proposal [125] in which the idea is to use "naked" Germanium detectors in a tank of liquid nitrogen. This enables maintaining the optimal operating temperature without the cryostats but due to its low stopping power, a huge amount of liquid nitrogen is needed.

In Paper II [48] we investigated the constraints the GENIUS experiment could set on the neutrino masses and mixing angles in a four-neutrino model assuming that the CP is conserved. The main results of our study are described in Sec. 4.1.

Quite recently a subset of Heidelberg-Moscow collaboration claimed that a refined statistical analysis of the 1990 - 2000 Heidelberg-Moscow data reveals a peak in the sum energy spectrum which they interpreted as an evidence of neutrinoless double beta decay corresponding the half-life of $T^{0\nu}_{1/2} = (0.8-35.07)\times 10^{25}$ and the effective Majorana mass of $\langle m\rangle = (0.11-0.56)$ eV (at 95 % C.L.) [126]. This claim was met with severe criticism in the community. It was suggested [127] that peak finding procedure used in [126] can produce spurious peaks in the region of interest and that [126] therefore does not provide sufficient evidence for its claim.

3.5 Physics potentials of future accelerator experiments

3.5.1 Second generation long-baseline accelerator experiments

The main goals of the KamLAND experiment [110] and the first generation long-baseline accelerator experiments, described in section 3.3.3, is to test the oscillation solution to the atmospheric and the solar neutrino problems, to measure the corresponding oscillation parameters [7] $\Delta m^2_{21}, \Delta m^2_{32}, \theta_{12}$ and θ_{23} within $\sim 10-20\%$ accuracy and to observe $\nu_\mu \leftrightarrow \nu_\tau$ oscillations. Better precision on solar and atmospheric oscillation parameters, determination of (or getting more stringent upper bound on) the value of the mixing angle θ_{13}, possibility to determine the sign of Δm^2_{32} (i.e. mass ordering of neutrinos) via the MSW matter effects, and, finally, observation of leptonic CP violation can be achieved only with neutrino beams with higher intensity: super-beams, beta-beams and neutrino factory beams, which are proposed to be employed in future experiments. Excellent review on the next generation oscillation experiments can be found in ref. [128].

Super-beams are conventionally produced accelerator neutrino beams whose large intensities follow from the large intensity of the primary proton beam. Indeed, the proton beam intensity with typical thermal power of 0.7 – 4 MW is close to the mechanical stability limit of the target material. Because of the high luminosity one can use the so-called off-axis beams which means that detector is located a few degrees off the main beam axis. This results in a mono-energetic beam with small electron neutrino contamination with reduced neutrino flux and average energy.

The JHF-Kamioka project [129], which is planned to start in 2007, will most probably be the first super-beam experiment. A high intensity narrow band neutrino beam of energy around 1 GeV will be produced by a high-intensity proton synchrotron at Japanese Hadron Facility (JHF), and detected 295 km away at the Kamioka site. In the first phase of the proposed experiment ("the JHF-SK project") the proton beam power will be 0.77 MW and Super-Kamiokande will be used as a detector. The physics goals are precision measurements of the atmospheric neutrino parameters $\sin^2 2\theta_{23}$ with 1 % and Δm^2_{atm} with $10^{-4}\,\mathrm{eV}^2$ preci-

[7] In this chapter the discussion is restricted to three-neutrino scenarios (see section 4.2).

sion, sensitivity to $\sin^2 2\theta_{13}$ down to ~ 0.006 and conformation of $\nu_\mu \to \nu_\tau$ oscillation or "discovery" of sterile neutrinos by detecting neutral current events [129]. In the planned second phase of the experiment ("the JHF-HK project") the accelerator would be upgraded to 4 MW in beam power and the neutrino off-axis beam would be pointed to the future Hyper-Kamiokande detector, a next-generation water Cherenkov detector with fiducial mass of 1 Mton. In this phase the sensitivity to $\sin^2 2\theta_{13}$ could be further improved by an order of magniture and, assuming the LMA solution for solar neutrinos, the leptonic CP violation could be observed if the CP phase δ is larger than $10^\circ - 20^\circ$ [129].

Other second generation long-baseline projects has been proposed in Europe and USA. For example, a super-beam could be produced at Fermilab [130] by upgrading the proton driver. The physics goals of this proposed experiment would be very similar to those of the JHF-SK and JHF-HK projects.

The third potential super-beam project [128,131] would collide a 2.2 GeV proton beam of 4 MW power from the Superconducting Proton Linac (SPL) which is being developed at CERN. In the proposal a super-beam of very low neutrino energy, 250 MeV on average, would be aimed at the Modane laboratory in the Fréjus tunnel, 130 km from CERN. As a target, large water Cherenkov detectors and diluted liquid scintillator detectors have been considered. According to ref. [128], with a 40 kton water Cherenkov detector, in a five-year run, the atmospheric oscillation parameters could be measured at about one order of magnitude better precision with respect to the expected precision of the first-generation long baseline experiments such as MINOS [111]. The sensitivity to $\sin^2 \theta_{13}$ could be improved by more than one order of magnitude compared with the present experimental limits. Maximal CP-violating phase could also be detected, but for serious CP violation studies a much larger detector, for example the proposed 440 kton water Cherenkov detector UNO [132], is needed.

The problem with conventionally produced ν_μ and $\overline{\nu}_\mu$ beams is that they are always contaminated by beam-related background which limits the sensitivity of the experiments. The proposed beta-beams [133,134], on the other hand, would be pure ν_e or $\overline{\nu}_e$ beams (depending on the isotope used) of relatively low energy, since they are produced from the β-decays of heavy ions circulating in a storage ring. If the same detector was exposed at the same time to ν_μ (or $\overline{\nu}_\mu$) super-beam and ν_e (or $\overline{\nu}_e$) beta-beam, the systematical errors would be reduced and a very good sensitivity to leptonic CP violation could be achieved [128,134].

3.5.2 Neutrino Factory

The third new type of beam considered is a neutrino factory beam [128,135] which is produced by muons decaying at long straight sections of a storage ring. The muons are produced from the pion decays, and the pions the same way as those for the super-beams. Therefore the high-intensity proton accelerator, such as the SPL at CERN, is required also for the neutrino factory. Pions, produced as the proton

beam hits the target, are collected and focused by a magnetic horn or a high-field solenoid as efficiently as possible after which they decay in a drift space. Next the phase space of the daughter muon is reduced by various proposed techniques (e.g. "phase rotation" and "ionization cooling", see refs. [135] for details). Finally the muons are reaccelerated to the desired final energy, typically 50 GeV, and the muon beam is injected into a storage ring with two or three straight sections. Decaying μ^-'s (μ^+'s) produce intense ν_μ's and $\overline{\nu}_e$'s ($\overline{\nu}_\mu$'s and ν_e's) in equal numbers so that the flavor content of the neutrino beam is precisely known.

Especially since neutrino factories are expected to be sensitive to the leptonic CP violation, they have inspired several phenomenological studies (see e.g. [136–145]), including our Paper I [47]. In Paper I we investigated the sensitivity of the neutrino factory to the CP violation in a four-neutrino model. The main results of our study and search for leptonic CP violation via neutrino oscillations in general are discussed in Sec. 4.3.

Comparison between the sensitivities of the super-beam experiments and neutrino factories has been performed e.g. in refs. [139, 140]. Figure 3.6, taken from ref. [140], shows how the expected sensitivity to the leptonic CP violation depends on the angle θ_{13} for different Δm^2_{21} in various experiments. It demonstrates how difficult it is to detect even maximal CP violating phase $\delta = \pi/2$ if Δm^2_{21} is not on the high side of the LMA solution. For small or close to π values of δ the sensitivity is naturally even worse.

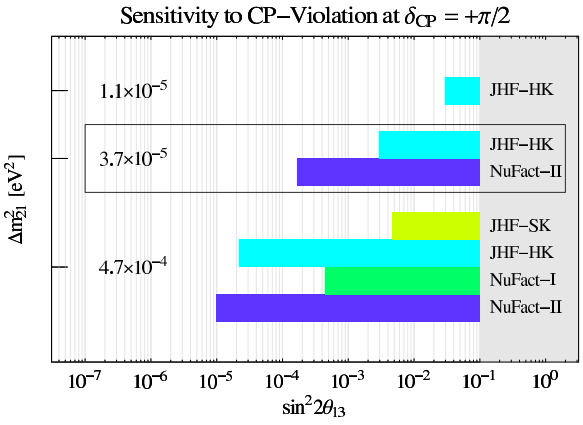

Figure 3.6: The $\sin^2 2\theta_{13}$ sensitivity range for maximal CP violation ($\delta = \pi/2$) for different Δm^2_{21} values according to [140]. Atmospheric oscillation parameters are chosen as $\Delta m^2_{31} = 3 \cdot 10^{-3}\text{eV}^2$ and $\sin^2 2\theta_{23} = 0.8$, and the solar neutrino mixing angle is set to $\sin^2 2\theta_{12} = 0.91$. JHF-SK, JHF-HK and NuMI ox-axis beam projects are chosen as prototypes of super-beam experiments and NuFact-I (NuFact-II) is a low (high)-luminosity version of the neutrino factory with target power of 0.75 (4) MW. Plot is from ref. [140].

Chapter 4

Phenomenological considerations

4.1 Direct determination of neutrino masses

Oscillation experiments are sensitive to the differences of squared neutrino masses, $\Delta m^2_{ji} = m^2_j - m^2_i$, and therefore, apart from some lower limits of the form

$$\max(m_j, m_i) \geq (|\Delta m^2_{ji}|)^{1/2}\,, \tag{4.1}$$

do not yield information about the masses themselves. One way to probe the absolute mass scale of neutrinos is to investigate the kinematics of various weak decays. Due to the smallness of neutrino masses, kinematical experiments cannot, with their present accuracy, distinguish the different mass components produced in a given decay but they measure just a mixing-weighted effective mass. For example, in the case of the electron neutrino, one measures the quantity

$$m^2_{\nu_e} = \sum_i |U_{ei}|^2 m^2_i\,. \tag{4.2}$$

The upper limit for the tau neutrino mass, obtained by studying the kinematics of the τ-decays into pions and ν_τ, is given by [146]

$$m_{\nu_\tau} < 18.2 \text{ MeV} \quad (95\ \%\ \text{C.L.})\,, \tag{4.3}$$

and the kinematical measurements of pion decays into muons and ν_μ yield the following upper limit[1] for the muon neutrino mass [22]:

$$m_{\nu_\mu} < 190 \text{ keV} \quad (90\ \%\ \text{C.L.})\,. \tag{4.4}$$

[1]Upper limit in eq. (4.4) is given by the Particle Data Group. Another often cited upper bound, $m_{\nu_\mu} < 170\,\text{keV}$ at 90 % C.L., is given in [147].

The mass of the electron neutrino is usually studied by investigating the β-spectrum of the tritium decay,

$$^3\mathrm{H} \rightarrow ^3\mathrm{He}^+ + e^- + \overline{\nu}_e \,. \tag{4.5}$$

The most stringent upper limit for the electron neutrino mass is given by the Troitsk [148] and the Mainz [149] experiments which both have obtained the limit

$$m_{\nu_e} \leq 2.2 \text{ eV} \quad (95\ \%\ \text{C.L.}). \tag{4.6}$$

The next generation tritium beta decay experiments are expected to reach sensitivities to sub-eV neutrino masses. For example, the proposed Karlsruhe Tritium Neutrino (KATRIN) experiment is estimated to be sensitive down to $m_{\nu_e} = 0.35\,\mathrm{eV}$ (at 90% C.L.) [150]. The discovery potential of future beta decay experiments is studied e.g. in ref. [151].

Neutrino masses are constrained also by cosmology. At present the most stringent upper limit on the sum of neutrino masses is obtained by observing the distribution of galaxies since massive neutrinos can have a significant effect on the formation of large-scale structures in the Universe. Neutrinos with masses in the eV range dropped out from thermal equilibrium in the early Universe when they still were relativistic. Forming the so-called hot component of the dark matter, they were able to free-stream over large distances until they become unrelativistic, thereby erasing small-scale structures. The power spectrum of density fluctuations is suppressed on small scales (on scales within the horizon when the neutrinos still were relativistic) by [152]

$$\frac{\Delta P_m}{P_m} \approx -8\frac{\Omega_\nu}{\Omega_m}\,, \tag{4.7}$$

where Ω_ν (Ω_m) is the contribution of neutrinos (matter) to the total mass-energy density of the Universe in units of the critical density. The neutrino contribution, on the other hand, is related to the sum of the neutrino masses by[2] [153]

$$\Omega_\nu h^2 = \frac{\sum_i m_i}{93.5\,\mathrm{eV}}\,, \tag{4.8}$$

where h is related to the Hubble parameter at present through $H_0 = 100\,h\,\mathrm{kms}^{-1}$ Mpc^{-1}. The combined analysis of the large scale structure data from the 2dF Galaxy Redshift Survey [28] and the recent WMAP data [8, 24] along with other cosmic microwave background data yields, according to the WMAP collaboration, an upper bound [24] $\Omega_\nu h^2 < 0.0076$ (95 % C.L.), which converts to the bound $\sum_i m_i < 0.7\,\mathrm{eV}$ on the neutrino masses.

The absolute mass scale of neutrinos can be studied also by searching for $0\nu\beta\beta$ process which is sensitive to the absolute value of the effective Majorana mass,

[2]It should be noted that the sum includes only light neutrino species which decoupled while still relativistic.

which in the three-flavor framework is given by

$$\begin{aligned} |\langle m \rangle| &= |\sum_{i=1}^{3} m_i U_{ei}^2| \\ &= |\, m_1 |U_{e1}|^2 + m_2 |U_{e2}|^2 e^{i\alpha_2} + m_3 |U_{e3}|^2 e^{i\alpha_3} \,|\,, \end{aligned} \tag{4.9}$$

where $m_i > 0$ and $\exp(i\alpha_j)$ are the CP-violating phases. If CP is conserved, the $\exp(i\alpha_j) = \eta_j$ factors represent the relative CP parities of the neutrinos ν_1 and ν_2, and ν_1 and ν_3, respectively, and they get the values $\eta_j = \pm 1$. Of course, the $0\nu\beta\beta$ process is possible only if massive neutrinos are Majorana particles. The most stringent upper limit, $|\langle m \rangle| < 0.35$ eV at 90 % C.L., is obtained, as mentioned in previous chapter, in Heidelberg-Moscow experiment [116]. Positive signal from the next generation $0\nu\beta\beta$ experiments, which are expected to be sensitive even down to $\langle m \rangle \sim 10^{-3} - 10^{-2}$ eV, could rule out some of the mass hierarchy models which are acceptable today, and also negative results would yield information about the absolute mass scale and mixings of neutrinos. Obviously, in determination of the absolute mass scale the kinematical measurements and the studies of $0\nu\beta\beta$ decay are largely complementary to each other and must be combined with the information obtained from the oscillation experiments. Many phenomenological studies concerning the present and the future experiments has been done on this subject [154, 155], including the work presented in Paper II [48].

In Paper II we investigated the constraints the proposed $0\nu\beta\beta$ experiment GENIUS [125] could set on neutrino masses and mixings relative to the present situation in a four-neutrino model, assuming that CP is conserved. We used an approximation in which the sterile neutrino mixings with the muon and tau neutrinos are largely neglected and the solar neutrino anomaly is explained by the so-called small mixing angle MSW solution (with $2 \cdot 10^{-3} \lesssim \sin^2 2\theta_{sol} \lesssim 10^{-2}$) so that the oscillations take place between the electron neutrinos and sterile neutrinos. In the mass model that we considered neutrino masses are divided into two degenerate pairs with masses m and $m + \Delta m$ so that the value of the mass gap between the pairs, Δm, is constrained by cosmology, the LSND and other short baseline experiments. There are two possible mass orderings, namely the Model A in which the neutrino pair responsible for the solar anomaly is lighter than the pair responsible for the atmospheric neutrino anomaly, and Model B in which the solar neutrino pair is heavier than the atmospheric neutrino pair.

In the Model A the $0\nu\beta\beta$ condition takes the form

$$|m\,(\sin^2\theta_{01} + \eta_1 \cos^2\theta_{01}) + (m + \Delta m)(\eta_2 \sin^2\theta_{12} + \eta_3 \sin^2\theta_{13})| < a, \tag{4.10}$$

where $\theta_{01} \simeq \theta_{sol}$. The future GENIUS experiment is expected to be sensitive down to $a = \mathcal{O}(10^{-3})$. In case that it does not detect the $0\nu\beta\beta$ process it induces an upper limit for mass m as a function of the quantity $b \equiv \sin^2\theta_{12} + \sin^2\theta_{13}$ or the quantity $b' \equiv \sin^2\theta_{12} - \sin^2\theta_{13}$, depending on the pattern of the relative CP

parities of the neutrinos. There exists eight possible patterns of the relative CP parities $\eta = (\eta_1, \eta_2, \eta_3)$, where $\eta_i = \pm 1$. In the case where $\eta_i = +1$ for $i = 1, 2, 3$, i.e. no cancellations between the contributions of different neutrinos occur, the upper bound for m is the most stringent, $m \lesssim 0.001$ eV. For all the other relative CP parity patterns the absolute mass bound is about an order of magnitude less stringent, $m \lesssim 0.024$ eV. In the case $\eta_i = +1$ also the upper bound obtained for b is rather stringent, $b \lesssim a$, whereas in other cases both a lower and an upper m-dependent limit on b or b' are obtained (see Fig. 1 in Paper II).

The Model B is in practical terms excluded by the present results from the $0\nu\beta\beta$ experiments as was previously noted in ref. [155].

4.2 Three-flavor effects on solar and atmospheric oscillations

For now, let us forget the LSND oscillation signal. As in the Chapter 3, the oscillation data is traditionally formulated in the two-neutrino oscillation scenario: Fig. 3.2 shows the allowed parameter region in the $(\Delta m^2_{sol}, \sin^2\theta_{sol})$ plane for the solar $\nu_e \leftrightarrow \nu_\mu/\nu_\tau$ oscillations, and the Fig. 3.3 shows the allowed parameter regions for the atmospheric $\nu_\mu \leftrightarrow \nu_\tau$ and $\nu_\mu \leftrightarrow \nu_s$ oscillations. Nowadays, and especially in future, as data is getting more and more accurate, one has to perform full three-flavor (3f) or four-flavor (4f) analyses also on solar and atmospheric data. Also, CP and T violation effects, which are hopefully probed in future long-baseline experiments, are specific to ≥ 3 flavor oscillations.

The 3f oscillation analysis involves seven parameters; two independent mass squared differences $\Delta m^2_{21}, \Delta m^2_{31}$, three mixing angles $\theta_{12}, \theta_{13}, \theta_{23}$, the sign$(\Delta m^2_{31})$ and the (Dirac) CP phase. The neutrino mixing matrix can be parameterized as in eq. (2.74).

Two mass orderings, depicted in Fig. 4.1, are compatible with the data. They are usually referred to in terms of the sign(Δm^2_{31}): $+1$ corresponds to the normal and -1 to the inverted mass hierarchy. The normal scheme allows the natural mass hierarchy, $m_1 \ll m_2 \ll m_3$, whereas the inverted scheme implies that $m_3 \ll m_1 \simeq m_2$. In both cases neutrinos can have quasi-degenerate masses, $m_1 \simeq m_2 \simeq m_3 \gg \Delta m^2_{21}, |\Delta m^2_{31}|$. According to data, the mass-squared differences responsible for the solar and the atmospheric neutrino oscillations have the following hierarchy:

$$\Delta m^2_{sol} \simeq \Delta m^2_{21} \ll |\Delta m^2_{31}| \simeq \Delta m^2_{atm}\,. \tag{4.11}$$

However, the mass squared difference corresponding to the LMA MSW solution can be as large as $\sim 10^{-4}\,\mathrm{eV}^2$, and therefore it may be that Δm^2_{sol} and Δm^2_{atm} differ actually only by one order of magnitude.

Also today the two-flavor analyses of solar and atmospheric neutrino data are good first approximations because of the hierarchy of the mass-squared differences,

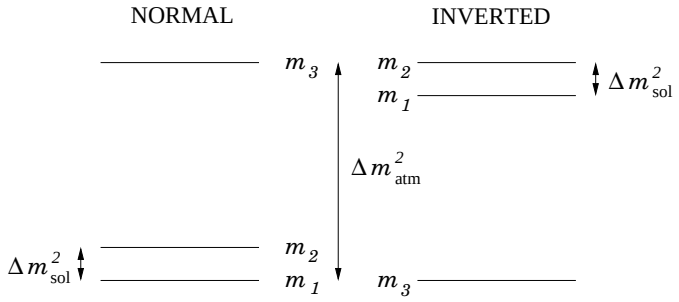

Figure 4.1: Mass schemes for 3ν oscillations.

eq. (4.11), and because the CHOOZ experiment [101] gives a rather stringent upper bound on $|U_{e3}| = \sin\theta_{13}$ [156]:

$$\sin\theta_{13} \leq 0.2 \quad (95\%\ \text{C.L.}). \tag{4.12}$$

The actual value of $|U_{e3}|$ is extremely important for reasons which will be discussed later.

To find oscillation probabilities in matter in the three-flavor scenarios, one has to solve the evolution equation $i(d/dt)\nu = H_M\nu$, where $\nu = (\nu_e\,\nu_\mu\,\nu_\tau)^T$ and

$$H_M = U\begin{pmatrix} E_1 & 0 & 0 \\ 0 & E_2 & 0 \\ 0 & 0 & E_3 \end{pmatrix} U^\dagger + \begin{pmatrix} V_{CC}(t) & 0 & 0 \\ 0 & 0 & 0 \\ 0 & 0 & 0 \end{pmatrix} \tag{4.13}$$

with the charged current induced matter potential $V_{CC} = \sqrt{2}G_F n_e$.

Analyses of the solar and the atmospheric neutrino oscillations usually are based on numerical simulations which take into account the varying matter density. However, in analysing the long-baseline accelerator neutrino experiment data it is not such a bad approximation to assume constant matter density, so that analytical expressions can be used. Exact analytical formulas for transition probabilities in matter with constant density can be found in [157], but since they are lengthy expressions, it is hard to see their physical implications. Therefore one usually uses simplified approximative formulas for transition probabilities by expanding in some small parameter, for example the angle θ_{13} and/or $\alpha = \Delta m^2_{21}/\Delta m^2_{31}$ (see e.g. ref. [138]).

3f effects on the oscillations of KamLAND and solar neutrinos

The solar neutrino experiments are sensitive to Δm^2_{21} and therefore, due to hierarchy (4.11), $\Delta m^2_{31} L/E \gg 1$ and fast oscillations with the oscillation length corresponding to atmospheric neutrino oscillations are averaged. Assuming the

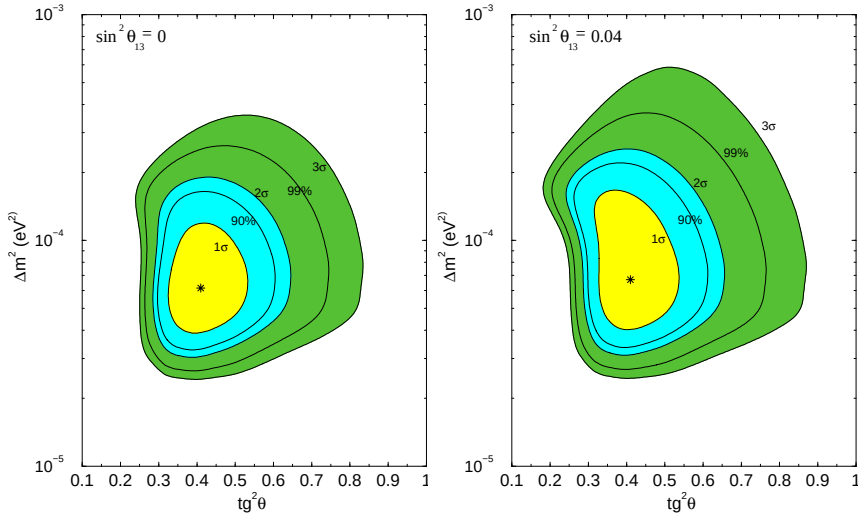

Figure 4.2: Allowed regions in the $\tan^2\theta_{12}, \Delta m^2_{21}$ plane from the global three-neutrino analysis of the solar neutrino data for $\sin^2\theta_{13} = 0$ and 0.04 (from de Holanda et al. [158]). The corresponding plots from the combined analysis of the solar neutrino data and the KamLAND data can be found in ref. [78].

LMA MSW solution to the solar neutrino problem, this applies also to the KamLAND [32] experiment.

In vacuum the three-neutrino survival probability takes the form

$$P^{3\nu}(\nu_\alpha \to \nu_\alpha) = \left(1 - |U_{\alpha 3}|^2\right)^2 \left[1 - 4\frac{|U_{\alpha 1}|^2|U_{\alpha 2}|^2}{(1-|U_{\alpha 3}|^2)^2}\sin^2\left(\Delta m^2_{21}\frac{L}{4E}\right)\right] + |U_{\alpha 3}|^4\,, \tag{4.14}$$

which for electron neutrinos, using the parameterization of eq. (2.74) for the mixing matrix, is given by

$$\begin{aligned} P^{3\nu}(\nu_e \to \nu_e) &= \cos^4\theta_{13}\left[1 - \sin^2(2\theta_{12})\sin^2\left(\Delta m^2_{21}\frac{L}{4E}\right)\right] + \sin^4\theta_{13} \\ &= \cos^4\theta_{13} P^{2\nu}(\nu_e \to \nu_e) + \sin^4\theta_{13}\,, \end{aligned} \tag{4.15}$$

where $P^{2\nu}$ is the two-flavor survival probability. This expression is applicable when analysing KamLAND results and it can differ from the two-flavour probability $P^{2\nu}$ by as much as $\sim 5-10$ %.

For solar neutrinos one should consider the effects of matter. It turns out that in case of mass hierarchy (4.11) and if Δm^2_{32} is much larger than the matter effect, i.e. $\Delta m^2_{32} \gg 2\sqrt{2}G_F N_e E_\nu \sin^2(2\theta_{13})$, matter effects on the evolution of ν_3 can be neglected and the survival probability in matter takes the following form [159]:

$$P^{3\nu}_{MSW}(\nu_e \to \nu_e) = \cos^4\theta_{13} P^{2\nu}_{MSW}(\nu_e \to \nu_e) + \sin^4\theta_{13}\,, \tag{4.16}$$

where $P^{2\nu}_{MSW}(\nu_e \to \nu_e)$ is the MSW probability in the two-generation limit[3], provided that the solar electron density has been modified at any point by $N_e \to \cos^2\theta_{13} N_e$. One can wonder whether the one-mass-scale dominance is justified in the analysis if it turns out that Δm^2_{31} and Δm^2_{21} differ by only one order of magnitude [161,162]. It has been shown that corrections due to violation of (4.11) are typically small and that the present solar neutrino data can indeed be described with three out of the seven parameters: $\Delta m^2_{12}, \theta_{12}$ and θ_{13} [162].

The expression (4.16) demonstrates that the effect of the angle θ_{13} is mainly an overall suppression of the survival probability. Also, in the limit $\theta_{13} \to 0$ the three-flavor analysis reduces to the two-flavor analysis. There are many three-flavor analyses of solar neutrino data in literature [158, 163]. Figure 4.2 shows the LMA MSW solution for two different values of $\sin^2\theta_{13}$ according to global statistical analysis on solar neutrino data performed in [158]. Clearly, small values of θ_{13}, which are allowed by the CHOOZ and the Palo Verde data, do not have dramatic effects in allowed values of the angle θ_{12} but increasing $\sin^2\theta_{13}$ loosens up the upper bound on Δm^2_{12}.

3f effects on the atmospheric oscillations

In the two-flavor framework ($\alpha \equiv \Delta m^2_{21}/\Delta m^2_{31} = \theta_{13} = 0$) atmospheric neutrino oscillations take place between ν_μ's and ν_τ's with maximal or close to maximal mixing and there are no matter effects since, as pointed out previously, matter has the same effect on muon and tau neutrinos. Therefore, the conversion probability $P(\nu_\mu \to \nu_\tau)$ takes the well-known vacuum form involving only the oscillation angle θ_{23} and the mass-squared difference $\Delta m^2_{31} = \Delta m^2_{32}$. In the three-flavor framework with $\theta_{13} \neq 0$ and/or $\alpha \neq 0$, on the other hand, Earth's varying matter density must be taken into account and evolution equation must be solved numerically in order to obtain the oscillation probabilities, which, in contrast with the two-flavor case, have weak sensitivity to the sign of Δm^2_{31}.

Let us consider the one-mass-scale dominance case, $\alpha = 0$. The constant matter density approximation is not necessarily very good when analysing the atmospheric neutrino data, but it does help to understand the 3f effects on the atmospheric neutrino oscillations. Transition probabilities, which can be found e.g. in refs. [106,164], show that the mixing angle θ_{12} can be rotated away so that θ_{13} is the only parameter which is common to both solar and atmospheric neutrino oscillations. Unlike the situation in the two-flavor scenarios, also subdominant oscillation channels $\nu_e \leftrightarrow \nu_{\mu,\tau}$ are present, and their oscillation amplitudes are controlled by the size of $|U_{e3}|^2 = \sin^2\theta_{13}$. If $\theta_{13} = 0$, the solar and the atmospheric oscillations are obviously completely decoupled. Many three-flavor analyses of the atmospheric neutrino data, in which the one-mass-scale dominance is assumed, can be found in literature [106, 164, 165]. Just like in the solar neutrino case,

[3]For $P^{2\nu}_{MSW}(\nu_e \to \nu_e)$ one can use analytical approximations, for example the so-called Parke's formula [160].

small values of θ_{13} allowed by the CHOOZ data have relatively small effect on the allowed Δm^2_{31} and θ_{23} parameter values given by the two-flavor analysis. It is perhaps worth mentioning that for $\theta_{13} \neq 0$ the allowed parameter region in the $\Delta m^2_{31}, \theta_{23}$ space loses its symmetry under the transformation $\theta_{23} \to \pi/4 - \theta_{23}$ (see e.g. Fig. 38 in ref. [106]). Three-flavor analyses which take into account non-vanishing values of both θ_{23} and α can be found for example in refs. [166, 167].

Contribution of the subdominant $\nu_e \leftrightarrow \nu_{\mu,\tau}$ oscillation channels to the number of μ-like events is subleading and therefore difficult to observe. Instead, if $\alpha \neq 0$, one could expect to see observable oscillation effects in the e-like events. Indeed, an excess of the e-like events has been observed in the low-energy part of the Super-K sub-GeV data, and it has been speculated that it might be, at least partly, due to subdominant oscillation channels [166, 167].

4.3 Search for leptonic CP violation

The Majorana CP phases of the leptonic mixing matrix U can be searched for by studying lepton number violating processes, like the $0\nu\beta\beta$ process. In case of three (four) generations of Majorana neutrinos there are three (six) physical phases in the neutrino mixing matrix, two (three) of which can in principle be probed by measuring the absolute value of the effective Majorana mass $|\langle m \rangle| = |\sum_i m_i U^2_{ei}|$. The search for CP violating Majorana phases via the $0\nu\beta\beta$ process is studied e.g. in refs. [168, 169].

4.3.1 Neutrino factories and the CP violation

A prominent way to find implications of the Dirac CP phase or phases in the leptonic mixing matrix is via neutrino oscillations. The probability of the neutrino flavor oscillation $\nu_\alpha \to \nu_\beta$ in vacuum can be written in the form

$$P(\nu_\alpha \to \nu_\beta) = \delta_{\alpha\beta} - \sum_{j<k} [4Y^{jk}_{\alpha\beta} \sin^2 \frac{\Delta m^2_{kj} L}{4E} - 2J^{jk}_{\alpha\beta} \sin \frac{\Delta m^2_{kj} L}{2E}] \,, \tag{4.17}$$

where

$$Y^{jk}_{\alpha\beta} \equiv \mathrm{Re}(U_{\alpha j} U^*_{\alpha k} U^*_{\beta j} U_{\beta k}) \quad \text{and} \quad J^{jk}_{\alpha\beta} \equiv \mathrm{Im}(U_{\alpha j} U^*_{\alpha k} U^*_{\beta j} U_{\beta k}) \,. \tag{4.18}$$

The probability of the CP conjugated channel, $P(\overline{\nu}_\alpha \to \overline{\nu}_\beta)$, is obtained by replacing U by U^*, which implies $J^{jk}_{\alpha\beta} \to -J^{jk}_{\alpha\beta}$. Therefore the difference of the transition probabilities,

$$\Delta P_{\alpha\beta} \equiv P(\nu_\alpha \to \nu_\beta) - P(\overline{\nu}_\alpha \to \overline{\nu}_\beta) \,, \tag{4.19}$$

is proportional to $J^{jk}_{\alpha\beta}$, the leptonic analogue of the Jarlskog invariant [170], and thus measures the CP violation originating from phases in the mixing matrix.

In practice, however, the detection of leptonic CP violation via oscillations is difficult. The oscillation experiment must be sensitive to the sub-leading squared mass difference or otherwise the CP-odd asymmetry $\Delta P_{\alpha\beta}$ is extremely small due to unitarity of the mixing matrix [141]. Indeed, this can be seen for example from the CP odd asymmetry for $\nu_e \leftrightarrow \nu_\mu$ oscillations, which in the three-flavor mixing scheme is given by[4]

$$\begin{aligned} \Delta P_{e\mu} &= 4 \sum_{j<k} J^{jk}_{e\mu} \sin \frac{\Delta m^2_{kj} L}{2E} \\ &= 4\, J^{CP}_\nu \Big(\sin \frac{\Delta m^2_{21} L}{2E} + \sin \frac{\Delta m^2_{32} L}{2E} + \sin \frac{\Delta m^2_{13} L}{2E} \Big) \end{aligned} \tag{4.20}$$

with

$$J^{CP}_\nu = c_{12} s_{12} c_{23} s_{23} c^2_{13} s_{13} \sin \delta \,, \tag{4.21}$$

where δ is the Dirac CP phase. From (4.20) and (4.21) it is also obvious that the odds to detect δ are better if Δm^2_{21} is on the high-side of the LMA MSW solution and that $\Delta P_{e\mu}$ vanishes if $\delta = 0$ or π. Also the smallness of the angle θ_{13} may cause problems. As already discussed, the present upper bound on θ_{13} is rather stringent, $\sin^2 \theta_{13} \lesssim 4 \cdot 10^{-2}$, and the angle θ_{13} can very well be zero or close to it. The possibility to detect the leptonic CP violation, at least in case of three neutrino flavors, clearly depends largely on the value of θ_{13}.

The proposed future oscillation experiments (e.g. neutrino factories), which are expected to be sensitive to the CP-violating phases, usually have very long baselines. In these experiments neutrinos travel long distances in the Earth matter which gives rise to the so called "fake" CP violation, an additional contribution to $\Delta P_{\alpha\beta}$ generated by the CP asymmetry of the earth matter. It may be difficult to extract the genuine CP violation effect from the matter effect, and this problem has been examined in many publications lately. One strategy is to look for tunable[5] parameter regions in which the CP odd term of the neutrino oscillation probability is dominated by vacuum mixing effects [142]. According to [142], an experiment which utilizes low-energy neutrino beam ($E \sim 100$ MeV) and relatively short baseline could be ideal. Another idea to isolate the genuine CP-violation term is to employ "the multiple detector difference method" [143], which means performing measurements with at least two detectors, using the same neutrino beam, at suitable distances from the neutrino source and from each other.

Also the so-called degeneracies can make it difficult to determine simultaneously the unknown mixing angle θ_{13} and the CP-violating phase δ in neutrino factories. Indeed, at a given neutrino energy and a fixed baseline, there are two values of the set (θ_{13}, δ) which give the same oscillation probabilities for neutrinos and antineutrinos [144]. The spectral analysis and the combination of baselines could solve this problem [144].

[4] In fact, it is easy to show that $\Delta P_{e\mu} = \Delta P_{\mu\tau} = \Delta P_{\tau e}$.

[5] Tunable parameters are such as energy of neutrino beam, baseline length, etc.

In Paper I [47] we studied the CP violation effects on the long-baseline neutrino oscillations at a neutrino factory experiment in the framework of a four-neutrino model. Especially we investigated the magnitude of the matter effect relative to the actual CP violation using an approximate analytical formula for the CP-odd asymmetry $\Delta P_{\alpha\beta}$ in matter by Minakata and Nunokawa [145], whose derivation is presented in Appendix A. For the analytical expressions of these quantities we used an approximation in which the mixing of the sterile neutrino with the muon and tau neutrinos are neglected. We also compared out results with the corresponding results in the three-neutrino case.

According to our results, with the parameter values typical to neutrino factories ($L = 732$ km, $E = 7$ GeV), the genuine CP violation term could be as large as $\mathcal{O}(10^{-2})$ whereas the matter effect is considerably smaller, of the order of $10^{-5} - 10^{-4}$. This is not so in the three-neutrino models where with certain parameter values the matter effect can be as important as the genuine CP violation term [137]. Therefore, finding implications of the actual leptonic CP violation can be easier if there exists a sterile neutrino along with the three active neutrinos.

4.4 Four-neutrino models

If the LSND results are not disregarded, three mass-squared differences of different orders of magnitude are needed to explain all the existing evidence of neutrino oscillations. To achieve that, the number of neutrinos taking part in oscillations must be at least four and, as discussed in sec. 2.1.1, the extra neutrinos must be sterile. Of course, one could add more than one sterile neutrino to the theory, but the four-neutrino models are the minimal framework that may be able to explain all data, and therefore they have been studied in detail. Also cosmology restricts the number of sterile neutrinos, as discussed in section 2.1.1.

Six type of 4-neutrino spectra, illustrated in Fig. 4.3, yield the required mass-squared differences $\Delta m^2_{sol}, \Delta m^2_{atm}$ and Δm^2_{LSND}. These spectra can divided into two groups. In the 3+1 models the group of three close-by masses, mainly responsible for solar and atmospheric oscillations, is separated from the fourth mass by a ~ 1 eV mass gap, corresponding to the LSND oscillations. Within the group of three masses the ordering can be either normal or inverted, and the group can be heavier or lighter than the isolated mass. In the 2+2 models two pairs of close-by masses are separated by the LSND mass gap so that either the solar or the atmospheric mass pair can be the heavier one. In the last few years the experimental information on the oscillation parameters has increased rapidly, and the 2+2 and 3+1 mass patterns have been favored by turns. At the time the Paper I and Paper II of this thesis were written, the 2+2 models were favored over the 3+1 models. Since then the situation has changed, and now it seems that both mass orderings are disfavored, except that the 3+1 schemes still have some marginally acceptable regions in the parameter space [171] (see Fig. 4.4).

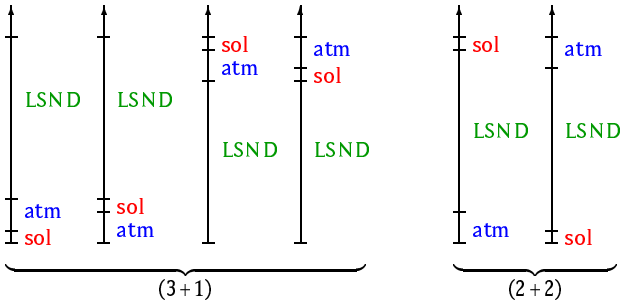

Figure 4.3: The six types of 4-neutrino mass spectra. Figure is from ref. [172].

4.4.1 The 3+1 models

The 3+1 models have been disfavored for a long time [173,174] because the LSND allowed parameter region is not compatible with the results from the short-baseline disappearance experiments. Indeed, in the 3+1 mass schemes the $\nu_\mu \to \nu_e$ oscillations corresponding to the LSND signal proceed through $\nu_\mu \to \nu_s \to \nu_e$ sequence, and $\nu_{\mu,e} \to \nu_s$ oscillations are strongly constrained by the short-baseline disappearance experiments.

More precisely, in the short-baseline experiments oscillations due to solar and atmospheric Δm^2's can usually be neglected, and the transition probability for the $\nu_\mu \to \nu_e$ (and $\overline{\nu}_\mu \to \overline{\nu}_e$) oscillations takes the two-neutrino form,

$$P(\nu_\mu \to \nu_e) = P(\overline{\nu}_\mu \to \overline{\nu}_e) = 4|U_{e4}|^2|U_{\mu 4}|^2 \sin^2 \frac{\Delta m^2_{LSND} L}{4E} \,. \tag{4.22}$$

Therefore the allowed parameter region of the two-flavor analysis on the LSND data, presented in Fig. 3.4, directly shows the allowed region in the Δm^2_{LSND}, $4|U_{e4}|^2|U_{\mu 4}|^2$ space with $\sin^2 2\theta$ identified by $4|U_{e4}|^2|U_{\mu 4}|^2$. Of course, the excluded parameter region of the KARMEN experiment [103] is similarly transferred to the new parameter space.

The matrix elements $|U_{e4}|$ and $|U_{\mu 4}|$ are, however, restricted also by short baseline disappearance experiments, e.g. the $\overline{\nu}_e$ disappearance experiment Bugey [100] and the ν_μ-disappearance experiment CDHS [175] where the survival probabilities are given by

$$P(\nu_\alpha \to \nu_\alpha) = P(\overline{\nu}_\alpha \to \overline{\nu}_\alpha) = 1 - 4|U_{\alpha 4}|^2(1 - |U_{\alpha 4}|^2) \sin^2 \frac{\Delta m^2_{LSND} L}{4E} \,. \tag{4.23}$$

Statistical analysis which takes into account results from the KARMEN, Bugey and CDHS experiments, from the NOMAD experiment [176], which looks for $\nu_\mu \to \nu_e$ oscillations, and the full atmospheric zenith-angle distribution data, has been presented in [172, 177]. Figure 4.4, taken from ref. [172], shows the LSND

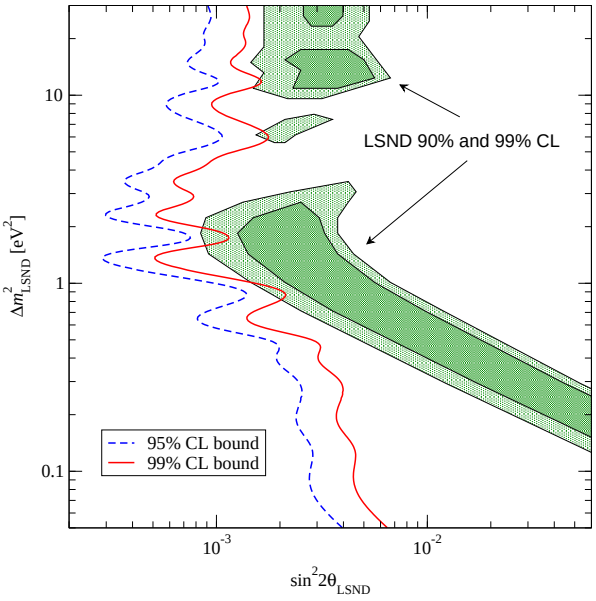

Figure 4.4: The LSND allowed region and the upper bounds on $\sin^2 2\theta = 4|U_{e4}|^2|U_{\mu 4}|^2$ at 95 and 99 % C.L. coming from various experiments. Intersecting areas indicate the marginal allowed parameter regions in the 3+1 scheme. The plot is from ref. [172].

allowed region and the Δm^2_{LSND}-dependent exclusion curve on $4|U_{e4}|^2|U_{\mu 4}|^2$ from atmospheric and short-baseline experiments. A few marginal allowed regions exist when both the LSND data and the bound are taken at the 99 % C.L.

It was concluded in [9] that the recent WMAP data [8] implies such a tight upper bound on $\sum_i m_i$ (see Sec. 4.1), and thus on Δm^2_{LSND}, that all the allowed windows in Fig. 4.4 are excluded. However, it was pointed out in [11] that neutrino mass bound depends on the total number of light neutrino species so that in case $N_\nu = 4$ the upper bound on $\sum_i m_i$ increases to 1.4 eV, which means that the LSND result is still allowed by cosmological observations.

4.4.2 The 2+2 models

In contrast with the 3+1 mass scheme, in the 2+2 mass ordering there must be a significant sterile component either in the solar or in the atmospheric neutrino oscillations or in both of them.

As mentioned, pure active-sterile oscillations are strongly disfavored explanations to both the solar and the atmospheric neutrino anomaly. In both cases transitions into the active-sterile admixture can take place, however. The Super-K atmospheric neutrino data allows up to a 19 % (26 %) contribution at 90 % (99 %) C.L. from ν_s as a sub-dominant oscillation partner [12, 13] and a sizable

sterile neutrino component could still be present also in the solar neutrino flux due to uncertainty in the ^{8}B neutrino flux [14].

Phenomenological considerations imply that the ν_μ is predominantly in the mass pair responsible for the atmospheric neutrino oscillations and ν_e is mainly in the pair which is responsible for the solar neutrino oscillations so that the atmospheric oscillations take place between ν_μ and [13]

$$\nu' = \cos\alpha\,\nu_\tau - \sin\alpha\,\nu_s + \mathcal{O}(\epsilon)\cdot\nu_e \tag{4.24}$$

and the solar oscillations take place between ν_e and

$$\nu'' = \sin\alpha\,\nu_\tau + \cos\alpha\,\nu_s + \mathcal{O}(\epsilon)\cdot\nu_\mu\,. \tag{4.25}$$

The fraction of ν_s present in atmospheric neutrino oscillations, $\eta_s^{atm} = \sin^2\alpha$, and the fraction of ν_s involved in the oscillations of the solar neutrinos, $\eta_s^{sol} = \cos^2\alpha$, should add up to unity in the 2+2 mass sceme [178]

$$\eta_s^{tot} \equiv \eta_s^{atm} + \eta_s^{sol} = 1\,. \tag{4.26}$$

This condition is in conflict with the solar and the atmospheric neutrino data. Indeed, as mentioned, the Super-K atmospheric data allowes the values $\eta_s^{atm} \leq 0.26$ (at 99 % C.L.) and according to ref. [179] the global solar neutrino data gives an upper limit of $\eta_s^{sol} \leq 0.45$ (at 99 % C.L.). Therefore, the 2+2 mass schemes are generally believed to be strongly disfavored by the solar and the atmospheric data[6].

It seems that all the four-neutrino models give poor fits to the data. As shown in [178], adding many sterile neutrinos to the 3+1 mixing scheme do not fit all the oscillation data much better than a single sterile neutrino. Therefore, if the MiniBooNE experiment will verify the LSND oscillation signal, we are facing a very interesting situation phenomenologically.

Recently CPT violation [54] has been proposed as a solution to the LSND oscillation signal. If CPT is not an exact symmetry of nature, more than two mass squared differences arise also in three-neutrino models as the neutrino and the antineutrino masses do not have to be the same. In case of CPT violation, MiniBooNE will not be able to confirm the LSND results, at least in its first phase, because it is looking for $\nu_\mu \to \nu_e$ oscillations. In case that CPT is violated, one has to look for $\overline{\nu}_\mu \to \overline{\nu}_e$ oscillation signal in order to confirm the LSND results [180].

[6]It should be noted that several different upper limits on η_s^{sol} and η_s^{atm} can be found in literature. E.g. ref. [180] quotes the values $\eta_s^{sol} \leq 0.18$ and $\eta_s^{atm} \leq 0.16$. Also, it has been argued that the sum rule (4.26) is relaxed as the matter effects and the small mixing angles are taken into account [181].

Chapter 5

Concluding remarks

Due to rapid increase in the amount of experimental data, neutrino physics phenomenology has been a particularly active research field in recent years and a lot of progress has taken place. Many models and ideas that seemed viable still a few years ago have become now disfavored or even excluded as a result of improved experimental accuracy and many new experiments that have been performed in recent times. So has happened also to the four-neutrino schemes considered in the original research papers of this thesis. New data from many experiments is expected in near future, and therefore neutrino physics phenomenology most likely continues to be a rapidly developing research field for many years to come.

However, the scientific problems that inspired our papers have been around for a long time and are most topical still today. The very fundamental question relating to the origin of neutrino masses is still unsolved: are neutrinos Dirac or Majorana particles? That is, are antineutrino and neutrino two different particles possessing different lepton numbers or just two spin orientations of one particle state? This question is answered if neutrinoless double beta decay is detected by future experiments.

Absolute value of neutrino masses also continues to be a challenging research topic. The smallness of neutrino masses is not at present explained properly by any theory since even though the see-saw mechanism generates small neutrino masses, it brings along a new large energy scale where all the lepton numbers are violated. What is this scale and what kind of physics does it contain? Detecting neutrinoless double beta decay in future experiments would not only establish the Majorana nature of neutrinos but would also be a valuable source of information on neutrino mixing angle elements and absolute values of neutrino masses.

Neutrino mixing matrix has turned out to be quite different from the quark mixing matrix, in contrast with what could naively be expected. Future long-baseline experiments will be able to determine the mixing parameters more precisely compared with the present situation, and some of the (distant) future projects, like the neutrino factories, are even expected to be able to detect im-

plications of leptonic CP violation, if it exists. Leptonic CP violation would be of course interesting from theory building point of view, but it could also have cosmological implications due to its role in the leptogenesis [182].

Another extremely important question is how many neutrino flavors are there. Do we need sterile neutrinos? If there exists a fourth neutrino flavor, neutrino physics phenomenology is naturally somewhat different from the three-neutrino case because there are more parameters involved. Specifically, finding indications of the leptonic CP violation could be easier in the four-neutrino case than in the three-neutrino case, as indicated by the results in Paper I [47]. It is also intuitively clear that chances to detect neutrinoless double beta decay could be better in the four-neutrino case since the LSND result suggests that at least one of the neutrino mass eigenvalues is rather large, $\gtrsim 0.5$ eV. However, it seems that all the four-neutrino models, which in principle could explain the results of the LSND laboratory experiment and the solar and the atmospheric data simultaneously in the framework of neutrino oscillations, are disfavored. The presently ongoing MiniBooNE experiment is of crucial importance because, if CPT is conserved, it will have the sensitivity to test the whole parameter region corresponding to the LSND signal.

Bibliography

[1] E. Fermi, Z. Phys. **88** (1934) 161.

[2] F. Reines and C. L. Cowan, Phys. Rev. **113** (1959) 273.

[3] G. Danby, J. M. Gaillard, K. Goulianos, L. M. Lederman, N. Mistry, M. Schwartz and J. Steinberger, Phys. Rev. Lett. **9** (1962) 36.

[4] K. Kodama *et al.* (DONUT Collaboration), Phys. Lett. B **504** (2001) 218, hep-ex/0012035.

[5] M. L. Perl *et al.*, Phys. Rev. Lett. **35** (1975) 1489; M. L. Perl *et al.*, Phys. Lett. B **63** (1976) 466.

[6] B. Pontecorvo, Sov. Phys. JETP **6** (1957) 429 [Zh. Eksp. Teor. Fiz. **33** (1957) 549]; B. Pontecorvo, Sov. Phys. JETP **7** (1958) 172 [Zh. Eksp. Teor. Fiz. **34** (1957) 247].

[7] Z. Maki, M. Nakagawa and S. Sakata, Prog. Theor. Phys. **28** (1962) 870.

[8] C. L. Bennett *et al.*, astro-ph/0302207.

[9] A. Pierce and H. Murayama, hep-ph/0302131.

[10] C. Giunti, hep-ph/0302173.

[11] S. Hannestad, astro-ph/0303076.

[12] M. Shiozawa (Super-Kamiokande Collaboration), presented at the Neutrino 2002 Conference, Munich, Germany, May 2002, http://neutrino2002.ph.tum.de/.

[13] E. K. Akhmedov, presented at the Neutrino 2002 Conference, Munich, Germany, May 2002, hep-ph/0207342.

[14] V. D. Barger, D. Marfatia and K. Whisnant, Phys. Rev. Lett. **88** (2002) 011302, hep-ph/0106207; J. N. Bahcall, M. C. Gonzalez-Garcia and C. Pena-Garay, JHEP **0207** (2002) 054, hep-ph/0204314; V. Barger, D. Marfatia, K. Whisnant and B. P. Wood, Phys. Lett. B **537** (2002) 179, hep-ph/0204253.

[15] S. L. Glashow, Nucl. Phys. **22** (1961) 579; A. Salam and J. C. Ward, Phys. Lett. **13** (1964) 168; S. Weinberg, Phys. Rev. Lett. **19** (1967) 1264; A. Salam, Originally printed in Ed. N. Svartholm: *Elementary Particle Theory*, Proceedings of the Nobel Symposium held 1968 At Lerum, Sweden, Stockholm, Almqvist & Wiksell (1968), 367-377.

[16] S. L. Glashow, J. Iliopoulos and L. Maiani, Phys. Rev. D **2** (1970) 1285; D. J. Gross and F. Wilczek, Phys. Rev. Lett. **30** (1973) 1343; H. D. Politzer, Phys. Rev. Lett. **30** (1973) 1346.

[17] P. W. Higgs, Phys. Lett. **12** (1964) 132; P. W. Higgs, Phys. Rev. Lett. **13** (1964) 508; G. S. Guralnik, C. R. Hagen and T. W. Kibble, Phys. Rev. Lett. **13** (1964) 585; T. W. Kibble, Phys. Rev. **155** (1967) 1554.

[18] G. 't Hooft, Nucl. Phys. B **33** (1971) 173; Nucl. Phys. B **35** (1971) 167.

[19] See e.g. S. Weinberg, *The Quantum Theory of Fields, Vol. 2*, Cambridge University Press (1996), Cambridge, UK; M. E. Peskin and D. V. Schroeder, *An Introduction to Quantum Field Theory*, Addison-Wesley Publishing Company (1995), Reading, USA; F. Mandl and G. Shaw, *Quantum Field Theory*, A Wiley-Interscience Publication (1984), Chichester, UK; L. H. Ryder, *Quantum Field Theory*, Cambridge University Press (1985), Cambridge, UK.

[20] N. Cabibbo, Phys. Rev. Lett. **10** (1963) 531.

[21] M. Kobayashi and T. Maskawa, Prog. Theor. Phys. **49** (1973) 652.

[22] K. Hagiwara *et al.* (Particle Data Group), Phys. Rev. D **66** (2002) 010001.

[23] D. G. Charlton, presented at the 30th SLAC Summer Institute on Particle Physics: Secrets of the B Meson (SSI 2002), SLAC, Menlo Park, California, Aug 2002, hep-ex/0211003.

[24] D. N. Spergel *et al.*, astro-ph/0302209.

[25] R. Barbieri and A. Dolgov, Phys. Lett. B **237** (1990) 440; Nucl. Phys. B **349** (1991) 743; K. Kainulainen, Phys. Lett. B **244** (1990) 191; K. Enqvist, K. Kainulainen and J. Maalampi, Phys. Lett. B **249** (1990) 531; Nucl. Phys. B **349** (1991) 754.

[26] K. Enqvist, K. Kainulainen and M. J. Thomson, Nucl. Phys. B **373** (1992) 498.

[27] K. Kainulainen and K. A. Olive, to appear in 'Neutrino Mass', Springer Tracts in Modern Physics, ed. by G. Altarelli and K. Winter, hep-ph/0206163.

[28] O. Elgaroy *et al.*, Phys. Rev. Lett. **89** (2002) 061301, astro-ph/0204152.

[29] B. Kayser, presented at TASI 2000, the Theoretical Advanced Study Institute in elementary particle physics held in Boulder, Colorado, USA, June 2000, hep-ph/0104147.

[30] R. N. Mohapatra and P. B. Pal, World Sci. Lect. Notes Phys. **60** (1998) 1.

[31] A. Aguilar *et al.* (LSND collaboration), Phys. Rev. D **64** (2001) 112007, hep-ex/0104049.

[32] K. Eguchi *et al.* (KamLAND Collaboration), Phys. Rev. Lett. **90** (2003) 021802, hep-ex/0212021.

[33] M. H. Ahn *et al.* (K2K Collaboration), Phys. Rev. Lett. **90** (2003) 041801, hep-ex/0212007.

[34] S. M. Bilenky, C. Giunti and W. Grimus, Prog. Part. Nucl. Phys. **43** (1999) 1, hep-ph/9812360.

[35] B. Kayser, F. Gibrat-Debu and F. Perrier, *"The Physics Of Massive Neutrinos"*, World Sci. Lect. Notes Phys. **25** (1989) 1.

[36] G. B. Gelmini and M. Roncadelli, Phys. Lett. B **99** (1981) 411.

[37] C. W. Kim and A. Pevsner, *Neutrinos In Physics And Astrophysics*, (Contemporary concepts in physics, 8), Harwood Academic Publishers (1993), Chur, Switzerland.

[38] M. Gell-Mann, P. Ramond and R. Slansky, proceedings of the Stony Brook Workshop, New York, 1979, published in *Supergravity*, edited by P. van Nieuwenhuizen and D. Z. Freedman, North Holland Publ. Co., Amsterdam, 1979; T. Yanagida, published in *Proceedings of the Workshop on the Unified theories and Baryon Number in the Universe*, Tsukuba, Japan, 1979, edited by O. Sawada and A. Sugamoto, KEK Report No. 79-18, Tsukuba, 1979.

[39] L. Wolfenstein, Nucl. Phys. B **186** (1981) 147.

[40] K. R. Balaji, A. Kalliomäki and J. Maalampi, Phys. Lett. B **524** (2002) 153. (Paper III of this thesis)

[41] N. Arkani-Hamed, S. Dimopoulos, G. R. Dvali and J. March-Russell, Phys. Rev. D **65** (2002) 024032, hep-ph/9811448.

[42] G. R. Dvali and A. Y. Smirnov, Nucl. Phys. B **563** (1999) 63, hep-ph/9904211.

[43] N. Arkani-Hamed, S. Dimopoulos and G. R. Dvali, Phys. Lett. B **429** (1998) 263, hep-ph/9803315.

[44] A. Barroso and J. Maalampi, Phys. Lett. B **132** (1983) 355.

[45] S. F. King, JHEP **0209** (2002) 0411, hep-ph/0204360.

[46] V. D. Barger, Y. B. Dai, K. Whisnant and B. L. Young, Phys. Rev. D **59** (1999) 113010, hep-ph/9901388.

[47] A. Kalliomäki, J. Maalampi and M. Tanimoto, Phys. Lett. B **469** (1999) 179, hep-ph/9909301. (Paper I of this thesis)

[48] A. Kalliomäki and J. Maalampi, Phys. Lett. B **484** (2000) 64, hep-ph/0003281. (Paper II of this thesis)

[49] W. Grimus, S. Mohanty and P. Stockinger, presented by W. Grimus at *Neutrino meeting*, Meeting in Honour of Samoil Bilenky's 70th Birthday, Torino, March 25-27, 1999, hep-ph/9909341.

[50] See e.g. B. Kayser, Phys. Rev. D **24** (1981) 110.

[51] C. Giunti, C. W. Kim, J. A. Lee and U. W. Lee, Phys. Rev. D **48** (1993) 4310, hep-ph/9305276; W. Grimus and P. Stockinger, Phys. Rev. D **54** (1996) 3414, hep-ph/9603430; Y. V. Shtanov, Phys. Rev. D **57** (1998) 4418, hep-ph/9706378; C. Giunti, C. W. Kim and U. W. Lee, Phys. Lett. B **421** (1998) 237, hep-ph/9709494; A. Ioannisian and A. Pilaftsis, Phys. Rev. D **59** (1999) 053003, hep-ph/9809503; W. Grimus, P. Stockinger and S. Mohanty, Phys. Rev. D **59** (1999) 013011, hep-ph/9807442; C. Y. Cardall, Phys. Rev. D **61** (2000) 073006, hep-ph/9909332;

[52] L. Wolfenstein, Phys. Rev. D **17** (1978) 2369.

[53] S. P. Mikheev and A. Y. Smirnov, Nuovo Cim. **9C** (1986) 17.

[54] See e.g. H. Murayama and T. Yanagida, Phys. Lett. B **520** (2001) 263, hep-ph/0010178; G. Barenboim, L. Borissov, J. Lykken and A. Y. Smirnov, JHEP **0210** (2002) 001, hep-ph/0108199; G. Barenboim, L. Borissov and J. Lykken, Phys. Lett. B **534** (2002) 106, hep-ph/0201080.

[55] C. G. Callan, R. F. Dashen and D. J. Gross, Phys. Lett. B **63** (1976) 334; R. Jackiw and C. Rebbi, Phys. Rev. Lett. **37** (1976) 172.

[56] J. H. Christenson, J. W. Cronin, V. L. Fitch and R. Turlay, Phys. Rev. Lett. **13** (1964) 138.

[57] B. Aubert *et al.* (BABAR Collaboration), Phys. Rev. Lett. **87** (2001) 091801, hep-ex/0107013; K. Abe *et al.* (Belle Collaboration), Phys. Rev. Lett. **87** (2001) 091802, hep-ex/0107061.

[58] S. M. Bilenky and S. T. Petcov, Rev. Mod. Phys. **59** (1987) 671 [Erratum-ibid. **61** (1989) 169].

[59] S. M. Bilenky, N. P. Nedelcheva and S. T. Petcov, Nucl. Phys. B **247** (1984) 61.

[60] S. Turck-Chieze, S. Cahen, M. Casse and C. Doom, Astrophys. J. **335** (1988) 415; J. N. Bahcall and R. K. Ulrich, Rev. Mod. Phys. **60** (1988) 297; J. N. Bahcall and M. H. Pinsonneault, Rev. Mod. Phys. **64** (1992) 885; J. N. Bahcall and M. H. Pinsonneault, Rev. Mod. Phys. **67** (1995) 781, hep-ph/9505425; J. N. Bahcall, S. Basu and M. H. Pinsonneault, Phys. Lett. B **433** (1998) 1, astro-ph/9805135.

[61] J. N. Bahcall, M. H. Pinsonneault and S. Basu, Astrophys. J. **555** (2001) 990, astro-ph/0010346.

[62] R. Davis, Jr., D. S. Harmer and K. C. Hoffman, Phys. Rev. Lett. **20** (1968) 1205.

[63] B. T. Cleveland *et al.*, Astrophys. J. **496** (1998) 505.

[64] J. N. Abdurashitov *et al.* (SAGE Collaboration), J. Exp. Theor. Phys. **95** (2002) 181 [Zh. Eksp. Teor. Fiz. **122** (2002) 211], astro-ph/0204245.

[65] W. Hampel *et al.* (GALLEX collaboration), Phys. Lett. B **447** (1999) 127.

[66] M. Altmann *et al.* (GNO collaboration), Phys. Lett. B**490** (2000) 16, hep-ex/0006034.

[67] T. Kirsten, presented at the Neutrino 2002 Conference, Munich, Germany, May 2002, http://neutrino2002.ph.tum.de/.

[68] Y. Fukuda *et al.* (Kamiokande collaboration), Phys. Rev. Lett. **77** (1996) 1683.

[69] Y. Fukuda *et al.* (Super-Kamiokande collaboration), Phys. Rev. Lett. **86** (2001) 5656, hep-ex/0103033; M. Smy *et al.* (Super-Kamiokande Collaboration), presented at Neutrino 2002 Conference, Munich, Germany, May 2002, http://neutrino2002.ph.tum.de/.

[70] S. Fukuda *et al.* (Super-Kamiokande Collaboration), Phys. Lett. B **539** (2002) 179, hep-ex/0205075.

[71] Q. R. Ahmad *et al.* (SNO Collaboration), Phys. Rev. Lett. **89** (2002) 011301, nucl-ex/0204008.

[72] Q. R. Ahmad *et al.* (SNO Collaboration), Phys. Rev. Lett. **89** (2002) 011302, nucl-ex/0204009.

[73] G. Alimonti *et al.* (Borexino Collaboration), Astropart. Phys. **16** (2002) 205, hep-ex/0012030. E. Meroni, presented at Europhysics Neutrino Oscillation Workshop (NOW 2000), Conca Specchiulla, Otranto, Lecce, Italy, Sep 2000, Nucl. Phys. Proc. Suppl. **100** (2001) 42; G. Ranucci *et al.* (BOREXINO Collaboration), presented at Neutrino 2000, Sudbury, Ontario, Canada, Jun 2000, Nucl. Phys. Proc. Suppl. **91** (2001) 58.

[74] G. L. Fogli, G. Lettera, E. Lisi, A. Marrone, A. Palazzo and A. Rotunno, Phys. Rev. D **66** (2002) 093008, hep-ph/0208026.

[75] G. L. Fogli, E. Lisi, A. Marrone, D. Montanino, A. Palazzo and A. M. Rotunno, Phys. Rev. D **67** (2003) 073002, hep-ph/0212127.

[76] L. Wolfenstein, Phys. Rev. D **17** (1978) 2369;

[77] C. S. Lim and W. J. Marciano, Phys. Rev. D **37** (1988) 1368; E. K. Akhmedov, Phys. Lett. B **213** (1988) 64. See also B. C. Chauhan and J. Pulido, Phys. Rev. D **66** (2002) 053006, hep-ph/0206193, and references therein.

[78] P. C. de Holanda and A. Y. Smirnov, JCAP **0302** (2003) 001, hep-ph/0212270.

[79] R. Becker-Szendy *et al.*, Phys. Rev. D **46** (1992) 3720.

[80] K. S. Hirata *et al.* (Kamiokande-II Collaboration), Phys. Lett. B **280** (1992) 146.

[81] Y. Fukuda *et al.* (Kamiokande Collaboration), Phys. Lett. B **335** (1994) 237.

[82] M. Shiozawa for the Super-K Collaboration, presented at the Neutrino 2002 Conference, Munich, Germany, May 2002, http://neutrino2002.ph.tum.de/.

[83] W. W. Allison *et al.* (Soudan-2 Collaboration), Phys. Lett. B **449** (1999) 137, hep-ex/9901024.

[84] See e.g. V. Agrawal, T. K. Gaisser, P. Lipari and T. Stanev, Phys. Rev. D **53** (1996) 1314, hep-ph/9509423; G. Barr, T. K. Gaisser and T. Stanev, Phys. Rev. D **39** (1989) 3532; G. Battistoni, A. Ferrari, P. Lipari, T. Montaruli, P. R. Sala and T. Rancati, Astropart. Phys. **12** (2000) 315, hep-ph/9907408; G. Fiorentini, V. A. Naumov and F. L. Villante, Phys. Lett. B **510** (2001) 173, hep-ph/0103322.

[85] F. Reines *et al.*, Phys. Rev. Lett. **15** (1965) 429; H. Achar *et al.*, Phys. Lett. **18** (1965) 196.

[86] K. Daum *et al.* (Frejus Collaboration), Z. Phys. C **66** (1995) 417.

[87] M. Aglietta *et al.* (NUSEX Collaboration), Europhys. Lett. **8** (1989) 611.

[88] M. Ambrosio *et al.* (MACRO Collaboration), Phys. Lett. B **434** (1998) 451, hep-ex/9807005.

[89] M. Ambrosio *et al.* (MACRO Collaboration), Phys. Lett. B **517** (2001) 59, hep-ex/0106049.

[90] E. N. Alekseev *et al.*, Phys. Part. Nucl. **29** (1998) 254 [Fiz. Elem. Chast. Atom. Yadra **29** (1998) 631]; M. M. Boliev, A. V. Butkevich, A. E. Chudakov, S. P. Mikheev, O. V. Suvorova and V. N. Zakidyshev, Nucl. Phys. Proc. Suppl. **70** (1999) 371.

[91] Y. Fukuda *et al.* (Super-Kamiokande Collaboration), Phys. Rev. Lett. **81** (1998) 1562, hep-ex/9807003.

[92] K. Scholberg (Super-Kamiokande Collaboration), presented at the 8th International Workshop on Neutrino Telescopes, Venice, Italy, Feb 1999, hep-ex/9905016.

[93] Y. Fukuda *et al.* (Super-Kamiokande Collaboration), Phys. Lett. B **467** (1999) 185, hep-ex/9908049.

[94] V. D. Barger, J. G. Learned, S. Pakvasa and T. J. Weiler, Phys. Rev. Lett. **82** (1999) 2640, astro-ph/9810121; V. D. Barger, J. G. Learned, P. Lipari, M. Lusignoli, S. Pakvasa and T. J. Weiler, Phys. Lett. B **462** (1999) 109, hep-ph/9907421.

[95] E. Lisi, A. Marrone and D. Montanino, Phys. Rev. Lett. **85** (2000) 1166, hep-ph/0002053.

[96] M. C. Gonzalez-Garcia *et al.*, Phys. Rev. Lett. **82** (1999) 3202, hep-ph/9809531.

[97] E. T. Kearns, Frascati Phys. Ser. **28** (2002) 413, hep-ex/0210019.

[98] S. Fukuda *et al.* (Super-Kamiokande Collaboration), Phys. Rev. Lett. **85** (2000) 3999, hep-ex/0009001.

[99] C. Athanassopoulos *et al.* (LSND Collaboration), Phys. Rev. Lett. **81** (1998) 1774, nucl-ex/9709006.

[100] Y. Declais *et al.* (Bugey Collaboration), Nucl. Phys. B **434** (1995) 503.

[101] M. Apollonio *et al.* (CHOOZ Collaboration), Phys. Lett. B **466** (1999) 415, hep-ex/9907037.

[102] See eg. S. J. Yellin, proceedings of Conference on Particle Physics and the Early Universe (COSMO 98), Monterey, CA, USA, Nov 1998, edited by D. Caldwell, AIP Conference Proceedings 478, Springer-Verlag, 1999, hep-ex/9902012.

[103] B. Armbruster *et al.* (KARMEN Collaboration), Phys. Rev. D **65** (2002) 112001, hep-ex/0203021.

[104] E. D. Church, K. Eitel, G. B. Mills and M. Steidl, Phys. Rev. D **66** (2002) 013001, hep-ex/0203023.

[105] A. O. Bazarko (BooNE Collaboration), Proceedings of the 31st International Conference on High Energy Physics (ICHEP 2002), Amsterdam, The Netherlands, Jul 2002, hep-ex/0210020.

[106] M. C. Gonzalez-Garcia and Y. Nir, hep-ph/0202058.

[107] F. Boehm *et al.*, Phys. Rev. D **64** (2001) 112001, hep-ex/0107009.

[108] G. Zacek *et al.*, Phys. Rev. D **34** (1986) 2621.

[109] G. S. Vidyakin *et al.*, JETP Lett. **59** (1994) 390 [Pisma Zh. Eksp. Teor. Fiz. **59** (1994) 364].

[110] A. Piepke (KamLAND Collaboration), Nucl. Phys. Proc. Suppl. **91** (2001) 99; V. D. Barger, D. Marfatia and B. P. Wood, Phys. Lett. B **498** (2001) 53, hep-ph/0011251.

[111] M. V. Diwan, presented at the 7th International Workshop on Tau Lepton Physics (TAU 02), Santa Cruz, California, Sep 2002, hep-ex/0211026.

[112] A. Rubbia, Nucl. Phys. Proc. Suppl. **91** (2000) 223, hep-ex/0008071.

[113] J. Rico (ICARUS Collaboration), presented at the 37th Rencontres de Moriond on Electroweak Interactions and Unified Theories, Les Arcs, France, Mar 2002, hep-ex/0205028; F. Arneodo *et al.*, Nucl. Instrum. Meth. A **461** (2001) 324.

[114] For reviews on present and future $0\nu\beta\beta$ experiments, see e.g. S. R. Elliott, presented at Neutrinos and Implications for Physics Beyond the Standard Model, Stony Brook, New York, Oct 2002, nucl-ex/0301011; S. R. Elliott and P. Vogel, Feb 2002, hep-ph/0202264.

[115] M. Gunther *et al.*, Phys. Rev. D **55** (1997) 54.

[116] H. V. Klapdor-Kleingrothaus *et al.*, presented by A. Dietz at the 3rd International Conference on Dark Matter in Astro and Particle Physics (Dark 2000), Heidelberg, Germany, Jul 2000, Eur. Phys. J. A **12** (2001) 147, hep-ph/0103062.

[117] C. E. Aalseth *et al.* (IGEX Collaboration), Phys. Rev. D **65** (2002) 092007, hep-ex/0202026.

[118] A. Alessandrello *et al.*, Phys. Lett. B **486** (2000) 13.

[119] R. Luscher *et al.*, Phys. Lett. B **434** (1998) 407.

[120] H. Ejiri *et al.*, Phys. Rev. C **63** (2001) 065501.

[121] X. Sarazin and D. Lalanne (NEMO Collaboration), Presented at the Neutrino 2000 Conference, Sudbury, Ontario, Canada, Jun 2000 and at ICHEP 2000, Osaka, Japan, 27 Jul - 2 Aug 2000, hep-ex/0006031.

[122] A. Alessandrello *et al.* (CUORE Collaboration), Phys. Atom. Nucl. **66** (2003) 452 [Yad. Fiz. **66** (2003) 480], hep-ex/0201038.

[123] M. Danilov *et al.*, Phys. Lett. B **480** (2000) 12, hep-ex/0002003.

[124] C. E. Aalseth *et al.* (Majorana Collaboration), presented at the 3rd International Conference on Nonaccelerator New Physics (NANPino 01), Dubna, Russia, Jun 2001, hep-ex/0201021.

[125] H. V. Klapdor-Kleingrothaus, presented at NOON 2000, Tokyo, Japan, Dec 2000, hep-ph/0103074; H. V. Klapdor-Kleingrothaus, Nucl. Phys. Proc. Suppl. **100** (2001) 350, hep-ph/0102277.

[126] H. V. Klapdor-Kleingrothaus, A. Dietz, H. L. Harney and I. V. Krivosheina, Mod. Phys. Lett. A **16** (2001) 2409, hep-ph/0201231.

[127] C. E. Aalseth *et al.*, Mod. Phys. Lett. A **17** (2002) 1475, hep-ex/0202018.

[128] M. Apollonio *et al.*, hep-ph/0210192.

[129] Y. Itow *et al.* (JHF Collaboration), hep-ex/0106019.

[130] D. Ayres *et al.*, hep-ex/0210005; G. Barenboim, A. De Gouvea, M. Szleper and M. Velasco, hep-ph/0204208; A. Para and M. Szleper, hep-ex/0110032.

[131] M. Mezzetto, presented at the NuFact workshop, London, July 2002, hep-ex/0302005; J. J. Gomez-Cadenas *et al.* (CERN working group on Super Beams Collaboration), hep-ph/0105297.

[132] C. K. Jung, published in the proceedings of International Workshop on Next Generation Nucleon Decay and Neutrino Detector (NNN 99), Stony Brook, New York, Sep 1999, hep-ex/0005046.

[133] P. Zucchelli, Phys. Lett. B **532** (2002) 166.

[134] M. Mezzetto, presented at the NuFact workshop, London, July 2002, hep-ex/0302007.

[135] See e.g. C. Albright *et al.*, May 2000, hep-ex/0008064; M. M. Alsharoa *et al.* (Muon Collider/Neutrino Factory Collaboration), October 2002, hep-ex/0207031; S. Geer, presented at the Neutrino 2002 Conference, Munich, Germany, May 2002, hep-ex/0207036.

[136] P. Hernandez and O. Yasuda, Nucl. Instrum. Meth. A **485** (2002) 811; P. Huber and W. Winter, hep-ph/0301257; J. Burguet-Castell, M. B. Gavela, J. J. Gomez-Cadenas, P. Hernandez and O. Mena, Nucl. Phys. B **646** (2002) 301, hep-ph/0207080;

A. Donini, D. Meloni and P. Migliozzi, Nucl. Phys. B **646** (2002) 321, hep-ph/0206034; A. Broncano and O. Mena, hep-ph/0203052; A. Bueno, M. Campanelli, S. Navas-Concha and A. Rubbia, Nucl. Phys. B **631** (2002) 239, hep-ph/0112297; M. Freund, P. Huber and M. Lindner, Nucl. Phys. B **615** (2001) 331, hep-ph/0105071; J. Burguet-Castell, M. B. Gavela, J. J. Gomez-Cadenas, P. Hernandez and O. Mena, Nucl. Phys. B **608** (2001) 301, hep-ph/0103258; P. Lipari, Phys. Rev. D **64** (2001) 033002, hep-ph/0102046; T. Hattori, T. Hasuike and S. Wakaizumi, Phys. Rev. D **65** (2002) 073027, hep-ph/0109124; V. D. Barger, S. Geer, R. Raja and K. Whisnant, Phys. Rev. D **62** (2000) 073002, hep-ph/0003184; V. D. Barger, S. Geer, R. Raja and K. Whisnant, Phys. Rev. D **62** (2000) 013004, hep-ph/9911524; A. De Rujula, M. B. Gavela and P. Hernandez, Nucl. Phys. B **547** (1999) 21, hep-ph/9811390; S. Geer, Phys. Rev. D **57** (1998) 6989 [Erratum-ibid. D **59** (1999) 039903], hep-ph/9712290.

[137] M. Tanimoto, Phys. Lett. B **462** (1999) 115, hep-ph/9906516.

[138] A. Cervera, A. Donini, M. B. Gavela, J. J. Gomez Cadenas, P. Hernandez, O. Mena and S. Rigolin, Nucl. Phys. B **579** (2000) 17 [Erratum-ibid. B **593** (2001) 731], hep-ph/0002108.

[139] P. Huber, M. Lindner and W. Winter, Nucl. Phys. B **645** (2002) 3, hep-ph/0204352.

[140] M. Lindner, presented at the Neutrino 2002 Conference, Munich, Germany, May 2002, hep-ph/0210377.

[141] S. M. Bilenky, C. Giunti and W. Grimus, Phys. Rev. D **58** (1998) 033001, hep-ph/9712537.

[142] H. Minakata and H. Nunokawa, Phys. Lett. B **495** (2000) 369, hep-ph/0004114.

[143] H. Minakata and H. Nunokawa, Phys. Lett. B **413** (1997) 369, hep-ph/9706281; J. Arafune, M. Koike and J. Sato, Phys. Rev. D **56** (1997) 3093 [Erratum-ibid. D **60** (1999) 119905], hep-ph/9703351.

[144] J. Burguet-Castell, M. B. Gavela, J. J. Gomez-Cadenas, P. Hernandez and O. Mena, Nucl. Phys. B **608** (2001) 301, hep-ph/0103258.

[145] H. Minakata and H. Nunokawa, Phys. Rev. D **57** (1998) 4403, hep-ph/9705208.

[146] R. Barate *et al.* (ALEPH Collaboration), Eur. Phys. J. C **2** (1998) 395.

[147] K. Assamagan *et al.*, Phys. Rev. D **53** (1996) 6065.

[148] Ch. Weinheimer, presented at the Neutrino 2002 Conference, Munich, Germany, May 2002, http://neutrino2002.ph.tum.de/.

[149] J. Bonn *et al.*, Nucl. Phys. Proc. Suppl. **91** (2001) 273.

[150] A. Osipowicz *et al.* (KATRIN Collaboration), hep-ex/0109033; C. Weinheimer (KATRIN Collaboration), Prog. Part. Nucl. Phys. **48** (2002) 141.

[151] Y. Farzan, O. L. Peres and A. Y. Smirnov, Nucl. Phys. B **612** (2001) 59, hep-ph/0105105.

[152] W. Hu, D. J. Eisenstein and M. Tegmark, Phys. Rev. Lett. **80** (1998) 5255, astro-ph/9712057.

[153] See e.g. J. A. Peacock, *Cosmological Physics*, Cambridge University Press (1999), Cambridge, UK.

[154] See e.g. S. M. Bilenky, C. Giunti, J. A. Grifols and E. Masso, hep-ph/0211462; H. V. Klapdor-Kleingrothaus, H. Pas and A. Y. Smirnov, Phys. Rev. D **63** (2001) 073005, hep-ph/0003219; S. Pascoli and S. T. Petcov, Phys. Lett. B **544** (2002) 239, hep-ph/0205022.

[155] C. Giunti, Phys. Rev. D **61** (2000) 036002, hep-ph/9906275; S. M. Bilenky, C. Giunti, W. Grimus, B. Kayser and S. T. Petcov, Phys. Lett. B **465** (1999) 193, hep-ph/9907234.

[156] S. M. Bilenky, presented at International School of Physics Enrico Fermi, Varenna, Lake Como, Italy, 6-16 Aug 2002, hep-ph/0210128.

[157] H. W. Zaglauer and K. H. Schwarzer, Z. Phys. C **40** (1988) 273.

[158] P. C. de Holanda and A. Y. Smirnov, Phys. Rev. D **66** (2002) 113005, hep-ph/0205241.

[159] T. K. Kuo and J. Pantaleone, Phys. Rev. Lett. **57** (1986) 1805; S. P. Mikheev and A. Y. Smirnov, Phys. Lett. B **200** (1988) 560.

[160] S. J. Parke, Phys. Rev. Lett. **57** (1986) 1275.

[161] C. S. Lim, K. Ogure and H. Tsujimoto, Phys. Rev. D **67** (2003) 033007, hep-ph/0210066.

[162] See G. L. Fogli, E. Lisi and A. Palazzo, Phys. Rev. D **65** (2002) 073019, hep-ph/0105080 and references therein.

[163] G. L. Fogli, E. Lisi and D. Montanino, Phys. Rev. D **54** (1996) 2048, hep-ph/9605273; G. L. Fogli, E. Lisi, D. Montanino and A. Palazzo, Phys. Rev. D **62** (2000) 113004, hep-ph/0005261; A. M. Gago, H. Nunokawa and R. Zukanovich-Funchal, Phys. Rev. D **63** (2001) 013005 [Erratum-ibid. D **64** (2001) 119902], hep-ph/0007270.

[164] G. L. Fogli, E. Lisi, D. Montanino and G. Scioscia, Phys. Rev. D **55** (1997) 4385, hep-ph/9607251.

[165] M. C. Gonzalez-Garcia, M. Maltoni, C. Pena-Garay and J. W. Valle, Phys. Rev. D **63** (2001) 033005, hep-ph/0009350; G. L. Fogli, E. Lisi and A. Marrone, Phys. Rev. D **64** (2001) 093005, hep-ph/0105139; G. L. Fogli, E. Lisi, A. Marrone and G. Scioscia, Phys. Rev. D **59** (1999) 033001, hep-ph/9808205; A. De Rujula, M. B. Gavela and P. Hernandez, Phys. Rev. D **63** (2001) 033001, hep-ph/0001124.

[166] M. C. Gonzalez-Garcia and M. Maltoni, Eur. Phys. J. C **26** (2003) 417, hep-ph/0202218.

[167] O. L. Peres and A. Y. Smirnov, Phys. Lett. B **456** (1999) 204, hep-ph/9902312; O. L. Peres and A. Y. Smirnov, Nucl. Phys. Proc. Suppl. **110** (2002) 355, hep-ph/0201069.

[168] K. Matsuda, T. Fukuyama and H. Nishiura, hep-ph/0302254; W. Rodejohann, hep-ph/0203214; S. Pascoli, S. T. Petcov and W. Rodejohann, Phys. Lett. B **549** (2002) 177, hep-ph/0209059; V. Barger, S. L. Glashow, P. Langacker and D. Marfatia, Phys. Lett. B **540** (2002) 247, hep-ph/0205290.

[169] S. M. Bilenky, S. Pascoli and S. T. Petcov, Phys. Rev. D **64** (2001) 113003, hep-ph/0104218; S. M. Bilenky, S. Pascoli and S. T. Petcov, Phys. Rev. D **64** (2001) 053010, hep-ph/0102265.

[170] C. Jarlskog, Phys. Rev. Lett. **55** (1985) 1039.

[171] M. Maltoni, T. Schwetz and J. W. Valle, Phys. Rev. D **65** (2002) 093004, hep-ph/0112103.

[172] M. Maltoni, T. Schwetz, M. A. Tortola and J. W. Valle, Nucl. Phys. Proc. Suppl. **114** (2003) 203, hep-ph/0209368.

[173] S. M. Bilenky, C. Giunti and W. Grimus, proceedings of the Neutrino 1996 conference, Helsinki, Finland, June 1996, edited by K. Enqvist *et al.*, p. 174, World Scientific, Singapore, 1997, hep-ph/9609343; V. D. Barger, S. Pakvasa, T. J. Weiler and K. Whisnant, Phys. Rev. D **58** (1998) 093016, hep-ph/9806328; S. M. Bilenky, C. Giunti, W. Grimus and T. Schwetz, Phys. Rev. D **60** (1999) 073007, hep-ph/9903454; W. Grimus and T. Schwetz, Eur. Phys. J. C **20** (2001) 1, hep-ph/0102252.

[174] S. M. Bilenky, C. Giunti and W. Grimus, Eur. Phys. J. C **1** (1998) 247, hep-ph/9607372.

[175] F. Dydak *et al.* (the CDHS collaboration), Phys. Lett. B **134** (1984) 281.

[176] M. Mezzetto (NOMAD Collaboration), Nucl. Phys. Proc. Suppl. **70** (1999) 214.

[177] M. Maltoni, T. Schwetz and J. W. Valle, Phys. Lett. B **518** (2001) 252, hep-ph/0107150; W. Grimus and T. Schwetz, Eur. Phys. J. C **20** (2001) 1, hep-ph/0102252.

[178] O. L. Peres and A. Y. Smirnov, Nucl. Phys. B **599** (2001) 3, hep-ph/0011054.

[179] M. Maltoni, T. Schwetz, M. A. Tortola and J. W. Valle, Nucl. Phys. B **643** (2002) 321, hep-ph/0207157.

[180] A. Strumia, Phys. Lett. B **539** (2002) 91, hep-ph/0201134.

[181] H. Päs, L. g. Song and T. J. Weiler, Phys. Rev. D **67** (2003) 073019, hep-ph/0209373.

[182] M. Fukugita and T. Yanagida, Phys. Lett. B **174** (1986) 45.

[183] M. Alonso and H. Valk, *Quantum Mechanics: Principles and Applications*, Addison Wesley Publishing Company (1973), Reading, USA.

Appendix A

Adiabatic neutrino evolution in matter

In case of varying matter density the matter effect on the CP-odd asymmetry $\Delta P_{\alpha\beta} = P(\nu_\alpha \to \nu_\beta) - P(\overline{\nu}_\alpha \to \overline{\nu}_\beta)$, can be calculated numerically. Approximative analytic formulas, applicable to the long-baseline neutrino experiments, can also be derived by considering the matter effect as the first-order correction in the perturbation theory. In this Appendix we present the derivation of the result of Minakata and Nunokawa [145] for the $\Delta P_{\alpha\beta}$ which was used in Paper I of this thesis.

Evolution equation for flavor neutrinos $\nu = (\nu_e, \nu_\mu, \nu_\tau)^T$ in the medium is given by

$$i\frac{d}{dx}\nu = H(x)\nu\,, \tag{A.1}$$

where the Hamiltonian in the flavor basis is

$$H = H_0 + H' = U\,\frac{1}{2E}\begin{pmatrix} m_1^2 & 0 & 0 \\ 0 & m_2 & 0 \\ 0 & 0 & m_3 \end{pmatrix} U^\dagger + \begin{pmatrix} a(x) & 0 & 0 \\ 0 & 0 & 0 \\ 0 & 0 & 0 \end{pmatrix}. \tag{A.2}$$

Matter effect is described by $a(x) = \pm\sqrt{2}G_F n_e(x)$, where $n_e(x)$ is the electron number density in the earth and $+$ $(-)$ sign is for neutrinos (antineutrinos). The unitary matrix U in eq. (A.2) diagonalizes H_0, the vacuum Hamiltonian in the flavor basis.

Introducing the unitary transformation $V(x)$ which diagonalizes the total Hamiltonian $H(x)$ locally,

$$V^\dagger(x)H(x)V(x) = H_d(x) = \mathrm{diag}(h_1(x), h_2(x), h_3(x))\,, \tag{A.3}$$

the mass eigenstate basis in matter can be defined by

$$\begin{pmatrix} \nu_{m_1} \\ \nu_{m_2} \\ \nu_{m_3} \end{pmatrix} = V^\dagger(x)\begin{pmatrix} \nu_e \\ \nu_\nu \\ \nu_\tau \end{pmatrix}, \tag{A.4}$$

and the eq. (A.2) in the matter-mass eigenstate basis is given by

$$i\frac{d}{dx}\begin{pmatrix}\nu_{m_1}\\ \nu_{m_2}\\ \nu_{m_3}\end{pmatrix} = H_d(x)\begin{pmatrix}\nu_{m_1}\\ \nu_{m_2}\\ \nu_{m_3}\end{pmatrix} + i\frac{d}{dx}V^\dagger(x)\cdot V(x)\begin{pmatrix}\nu_{m_1}\\ \nu_{m_2}\\ \nu_{m_3}\end{pmatrix}. \tag{A.5}$$

In the adiabatic approximation the second term in the right-hand side is assumed to be so small that it can be ignored. This is a good approximation as long as the matter density varies slowly [145]. The solution for the evolution equation under the adiabatic approximation is given by

$$\nu_\alpha(x) = V_{\alpha i}(x)\,\exp\Big[-i\int_0^x dy h_i(y)\Big]V^*_{\beta i}(0)\nu_\beta(0)\,. \tag{A.6}$$

The probability to have neutrino ν_α at $x = L$ is then

$$\begin{aligned}|\nu_\alpha(L)|^2 &= V_{\alpha i}(L)\,\exp\Big[-i\int_0^x dy h_i(y)\Big]V^*_{\delta i}(0)\nu_\delta(0)\,\times\\ &\quad V^*_{\alpha j}(L)\,\exp\Big[i\int_0^x dy h_j(y)\Big]V_{\delta j}(0)\nu_\delta(0)^*\,,\end{aligned} \tag{A.7}$$

and if ν_β is created at $x = 0$ and ν_α is detected at $x = L$, the probability of neutrino oscillation $\nu_\beta \to \nu_\alpha$ is given by

$$P(\nu_\beta\to\nu_\alpha) = \sum_{ij} V_{\alpha i}(L)V^*_{\alpha j}(L)V^*_{\beta i}(0)V_{\beta j}(0)\,\exp\Big\{-i\int_0^L dx[h_i(x)-h_j(x)]\Big\}. \tag{A.8}$$

An idealized situation $V(0) \simeq V(L) \equiv V(a)$, where a refers to any point just below the earth surface with matter density ~ 2.7 g/cm^3, describes the experimental conditions suffiently well according to [145]. Like in the vacuum oscillation case, one can rewrite oscillation probability in a form

$$\begin{aligned}P(\nu_\beta\to\nu_\alpha) &= -4\sum_{j>i}\mathrm{Re}[V_{\alpha i}(a)V^*_{\alpha j}(a)V^*_{\beta i}(a)V_{\beta j}(a)]\sin^2[\frac{1}{2}I_{ij}(a)]\\ &+ 2\sum_{j>i}\mathrm{Im}[V_{\alpha i}(a)V^*_{\alpha j}(a)V^*_{\beta i}(a)V_{\beta j}(a)]\sin[I_{ij}(a)]\,,\end{aligned} \tag{A.9}$$

where

$$I_{ij}(a) = \int_0^L dx[h_i(x)-h_j(x)]\,. \tag{A.10}$$

A.1 Perturbative treatment of matter effect

The perturbative treatment of the matter effect can be used if the following condition is satisfied:

$$\frac{\Delta m^2}{E} = 10^{-12}\Big(\frac{\Delta m^2}{10^{-3}\,\mathrm{eV}^2}\Big)\Big(\frac{E}{1\mathrm{GeV}}\Big)^{-1}\,\mathrm{eV}$$

$$\gg \quad a = 1.04 \times 10^{-13} \Big(\frac{\rho}{2.7\mathrm{g/cm}^3}\Big)\Big(\frac{Y_e}{0.5}\Big)\,\mathrm{eV}\,, \tag{A.11}$$

where $Y_e = N_p/(N_p + N_n)$ is the electron fraction, i.e. the ratio of electrons to baryons (neutrons and protons) in the matter. In long-baseline experiments neutrino energies are typically $\gtrsim 1$ GeV, and therefore one must consider mass spectra where the mass-squard differences satisfy $\Delta m^2 \gtrsim 10^{-3}\,\mathrm{eV}^2$. The mass scale difference corresponding to the solar neutrino oscillations $\Delta m^2_{sol} \sim 10^{-5}\mathrm{eV}^2$ clearly does not satisfy condition (A.11) in long-baseline experiments.

In building the stationary state matter perturbation theory, one can take the vacuum mass eigenstate ν_i $(i = 1, 2, 3)$ as the basis. In vacuum mass basis the vacuum Hamiltonians H_0, defined in eq. (A.2), is given by

$$\tilde{H}_0 = U^\dagger H_0 U = \frac{1}{2E}\,\mathrm{diag}(m_1^2, m_2^2, m_3^2)\,, \tag{A.12}$$

and the vacuum mass eigenstate is given by

$$\nu_i(x) = e^{-ih_i^{(0)}x}\nu_i\,, \tag{A.13}$$

where $h_i^{(0)} = m_i^2/2E$. The matter induced part of the Hamiltonian, $(H')_{\alpha\beta} = a\delta_{\alpha e}\delta_{\beta e}$ is given in this basis as

$$(\tilde{H}')_{ji} = a(U^\dagger)_{je}U_{ei} = aU^*_{ej}U_{ei}\,, \tag{A.14}$$

and thus the matter mass eigenstate to first order in a (see, e.g. [183]) is given by

$$\nu_{mi} = \nu_i + \sum_{j\neq i}\frac{(\tilde{H}')_{ij}}{E_i - E_j}\nu_j = \nu_i + \sum_{j\neq i}\frac{aU_{ej}U^*_{ei}}{h_i^{(0)} - h_j^{(0)}}\nu_j\,, \tag{A.15}$$

which can be inverted to

$$\nu_i = \nu_{mi} - \sum_{j\neq i}\frac{aU_{ej}U^*_{ei}}{h_i^{(0)} - h_j^{(0)}}\nu_{mj}\,. \tag{A.16}$$

Since the relation between the flavor and the vacuum mass eigenstates is $\nu_\alpha = U_{\alpha i}\nu_i$, the flavor eigenstate is given by

$$\nu_\alpha = \sum_i \Big[U_{\alpha i}\delta_{ij} - \sum_{j\neq i}\frac{U_{\alpha i}U^*_{ei}U_{ej}}{h_i^{(0)} - h_j^{(0)}}a\Big]\nu_{mj}\,, \tag{A.17}$$

and since $\nu_\alpha = \sum_i V_{\alpha i}\nu_{mi}$, the matrix element of V to first order in a is

$$V_{\alpha i} = U_{\alpha i} + (\delta V)_{\alpha i} = U_{\alpha i} - \sum_{j\neq i}\frac{U_{\alpha j}U^*_{ej}U_{ei}}{h_j^{(0)} - h_i^{(0)}}a\,. \tag{A.18}$$

The product of the four matrix elements in eq. (A.9) can be written schematically to the first order in a as

$$VVVV = UUUU + UUU\delta V\,, \tag{A.19}$$

where

$$UUU\delta V \equiv UUU\delta V + UU\delta VU + U\delta VUU + \delta VUUU\,. \tag{A.20}$$

Taking into account how $UUUU$ and $UUU\delta V$ terms transform in changing the sign of the CP phase $\delta \to -\delta$ and the matter term $a \to -a$, the CP odd neutrino - antineutrino difference can be written as

$$\begin{aligned}
\Delta P(\nu_\beta \to \nu_\alpha) &= P(\nu_\beta \to \nu_\alpha; \delta, a) - P(\nu_\beta \to \nu_\alpha; -\delta, -a) \\
&= -4 \sum_{j>i} \mathrm{Re}(UUUU)_{\alpha\beta;ij} \Big[\sin^2\{\frac{1}{2} I_{ij}(a)\} - \sin^2\{\frac{1}{2} I_{ij}(-a)\} \Big] \\
&\quad +2 \sum_{j>i} \mathrm{Im}(UUUU)_{\alpha\beta;ij} \Big[\sin I_{ij}(a) + \sin I_{ij}(-a) \Big] \\
&\quad -4 \sum_{j>i} \mathrm{Re}(UUU\delta V)_{\alpha\beta;ij} \Big[\sin^2\{\frac{1}{2} I_{ij}(a)\} + \sin^2\{\frac{1}{2} I_{ij}(-a)\} \Big] \\
&\quad +2 \sum_{j>i} \mathrm{Im}(UUU\delta V)_{\alpha\beta;ij} \Big[\sin I_{ij}(a) - \sin I_{ij}(-a) \Big]\,,
\end{aligned} \tag{A.21}$$

where $(UUUU)_{\alpha\beta;ij} = U_{\alpha i} U^*_{\alpha j} U^*_{\beta i} U_{\beta j}$.